NORWEGIAN SEISMIC ARRAY NORSAR

EARTHQUAKE HAZARD OFFSHORE NORWAY

A study for the NTNF «Safety Offshore» Committee

by

Frode Ringdal, Eystein S. Husebye, Hilmar Bungum,
Svein Mykkeltveit and Ottar A. Sandvin

EARTHQUAKE HAZARD OFFSHORE NORWAY
A study for the NTNF «Safety Offshore» Committee

by

Frode Ringdal, Eystein S. Husebye, Hilmar Bungum,
Svein Mykkeltveit and Ottar A. Sandvin

NORSAR Contribution No. 302

February 1982

NTNF/NORSAR
POST BOX 51
N-2007 Kjeller
Norway

EARTHQUAKE HAZARD OFFSHORE NORWAY

A Study for the NTNF 'Safety Offshore' Committee

Table of Contents

		Page
	SUMMARY AND RECOMMENDATIONS	5
1.	INTRODUCTION	7
2.	TECTONIC PROCESSES; INTER- AND INTRAPLATE MOVEMENTS	9
3.	THE GENERAL FENNOSCANDIAN REGION INCLUDING ADJACENT SEAS - ITS TECTONIC SETTING	11
	3.1 Tectonics of mainly Precambrian times (3000-300 mybp)	11
	3.2 Tectonics of Cambrian-Present times	12
	3.3 Neotectonic movements - Seismotectonic modeling	13
	3.4 Tectonic evolution of the continental shelf between 62-69oN	16
4.	EARTHQUAKE OCCURRENCE - INTER- AND INTRAPLATE EARTHQUAKES	19
5.	EARTHQUAKE OCCURRENCE ON THE NORWEGIAN CONTINENTAL SHELF	21
	5.1 Data bearing on earthquake occurrence	21
	5.2 Seismicity maps for Fennoscandia	22
	5.3 The largest known earthquakes offshore Norway	26
	5.4 Precision of estimated earthquake parameters	30
6.	THE MELØY, N. NORWAY, EARTHQUAKE SEQUENCE 1978/79	31
	6.1 The earthquake sequence	31
	6.2 Focal mechanisms, tectonic implications	32
	6.3 Frequency Characteristics, Source Spectra	33
	6.4 Seismic Moments/Source Parameters	34
7.	DETECTABILITY OF SEISMIC EVENTS OFFSHORE NORWAY	37
	7.1 Introductory remarks	37
	7.2 Development of a detectability map offshore Norwayqm37	
8.	STRONG-MOTION ATTENUATION	43
	8.1 World-wide attenuation relationships	43
	8.2 Attenuation relationships relevant to the Norwegian Continental Shelf	44
9.	DEVELOPMENT OF SEISMIC RISK MAPS - GENERAL CONSIDERATIONS	49
	9.1 ntroduction	49
	9.2 Statistical prediction	49
	9.3 Seismic risk versus other environmental risks	49
10.	DEVELOPMENT OF SEISMIC ZONING MAPS	51
	10.1 Introduction	51
	10.2 Method and parameters	51
	10.3 Seismic zoning maps offshore Norway	53
11.	DESIGN SPECTRA FOR THE NORWEGIAN CONTINENTAL SHELF	57
	11.1 Design spectra - General considerations	57
	11.2 Design spectra for Norwegian Continental Shelf areas	58
	11.3 Time histories	60
	REFERENCES	63

Summary and recommendations

Summary

This report forms part of a comprehensive research effort aimed at obtaining an assessment of the risk of earthquake damage to Norwegian offshore installations. This research, in which NTNF/NORSAR has participated along with the Norwegian Geotechnical Institute, Det norske Veritas and Norwegian Contractors has been undertaken as part of the NTNF "Safety Offshore" program. The work conducted by NTNF/NORSAR, and which is the topic of this report, is subdivided into 3 parts: i) an outline of the geological and tectonic setting of the Norwegian continental shelf area, ii) a study of the seismicity of this region and iii) an assessment of the possibility of occurrence of large, damaging earthquakes here. In summary, the main results of the study presented in this report are as follows:

1. Tectonic Evolution

The most prominent stages of the tectonic development of the Norwegian continental shelf are, in geological terms: i) the Caledonide orogeny, ii) the Hercynian orogeny, iii) several taphrogenic stages in Permian-Cretaceous times, iv) the Kimmerian tectonic movements and v) the opening of the Norwegian Sea. Each of these stages are discussed in some detail in the report. The present-day uplift of Fennoscandia is also commented upon. This uplift, which amounts to maximum 1 cm/yr is generally attributed to glacial rebound, although alternative explanations involving a dominant tectonic component have also been forwarded.

2. Tectonic Settings

The old, stable cratonic blocks of Fennoscandia and Western Russia are separated from the rest of Europe by a dominant fault zone often denoted the Toornquist line. The area south and west of this line, which includes the North Sea, is a more fragmentary part of the Eurasian plate, and is characterized by numerous faults, some of which are still tectonically active. Further north, several striking features may be identified and evidence of block faulting has been observed in the Helgeland and Vestfjorden basins. Neotectonic movements (i.e., crustal movements dating back not more than 10,000 years) have been identified in several areas in Scandinavia, and in particular the Paarve fault in N. Sweden is worth mentioning here. The length of this fault is 150-200 km and its largest vertical slip is 25-30 m. I instances offshore huge "landslides"of unconsolidated sediments have been reported, and this may not unreasonably be taken as evidence of past earthquake activity.

3. Earthquake Occurrence

Most of the world's earthquakes occur in narrow zones along so-called plate boundaries, and are denoted *interplate* earthquakes. The Norwegian continental shelf is well removed from the nearest plate boundary, and is therefore characterized by a relatively low (so-called *intraplate*) earthquake activity. Nonetheless, clear zones of significant seismic activity may be identified in Scandinavia, with the Norwegian west coast and continental shelf being among the most active areas (Fig. 5.2-5.4). The seismicity maps presented in this report are based upon earthquake catalogues compiled by NTNF/NORSAR and covering the period from about 1500 and up to 1980. Particular attention is given to the recent Meløy, Nordland, earthquake sequence 1978/79, which so far includes more than 10,000 recorded earthquakes, about 60 of which were strong enough to be felt.

4. The Largest Earthquakes

During the past 200 years, several earthquakes of estimated magnitude 5.5- 6.5 have occurred in Norway and adjacent seas. The 1927 North Sea earthquake was felt in Scotland, the Shetland Islands, most of southern Norway and parts of Denmark. An even larger earthquake occurred in 1931 further south, near the Dogger bank. Further north, large earthquakes took place in 1866, near Kristiansund and 1819 near Lurøy, Nordland; the latter location is quite close to the source area of the recent Meløy earthquake sequence. In general, the largest known earthquakes of Northern Europe have occurred offshore, thus making any assessment of their risk potential difficult due to lack of observations. Although reported earthquakes in this area have estimated magnitudes of 6.0-6.5 at the most, the future occurrence of even larger events cannot be ruled out. Earthquakes of magnitudes 7.0-7.5 are in fact known to have occurred in areas tectonically similar to Scandinavia, e.g., in eastern North America and in the Canadian Arctic.

5. Assessment of Seismic Risk Offshore Norway

For engineering purposes, the seismic risk at a given site is often expressed in terms of the expected maximum peak ground acceleration to be caused by an earthquake during a specified time period. In this report such acceleration values have been estimated, and the offshore area has been subdivided into seismic hazard zones based on these results. For offshore areas of significant seismic activity, such as the coasts of Møre/Hordaland or Nordland, our results indicate peak acceleration values at the base rock of about 0.05 g at a probability of exceedance of 10^{-2} per year and about 0.2 g at a probability of exceedance of 10^{-4} per year. These results indicate that the seismic risk offshore Norway is similar to the seismic risk offshore Eastern USA, as given by the Report API RP2A of the American Petroleum Institute.

Recommendations

The study of historical earthquake activity in Scandinavia and adjacent seas, as documented in this report, has shown that large earthquakes with magnitude 6 and above have occurred and are likely to occur in the future on the Norwegian continental shelf. Such earthquakes have clearly a destructive potential, and cannot be ignored in a safety context. Preliminary calculations have shown that the probability of a large earthquake occur-

ring close to a given offshore installation is low, *but not negligible*. While these calculations have been based upon what is considered reasonable estimates of seismicity, seismic wave attenuation and magnitude/acceleration relationships, there are still many unknown or uncertain parameters in the risk model. We therefore recommend that further research be carried out in order to permit future updates of the estimated seismic hazard offshore Norway. The most pressing topics to be investigated are:

- More detailed evaluation of focal depths and source mechanisms of selected Scandinavian earthquakes.
- Further development of regional magnitude-frequency recurrence relationships of earthquakes.
- Further improvements in seismic wave attenuation models for Scandinavia including the adjacent continental shelf areas.
- Elaboration of the seismic risk estimates using more refined parameter values and seismicity estimates.
- Establishing a model for generalized seismic risk analysis, i.e., a model including options for analyzing *consequences* of potential earthquake damage. Initial steps toward developing such a model have been taken in the subproject SP6 of the current research project.

Finally, we would like to emphasize that the basic shortcoming in seismic risk studies in Scandinavia is the lack of high-quality seismic data. NTNF/ NORSAR has recently established a local network in Southern Norway, as part of a project sponsored by NVE and NTNF. Supplementing this network with seismographs along the Norwegian coast, including Northern Norway, would significantly improve the seismic surveillance capabilities offshore Norway. Installing ocean-bottom seismographs on the Norwegian continental shelf itself has up to now not been practical. The main reasons are the high initial costs and the relatively low sensitivity and unreliable operation of such installations. However, the future technology trend in this context appears to be that of installing seismometers in boreholes and at depths of 400-500 meters below the ocean bottom - preliminary, promising results have been reported by a U.S. government agency.

1. Introduction

This document gives the results of a study undertaken by NTNF/NORSAR within the NTNF "Safety Offshore" program. It forms part of a comprehensive research effort to assess the risk of earthquake damage to Norwegian offshore installations. NORSAR has participated in this research in cooperation with Norwegian Geotechnical Institute, Det norske Veritas and Norwegian Contractors.

The scope of this report is to present recent research results related to the tectonic and seismic environment of Norway and adjacent seas. Its primary purpose is to provide background material for the "Safety Offshore" committee so that a conclusion may be drawn as to whether or not earthquakes contribute a significant risk factor on the Norwegian continental shelf. With this in mind, emphasis has been laid upon assessments of large-scale tectonic structures and associated movements, and special attention has been given to studying the largest earthquakes known to have occurred offshore Norway. Estimates of expected ground acceleration due to earthquakes offshore Norway for given return periods have also been included.

The organization of the report is as follows: Chapter 2 contains an outline of basic inter- and intraplate tectonic processes, followed by a more detailed discussion of past and present tectonic development in Fennoscandia in Chapter 3. After a more general discussion of earthquake occurrence in Chapter 4 then follows, in Chapter 5, a detailed and thorough treatment of earthquakes on the Norwegian continental shelf, with special emphasis on the largest known earthquakes. The important Meløy earthquakes are then discussed in Chapter 6; Chapter 7 contains a detectability study for offshore Norway, and in Chapter 8 a study of attenuation relationships relevant to the Norwegian continental shelf is presented. The following two chapters then contain the seismic risk analysis, with general considerations in Chapter 9, and the method followed by risk maps for acceleration, velocity and displacement in Chapter 10. Finally, in Chapter 11 are listed some strong-motion records that should be appropriate for the area offshore Norway.

2. Tectonic processes; inter- and intraplate movements

Earthquake occurrence is a clear manifestation that the earth is not in a state of equilibrium. It is well established that relative movements take place within the uppermost, crystalline layers of the earth, which are often denoted the crust/upper mantle or the lithosphere. If we go back in time, say to the middle of the last century, ideas concerning large-scale movements in the crust were discussed only among progressive geologists. However, at the turn of the century the accumulated geological and biological evidence in favor of such movements was rather convincing, and were synthesized in the famous Wegener (1929) hypothesis of continental drift. Notwithstanding the fact that Wegener was a meteorologist, his drift hypothesis was strongly opposed by leadings geophysicists like Harold Jeffreys in Cambridge on the grounds that there was *no* satisfactory mechanical mechanism to explain the decoupling of the rigid continents from underlying strata.

In the early sixties, however, the emergence of a multitude of precise geophysical observations made it clear that Wegener's hypothesis was basically correct; that is, continents have moved and do move relative to each other. The new theory proposed that much larger plates of lithospheric thicknesses, overlying the soft, "semimolten" asthenosphere, were in relative motion. This modern counterpart to Wegener's continental drift hypothesis was called the theory of plate tectonics and gives a reasonable explanation of past and present geographical continent positions, why and where we have prominent earthquake and volcanic belts, and so on. Notice that the previous concept of continental drift has been substituted by plate movements reflecting that the size of the moving fragments on the earth's surface mostly are larger than the continents themselves, i.e., including adjacent oceanic regions. Since the earth is not expanding and these plates are continuously moving, this in turn immediately implies that the underlying dynamic processes are sometimes constructive - plate accretion, and sometimes destructive - subduction of plates into the earth's mantle.

There are several reasons why we consider plate tectonics important in the context of potential seismic hazards for the North Sea and other parts of the Norwegian offshore areas. The foremost is that a good understanding of the past tectonic processes and associated, preserved imprints on the lithosphere in the whole Fennoscandian region provide some insight into present-day tectonic processes and also may indicate which areas and processes that deserve special attention. On a global scale such processes are reasonably well understood today due to a relative abundance in available geophysical information, while the data on local tectonic movements are much poorer. Consequently the following brief review of the tectonic evolution of Fennoscandia dating back some 3 billion years will mainly deal with *large-scale* features, which also reflect the scarcity of relevant information as we go back in time.

Northwest Europe is an integral part of the Eurasian plate, which since the breakup of Pangaea, a conceptional supercontinent comprising all the present-day continental areas, has generally moved northward with an average speed of about 2 cm/year. Modern hypotheses on plate tectonics hold that the individual plates largely act as rigid bodies and henceforth that tectonic deformation within plates is small. This is the reason for the sharp distinction between *intraplate* (within-plate) tectonics and *interplate* (between-plate) tectonics.

Most of the mechanical energy associated with plate movements is released at plate boundaries so the global earthquake activity is mainly confined to such areas. A consequence here is that the interplate stress field decoupled from that of intraplate areas. This does not imply that large, destructive earthquakes do not take place within plates. In fact, numerous examples to the contrary (for example, in China) have been documented throughout historical times.

The size and position of plates are subjected to continuous changes, and the most spectacular process here is when two plates of mainly continental composition collide. Notice that the lithosphere has a thickness of around 200 km beneath continents but only around 100 km beneath deep-oceanic areas. The result of such a process is usually the creation of mountain chains like the Caledonides of western Norway formed some 400 mill. years ago, while a much more recent example is the Himalayas which has been and is being formed by the present-day collision between Eurasia and the Indian subcontinent. Another tectonic process of interest in our context is that of continental rifting, which unless aborted will result in a breaking up of a continental plate in two parts which subsequently drift apart. A typical example here is the westward drift of North America and Greenland, once attached to NW Europe, which started roughly 58 mill. years ago. This drifting process is intimately associated with the creation of new oceanic lithosphere (and in this particular case, the Norwegian and Greenland Seas). There are also processes tied to plate destruction. For example, when a dominantly continental plate collides with an oceanic type one, the latter is subducted below the former and in due time assimilated within the relatively hot upper mantle and is not traceable after a time span of roughly 30 mill. years. An example here is that prior to the formation of the Caledonides, an intermediate Iapetus ocean or a proto-Atlantic is thought to have been subducted beneath NW Europe, and fragments of this pre-Caledonide oceanic area are traceable today (e.g., see Tozer and Schenk, 1978; Mykkeltveit et al, 1980). The interplate tectonic processes discussed above are schematically illustrated in Fig. 2.1.

In the foregoing we have mainly dealt with movement *between* plates, which sharply contrasts with those taking place *within* plates. In general intraplate tectonic movements are very modest, in particular shear movements are less pronounced, thus explaining why plates are treated as rigid bodies. A nearby, notable exception is the reported horizontal, or strike-slip movements associated with a recent outburst of earthquake activity in the Heer

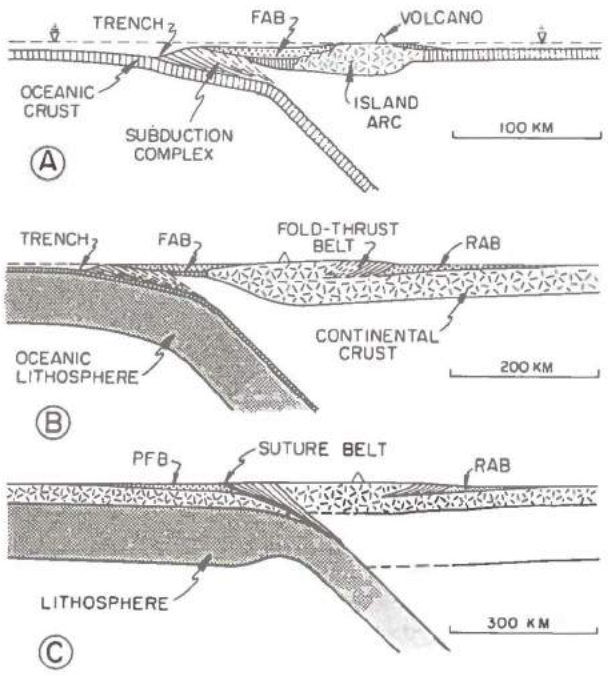

Fig. 2.1a.
Schematic diagrams of orogen types: (A) intra-oceanic arc orogen, (B) continental-margin arc orogen, (C) intercontinental collision orogen. Types of orogenic basins shown by stipples include: FAB - forearc basin; RAB - retroarc foreland basin; PFB - peripheral foreland basin. (After Dickinson, 1977)

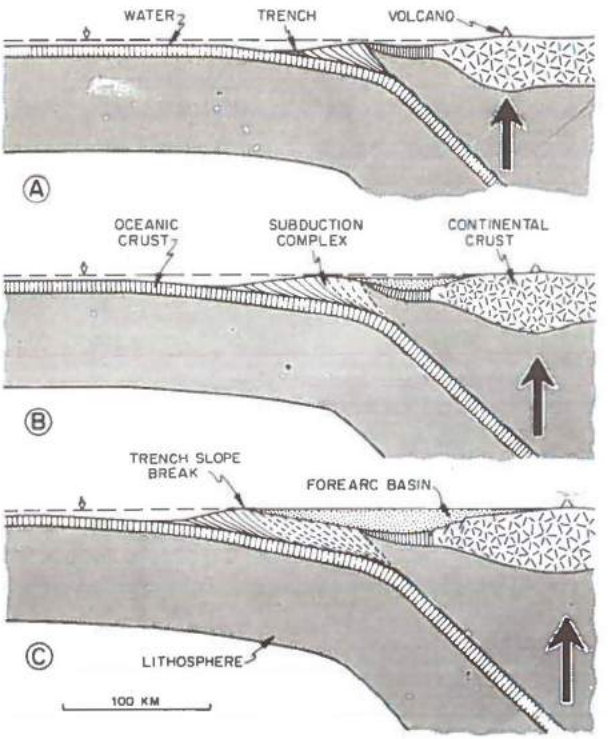

Fig. 2.1b.
Idealized diagram showing inferred evolution (A to B to C) of the accretionary prism of a arc-trench system: A, incipient stage; B, starved forearc basin; C, full forearc basin. Solid lines within subduction complex denote active imbricate zones, whereas dashed lines denote inactive structures. Large arrows show path of magma transit from seismic zone to magmatic arc.

Land area, (Bungum et al, 1981). While large-scale lateral movements within plates are exceptional, vertical movements are not so, as easily testified by geological rock records or simply by precision leveling profiling. A prominent example here is the on-going Fennoscandian glacial rebound, which is likely to result in a total uplift amounting to around 800 meters, of which 250-300 m probably remains (Bjerhammar, 1982; Mörner, 1980). Focal mechanism solutions of intraplate earthquakes as well as in situ stress measurements within continents generally indicate a domination of horizontal compressive stress (Stein et al, 1979).

A conspicuous feature of intraplate tectonic processes is the existence of large, prolonged depressions which are variously denoted aulacogens, rifts and graben structures. We note in passing that major oil fields in the North Sea like the Statfjord field are located within such rift and graben structures. The formation of this kind of intraplate tectonic structures has been much discussed, and is generally attributed to lithospheric stretching as the initial step in the post-rifting sedimentation process (e.g., McKenzie, 1978; Christie and Sclater, 1980; Jarvis and McKenzie, 1980; and Donato and Tully, 1981).

To summarize the discussion so far, tectonic movement at plate boundaries and associated earthquake activity are reasonably well understood, but not so for intraplate tectonic movements and associated earthquake activity. In the latter case, however, earthquake occurrence appears to correlate to some extent with proiminent weakness zones like paleorifts and megafaults. This in turn is the motivation for the forthcoming discussion of the tectonic history of NW Europe. The guiding scientific principle is that earthquake occurrence both in time and space within a given area is a non-random process, though random modeling sometimes serves as a convenient research tool due to lack of precise geological and geophysical data.

3. The general Fennoscandian region including adjacent seas - its tectonic setting

The theory of plate tectonics has enabled the oceans and continents to be studied in entirely new ways, and furthermore allows reasonably precise assumptions to be made about the stage by stage evolution of the oceanic lithosphere and past movements of the continents at least back to about Permian times (ca 200 mybp) or the mentioned breakup of Pangaea. The reconstruction of past tectonic movements becomes increasingly difficult with increasing geological ages for the obvious reason that the non-uniqueness problems in interpretation of geological and geophysical information are severely aggravated by scarcity of data. Another complicating factor is that parts of past tectonic movements are irreversible - a nearby example is the hypothesized subduction and subsequent destruction of a pre-Caledonide Iapetus ocean around 500 mybp. Notwithstanding these difficulties, in the following we will briefly outline the tectonic setting of the areas in question, and the natural starting point is the Archean rocks of pre-Cambrian times.

3.1 Tectonics of mainly Precambrian times (3000-300 mybp)

Manifestations of tectonic movements prior to Cambrian times are found in the very old Fennoscandian crystalline rocks which in exceptional cases date back more than 3000 mybp. There is some discussion on whether Archean tectonic processes were of the same kind as those of post-Cambrian times. Anyway, extensive geological studies have clearly demonstrated that at least Fennoscandia has been subjected to several orogenic cycles (e.g., see Windley, 1979, and Yanshin, 1966), and the essence of these studies is synthesized in Table 3.1 and Fig. 3.1. We will not comment further on this subject because the associated tectonic movements are not well understood and although recent seismicity and neotectonic studies indicate that these paleoruptures may be of some importance in regard of present-day stress release (e.g., see Husebye et al, 1975; Gelfand et al, 1975; Sykes, 1978; Richardson and Solomon, 1979).

The period 800-300 mybp is interesting as we now see the contours of the present-day NW Europe. The old, stable cratonic blocks of Fennoscandia and western Russia are in this period being "separated" from the rest of Europe (ages of exposed rocks generally less than 600-700 mill. years) by a dominant fault zone often denoted the Törnquist-Teissyre lineament or the Fennoscandian Border Zone. This major tectonic feature, traced from Jutland- Skagerrak in the north to the Black Sea and possibly further south, was tectonically active even in Tertiary times and possibly also in Quartiary times.

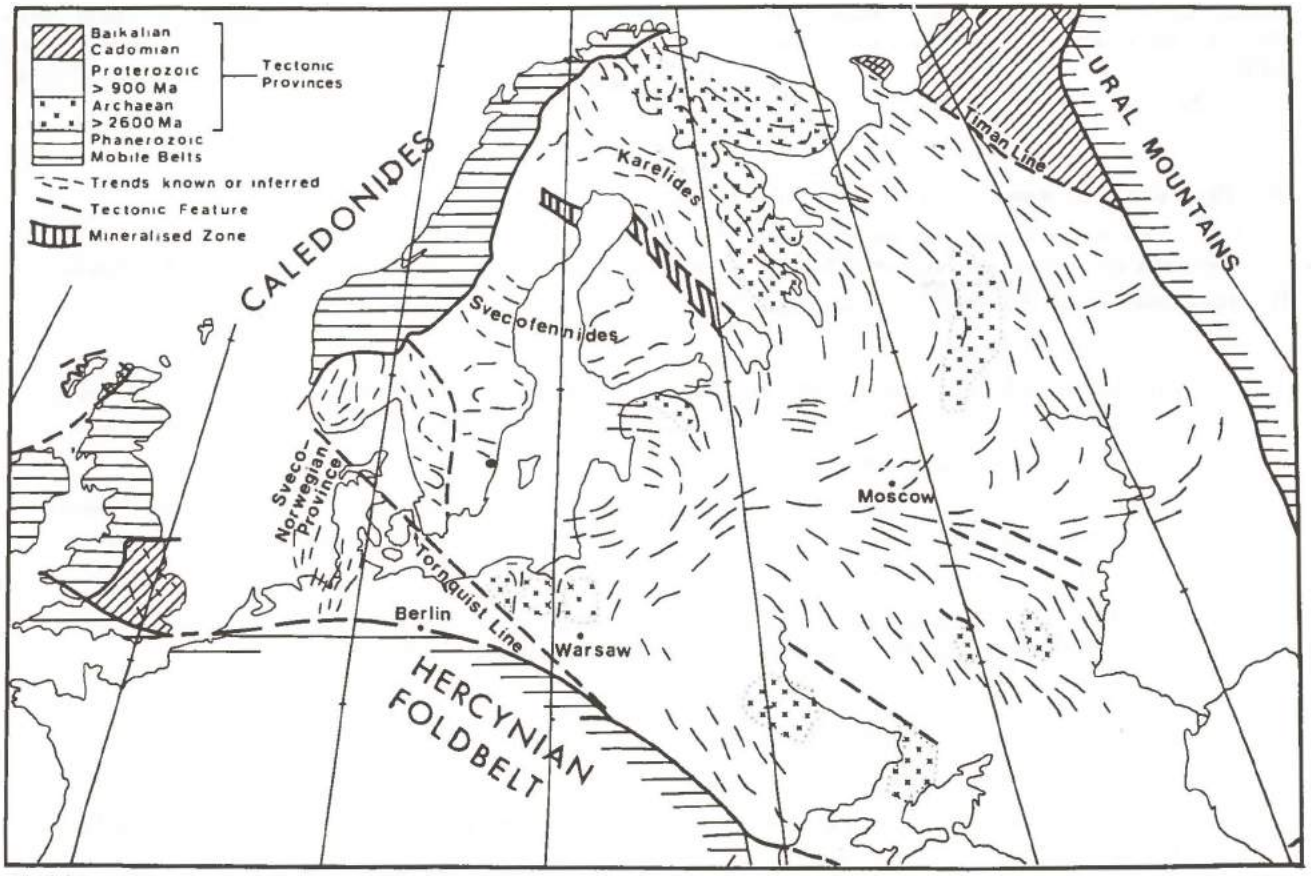

Fig 3.1
Schematic map of the Eo-European craton. The Archaean areas distinguished represent massifs in which Proterozoic tectonic effects are slight; regenerated Archaean rocks in proterozoic provinces are not shown. Map reproducted from Watson (1977)

3.2 Tectonics of Cambrian-Present times

Research aimed at the geotectonic evolution of NW Europe has been greatly encouraged by the associated oil and gas potential, and the evolution of this region is now reasonably well understood, particularly after Permian times when large-scale sedimentation of this region started (e.g., see Illing and Hobson, 1981). Major stages in the tectonic evolution of the North Sea area are tabulated in Table 3.2, and supplementary comments are as follows:

The Caledonide orogeny. The tectonic model of this orogeny is centered on a collision between the Eurasian and N. American plates including subduction of a presumed intervening Iapetus (proto-Atlantic) ocean. As mentioned, collision of predominantly continental plates results in mountain chains, and in this particular case prominent remnants (the Caledonides) are found in Spitsbergen, East Greenland, Western Norway, Scotland and eastern part of Canada (e.g., see Tozer and Schenk, 1978). Interestingly, rocks claimed to be associated with this orogeny have also been found in the southern part of the North Sea, Poland and Barents Sea, suggesting *intraplate* tectonic movements outside the stable Fennoscandian craton as illustrated in Fig. 3.2.

The Hercynian orogeny. This orogeny is sometimes interpreted in terms og a continent-continent collision between the Eurasian and African and possibly N. American plates generating a mountain-folding belt stretching from Ireland-S. England over Brabant, Central Germany and further eastward. The consolidation of the Hercynian (Variscan) fold belt was accompanied by the emplacement of a right lateral tranform fault system which linked the southern Uralides and northern Appalachians, and which crossed Europe where it caused the development of a complex pattern of conjugate shear faults and related pull-apart structures (see Fig. 3.3). This fault system remained active until the late Early Permian. For references, e.g., see Krebs (1977), Windley (1977) and Ziegler (1981).

The North Sea taphrogenic stages in Permian-Cretaceous times.

In Permian times tensional stresses come into being in view of the development of the Oslo Rift - Oslo Graben system during this period. During lower Permian subsidence started in two essentially east-west oriented (intracratonic) basins, partly covering present-day North Sea. The mid North Sea-Ringkøbing-Fyn High also came into existence as a continuous barrier separating the northern basin (Scotland-Norway-Denmark) from the southern one (England-Poland).

During the Triassic the tendency of an essentially north-south rifting system was further accentuated - the Central Graben breached the North Sea-Ringkøbing-Fyn High and the Viking Graben came into existence. The evolution of the central rift systems also continued, and during the Jurassic had become the dominant structural element of the North Sea.

After the initial rifting cycle the North Sea has continued to subside until present, but in the later stages on a significantly broader scale. The challenging geophysical problems are the "mechanism(s)" maintaining the subsidence of the area so as to accomodate a continuous sediment deposition. Recently two classes of hypotheses have been forwarded to explain the subsidence process; in one case large wavelength tectonic processes are introduced including a postulated "stretching" of the subsiding area in question, while in the second case, which indeed appears to be a viable alternative, the sedimentary load results in a net down-warping via an isostatic compensation mechanism (e.g., see Beaumont, 1978; Jarvis and McKenzie, 1980; Sclater and Christie, 1980; Donato and Tully, 1981).

Kimmerian tectonics. A period of significant tectonic activity is the Kimmerian phases, which in Upper Jurassic - Lower Cretaceous affected the entire North Sea area and is generally rated as a major rifting phase. For ex-

A. The pre-cratonic stage (Svecokarelium 2600-1800) m.y)

Eo-Europa occupied mainly by mobile tectonic provinces; Archaean tectonic systems succeeded by Early Proterozoic tectonic systems in which mobile (Karelide and Svecofennide) belts surrounded many small stable massifs.

B. The cratonic stage - Europa forms a single mass (1800-300 m.y.)

(i) Gotium (ca 1800-1100 m.y.)

The nucleus of Eo-Euoropa probably forms part of a craton of huge dimensions including parts of Greenland and North America; Sveconorwegian province added to eocraton at about the end of this phase.

(ii) Dalslandium (ca 1100-800 m.y.)

Phase of extension and/or disruption. Positioning of future aledonides and Hercynides. At the end of period (Jothnian) the American, African and Eurasian plates probably in collision - the Grenville orogeny.

(iii) Eocambrian-Palaezoic (ca 800-300 m.y.)

Complex phases of collision and orogeny in the marginal mobile belts. Eo-Europa once more forms part of a huge craton including much of Greenland, North America and Siberia.

(iv) Late Paleozoic (ca 300-200 m.y.)

Life span of largest supercontinental craton.

(v) Mesozoic-Cenozoic (ca 200-0 m.y.)

Phase of extension and disruption of supercontinental craton. Eo-Europa now becomes part of the Eurasian craton.

Table 3.1.
Eo-Europa in relation to successive global tectonic systems - material taken mainly from Stephansson and Carlsson (1976), Watson (1977) and Windley (1977).

ample, in the Viking Graben the associated tectonic movements resulted in a strong, block-faulted submarine relief of some 2-3000 meters.

Opening of the Norwegian Sea. Rifting movements in the North Sea petered out gradually during Upper Cretaceous-Early Tertiary and thus apparently was un related to the opening process of the Norwegian Sea, or in other words the Norway-Greenland separation (e.g., see Talwani and Eldholm, 1977). However, the North Sea subsidence continued, and we also have clear evidence of a contemporary uplift of Scandinavia, particularly Western Norway. The present-day uplift of Fennoscandia, is (Bjerhammar, 1982) considered unrelated to the above Tertiary uplift.

The North Sea tectonic evolution - A brief summary

Due to the proven hydrocarbon potential of the North Sea, this area has been mapped both geologically and geophysically in considerable detail and consequently the major stages of its tectonic evolution are reasonably well known, e.g., see Illing and Hobson, 1981. The dominant tectonic feature in the context of seismic risk assessment for the area in question is summarized in Fig. 5.6, where the largest *known* occurring earthquakes in the general North Sea area are depicted. Additional details for the Norwegian sector south of 62^{o}N latitude are presented in Fig. 3.4. The use of this information in a seismo- tectonic context for risk analysis is the topic of a later chapter.

3.3 Neotectonic movements - Seismotectonic modeling

The U.S. Atomic Energy Commission in their guidelines for seismic hazard assessment for areas where nuclear power plants are to be located emphasize that no neotectonic movements (dating back at most a few 10^5 years) should have taken place in the vicinity of the suggested

TIME PERIOD	TYPE OF TECTONIC MOVEMENT Eurasia	North Sea Area	Main Effect
Quarternary (present)	Eurasian plate moving NE. Glaciation	Sedimentation, glacial rebound	Sedimentation & subsidence
U. Tertiary	Alpine subduction in W. Tethys Sea	Alpine orogeny	Sedimentation & subsidence
L. Tertiary	Spreading & rifting in N. Atlantic. Opening of Bay of Biscay	Laramide tectonisms. Fennoscandia uplift.	Rifting, wrenching & inversion
Cretaceous	Relatively modest tectonic activity	Modest tectonic activity	Sedimentation & subsidence
Jurassic	Rifting in N. Atlantic incipient spreading	Kimmerian tectonism	Rifting, wrenching, volcanism & subsidence
Triassic	Break-up of Pangaea	Modest tectonic activity	Sedimentation & subsidence
Permian	Post-Hercynian orogeny movements & rifting	Subsidence & marginal rifts	Oslo rift formation
Carbon-iferous	Hercynian orogeny	Hercynian orogeny	Mostly marginal tectonic movements
Devonian Silurian Ordovician	Caledonian orogeny Closure of the Iapetus ocean	Caledonian orogeny	Formation of the Caledonides Cratonization, rifting, wrenching, volcanism
Cambrian & Precambrian	(See Fig. 3.1 and Table 3.1)		

Table 3.2
Chart summarizing tectonic development of the general North Sea area. The underlying data have been taken from a variety of sources which are partly contradictory. Major references are Woodland (1975), Ziegler (1977) and Illing and Hobson (1981). This in turn reflects an occasional scarcity of basic information available but also some confusion of types and time spans of tectonic processes affecting NW Europe, particulary in Paleozoic times.

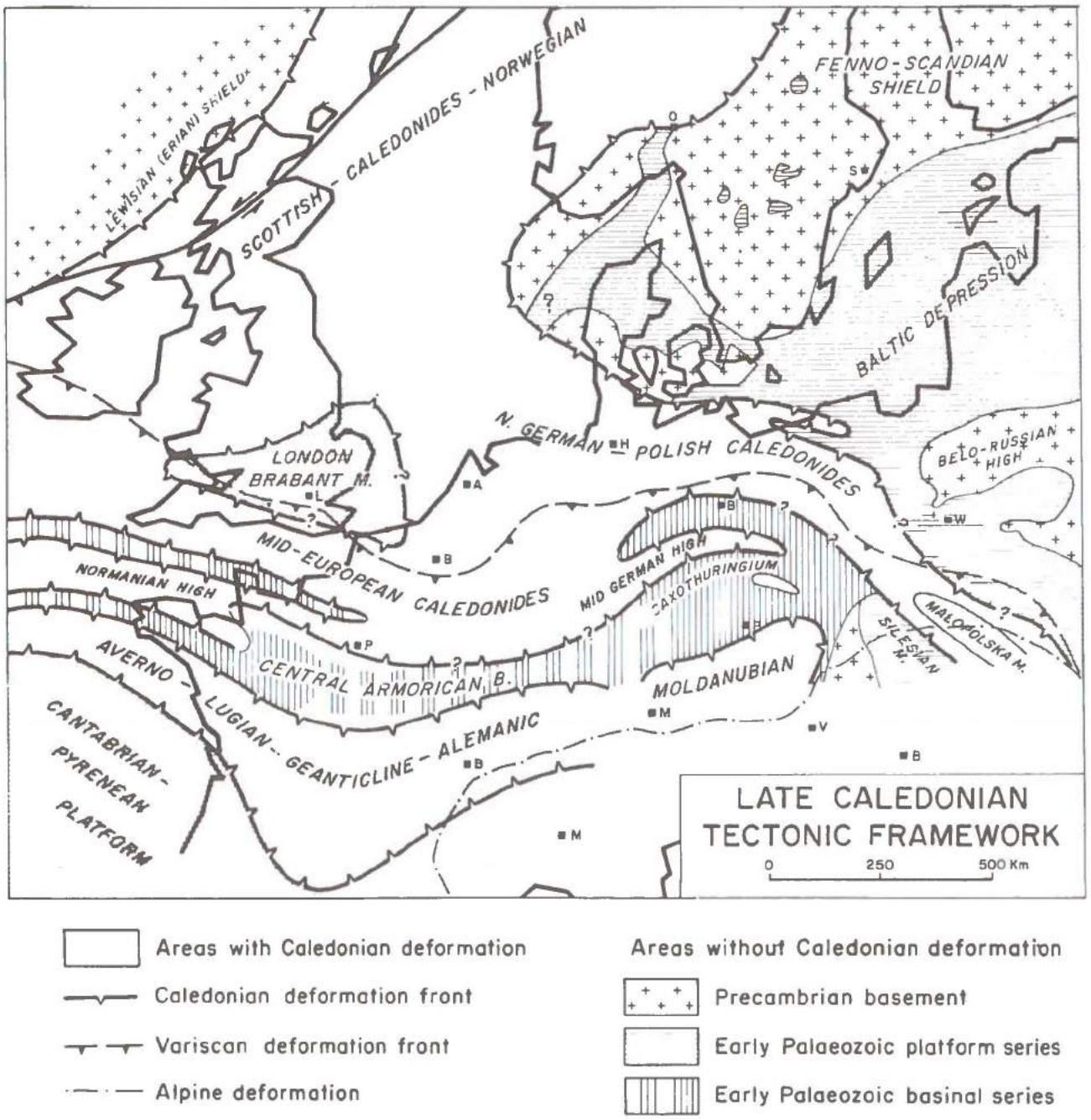

Fig. 3.2.
Late Caledonian tectonic framework of northwest Europe. (Figure reproducted after Ziegler, 1981)

location. The rationale for this formulation is obviously that tectonic movement (that is large earthquakes) therefore may occur again in the same area in the near future. However, the wisdom of that inference has lately been questioned on the grounds that it tends to ignore an equally obvious fact, namely, that even very large earthquakes (say $M \geqslant 7$) do not necessarily result in surface faulting. An extreme example here is that the discussed neotectonic principle would have permitted the epicentral area of the large Missouri earthquakes of 1811/12 to be rated as safe in an earthquake hazard context. Consequently, *both* recent tectonic movements (say during the past 10^5 years or less) and seismotectonic modeling (fault age not a critical constraint) must be considered in seismic risk assessments.

Neotectonic movements in Fennoscandia

With neotectonics is meant clear evidence of crustal movements preferably observable on the earth's surface dating back not more than 10^5 years. N. Sweden and N. Finland exhibit examples of such movements and the most impressive one is the Parve fault of presumed postglacial origin in Swedish Lappland. The length of this fault is about 150-200 km and the largest vertical slip of the order of 25-30 meters (Lundquist and Lagerbäck, 1976). The underlying tectonic process here is not well understood at present. Neo-tectonic movements have also been suggested as having taken place in Southern Norway (Løset, 1981). Huge offshore "landslides" of unconsolidated sediments have been reported from several areas, and

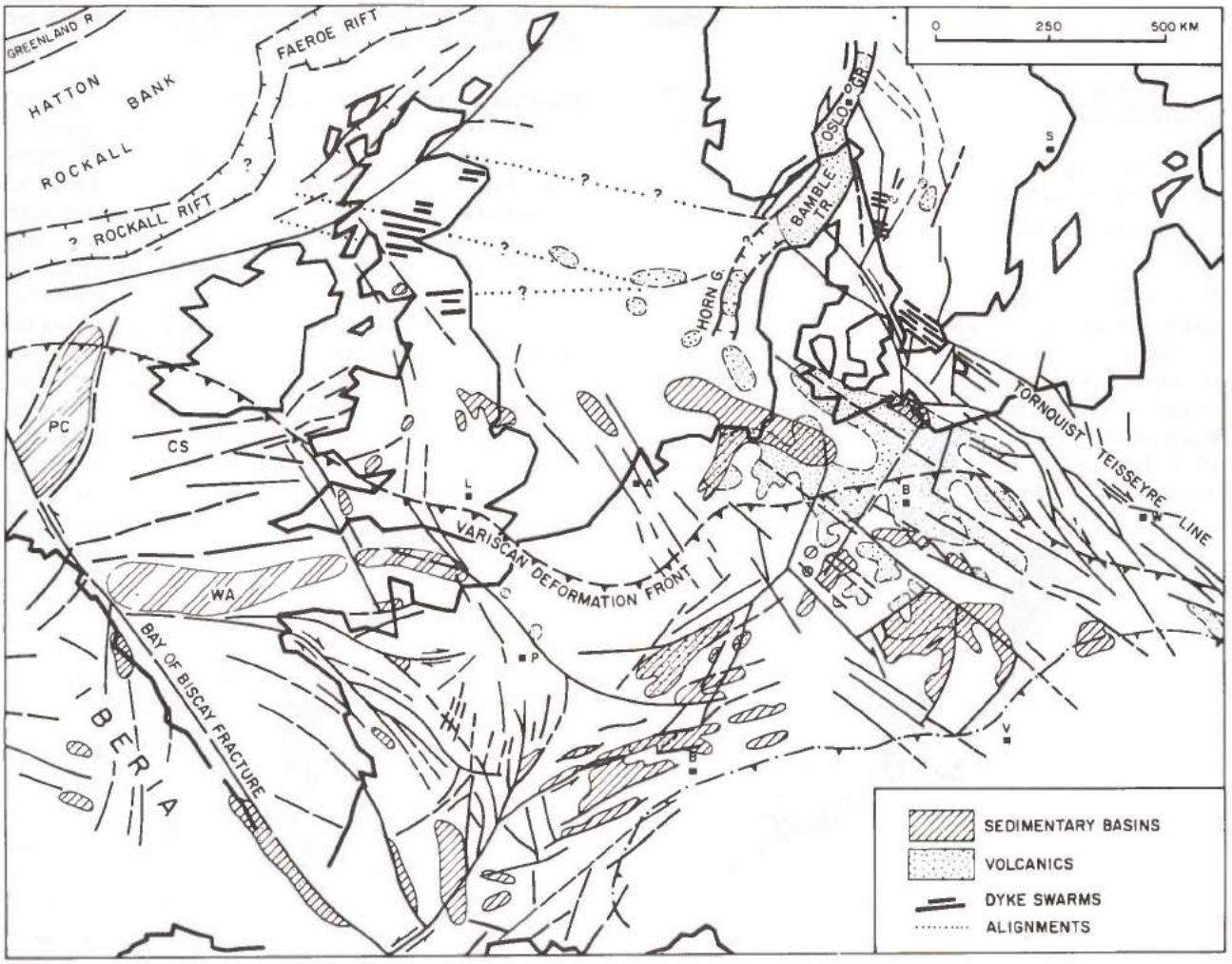

Fig 3.3.
Late Hercynian (Variscan) tectonic framework of northwest Europe. (Figure after Ziegler, 1981)

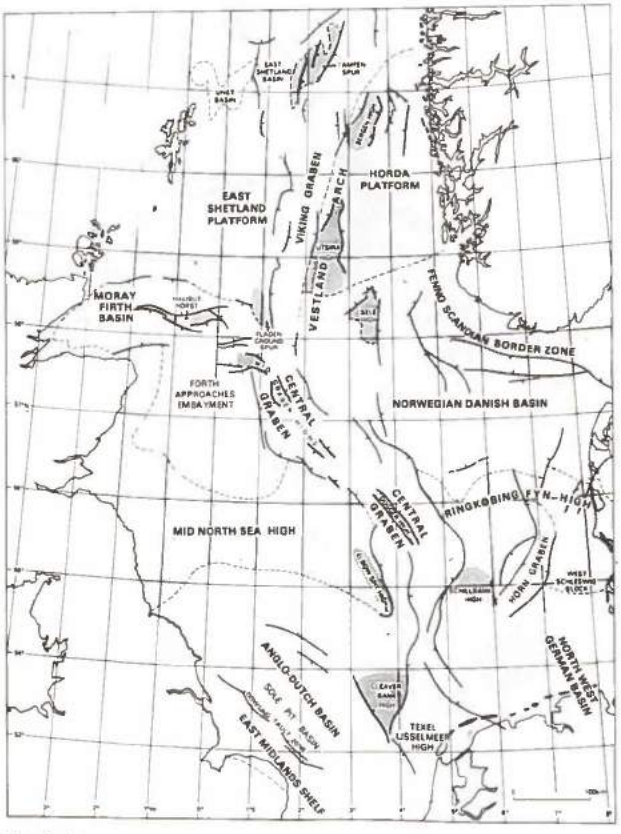

Fig. 3.4.
Major structural units in the North Sea. (Figure after Day et al. 1981.)

may be taken as indirect evidence of past earthquake activity. Such an explanation is at least not unreasonable as of today the earthquake activity, say from Møre to Troms and along the shelf edge is quite significant.

To summarize, prominent post-glacial tectonic movements have taken place in Fennoscandia, and if these movements represent fracturing processes, the corresponding maximum magnitudes (scaled after present-day fault dimensions) would be of the order of 7.0-7.5 units on the Richter scale.

Seismotectonic modeling

In the context of seismic hazard assessment we mean by seismotectonic modeling specific procedures by which information on past tectonic processes is incorporated in the actual seismic risk analysis. The rationale behind this approach is two-fold: i) the fault pattern within an area of aperture, say, 300-500 km, appears to be "indestructible", even over geological time spans of the order of 10^8 years - in other words if an area is repeatedly subjected to orogenic cycles, the repeated stress releases would predominantly follow the established fault pattern; ii) major earthquakes and consequently the most destructive ones have large fault length dimensions, say, of the order of 50-300 km. Naturally, such earthquakes cannot be accomodated within smaller faults, say, of length 5-10 km. In offshore areas even major faults in the crystalline basement might be very difficult to detect, but such problems may at least partly be offset by statistical simulations.

3.4 Tectonic Evolution of the Continental Shelf between 62-69°

In discussing the tectonic evolution of this area we make a sharp distinction between pre- and post-Cenozoic times (say, around 58 mybp) as this marks the initial rifting phase, which subsequently resulted in a total separation between W. Norway and Greenland, including accretion of new oceanic areas - the Norwegian and Greenland Seas.

The western Norway shelf area (north of 62°N) has been mapped in significantly less detail than the North Sea. Incidentally, it is just now that more comprehensive analysis of this area has become more generally available (Anonymous, 1979; Binns, 1978; Eldholm and Talwani, 1977; Kjøde et al, 1978; Oftedahl, 1980; Sturt and Roberts, 1978; Talwani and Eldholm, 1977; Jørgensen and Navrestad, 1981; Rønnevik, 1981). Paleographic maps sketching the tectonic evolution of western Norway and the Barents Sea are shown in Fig. 3.5.

Pre-Cenozoic time. After the Caledonian orogeny the present-day W. Norway shelf area (and its E. Greenland counterpart) constituted an epicontinental sedimentary basin. Just like the North Sea also this area was subjected to extensional forces including graben formations with subsequent sedimentation which in more extreme areas resulted in strata of up to 9 km thicknesses. The above loosely referenced tectonic activity resulted in several structural features, the most prominent among these being the Helgeland basin, and the Nordland and Vega crests (ridges). Several seismic profiling surveys have not unexpectedly provided clear evidence of block faulting in the Helgeland and Vestfjorden basins. Finally, the Upper Cretaceous period appears to be a tectonically quiet one like it was for the North Sea (Jørgensen and Navrestad, 1981).

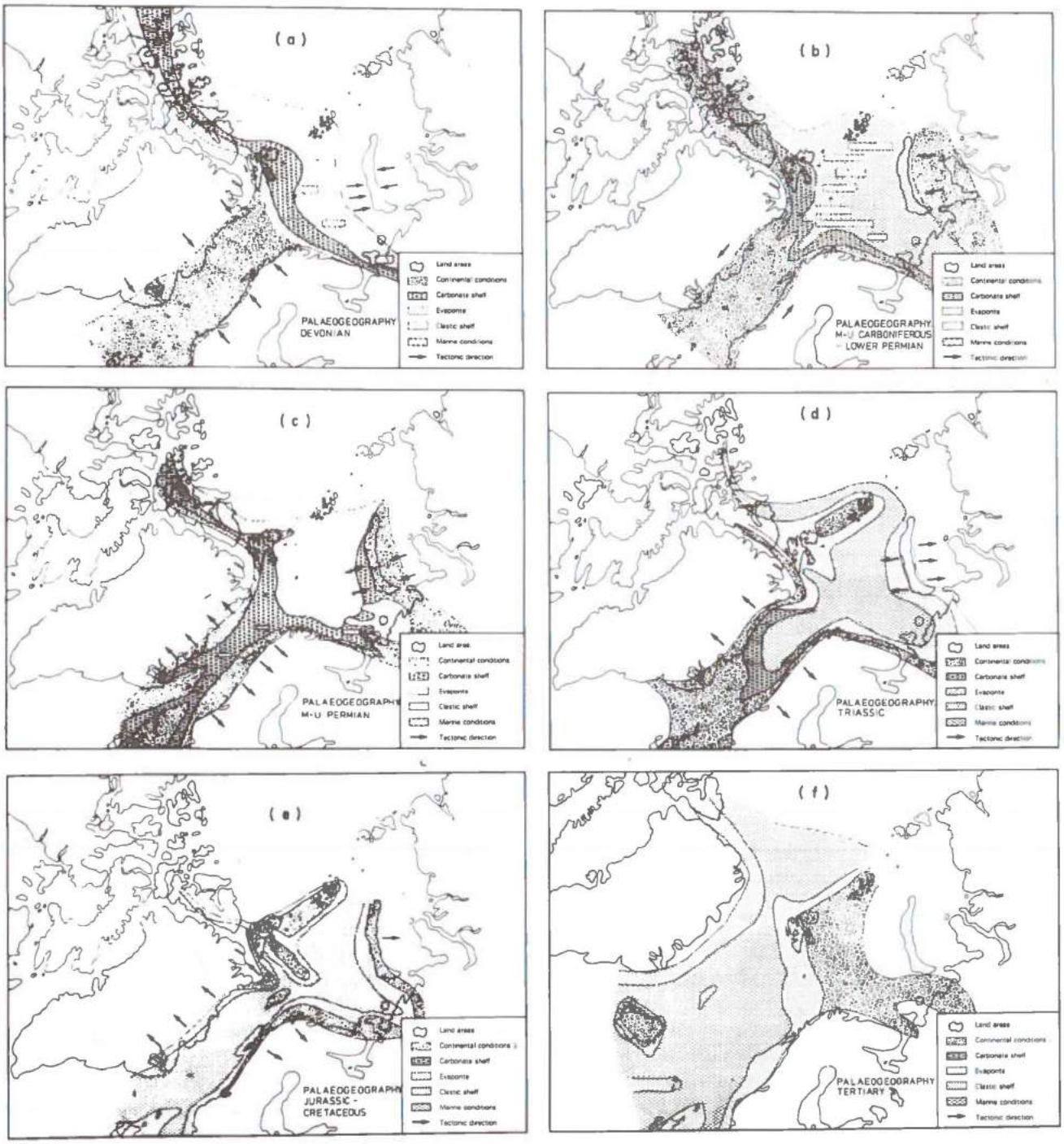

Fig 3.5.
Poleogranpic maps: (a) Devonian; (b) Middle Carboniferous-Lower permian; (c) Middle Upper Permian; (d) Traiassic; (e) Jurassic-Cretaceous; (f) Tertiary. (Figure after Rønnevik, 1981).

Early Cenozoic and later times. The really spectacular tectonic events are the opening of the Norwegian Sea commencing some 58 m.y. ago and also the Tertiary uplift of mainland Fennoscandia, which are estimated to be of the order of nearly 2000 m. The westward drift of Greenland meant accretion of the new *oceanic* sea floor. The relatively abrupt transition from a continental-to-oceanic crust is denoted escarpments, and are causually connected to exceptional basaltic injections in the initial rifting phase (Talwani and Eldholm, 1977). An anomalous feature is the so-called Vøring plateau, the formation of which is probably associated with a shift in the spreading axis after only about 2 mill. years. As regards the uplift of mainland Fennoscandia, hypothesized major faults associated with this asymmetric movement are found outside SW Norway, while similar manifestations to our knowledge have not yet been reported off-coast further north.

To summarize, also western Norway (between 62^{o}-69^{o}N) exhibits striking tectonic features and also (onshore) evidence of neotectonic movements. As will be demonstrated in Chapter 5, the observed seismic activity is also *remarkable* in particular with earthquake occurrence along the shelf edge and in an oceanic zone extending from Lofoten to the Mohn's/ Knipovich mid-oceanic ridge intersections in the Norwegian Sea (Husebye et al, 1975).

4. Earthquake occurrence - inter- and intraplate earthquakes

Most of the world's earthquakes occur in narrow bands that can be clearly identified on a global seismicity map (Fig. 4.1). With the emergence of the plate tectonic concept in the 1960's (Chapter 2) an attempted unified theory was forwarded to explain the earthquake occurrence along plate boundaries as resulting from relative motion of large lithospheric plates. Today, such earthquakes are commonly called *interplate* earthquakes, and their mechanisms and causes are fairly well understood.

A considerably more difficult problem is the occurrence of earthquakes within plates. Such earthquakes, which are denoted *intraplate* earthquakes, occur much less frequently and generally seem to exhibit less clear tectonic patterns. Norway and the Norwegian continental shelf are located well within what is called the Eurasian plate, and are thus an intraplate region.

Before studying in detail the earthquake occurrence in Scandinavia and adjacent seas (Chapter 5), it is of interest to summarize some basic facts about global seismicity, with special emphasis on intraplate earthquakes. Conceptionally, an earthquake represents a sudden release of accumulated stress along a zone of weakness (or fault) in the crust or lithosphere (e.g., see Doornbos, 1981; Knopoff, 1981; and Madariaga, 1981). Fault sizes may vary considerably, and the largest earthquakes can cause displacement along faults of several hundred kilometers' length. While all continents and continental shelves show an abundance of faults, only very few of these faults are today seismically active. Thus a geological study is by itself not sufficient to point out potential areas of seismic hazard. A futher complication is that the large majority of earthquakes, including numerous destructive ones, do not cause surface ruptures, though imprints of previous movements are clear. In some cases the entire fault may be buried under thick layers of sediments, making it impossible to be identified through surface surveys.

Earthquakes occur at depths ranging from 0 to 700 km. The deeper earthquakes occur only in lithospheric subduction zones (see Chapter 2) and most earthquakes can be classified as shallow, i.e., having depths of 70 km or less. Known intraplate earthquakes are of the shallow type with a few exceptions, notably some events occurring in Rumania and Pamir/Hindu-Kush which are associated with fossilized subduction zones.

Earthquakes are detected and located through the elastic waves they generate. These waves propagate through the interior of the earth or along its surface, and can be registered by sensitive instruments called seismometers thousands of kilometers away. By associating wave arrival times at widely distributed stations, one can automatically determine the earthquake location, usually to within 15 km accuracy today for well-recorded earthquakes.

The elastic waves generated by an earthquake can be classified into:

a) **Body waves** propagating through the earth's interior
   - P waves of the compressional type
   - S waves of the shear type

b) **Surface waves** propagating along the earth's outer layers
   - Rayleigh waves, characterized by elliptical pozation in the vertical plane
   - Love waves, which are polarized in the horizontal plane.

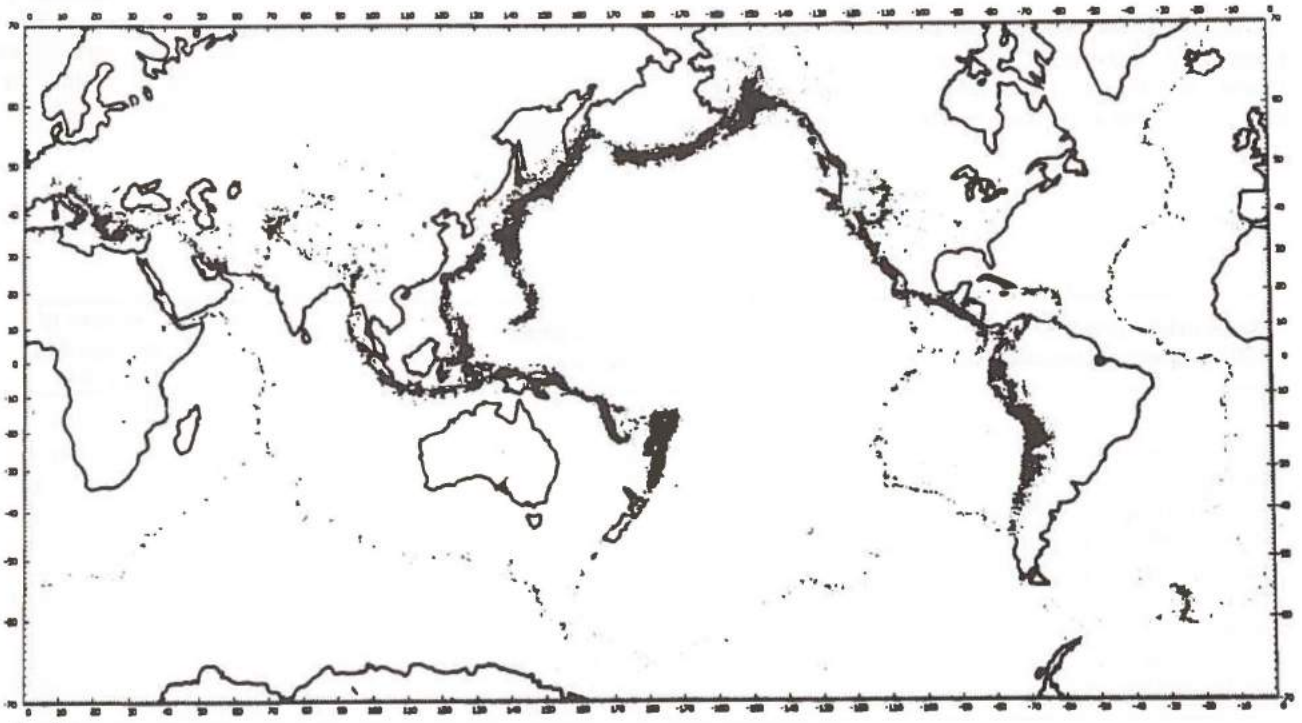

Fig. 4.1.
Seismicity of the world, 1967-1979.

While the P waves are most important for earthquake detection and location, the shear waves (and in particular the horizontal component) are of most concern to the engineer.

A number of ways have been proposed to measure the *size* of an earthquake, and some of these will be further discussed in Chapter 5. The most widely used measure so far is the Richter magnitude, which is based on the maximum deflection of the signals recorded by a seismograph (Richter, 1958). The scale is logarithmic and contains a correction factor which is introduced in order to compensate for the weakening of seismic waves as they spread away from the source. Recently, an extension of the Richter scale, applicable to the largest events, has been introduced by Kanamori (1977). The largest Richter-Kanamori magnitude yet reported is 9.5, while the most sensitive local seismographs can record microearthquakes of magnitudes below 0. Most destructive earthquakes have magnitudes above 6, but there are examples of very shallow, low magnitude shocks which have had disastrous effects, such as the 1960 Skopje earthquake (M = 5.5) and the 1960 Agadir earthquake (M = 5.8), which each claimed thousands of human lives.

Table 4.1 shows how magnitude of shallow earthquakes can be related in a rough way to earthquake effects, and also indicates the number of earthquakes per year. We do emphasize the great variability in effects as a function of among others distance to source, local geology and not least, construction quality, and the table should only be considered an illustration of the potential hazards. The rightmost column shows how the number of earthquakes increases with decreasing magnitude; typically a decrease of 1 magnitude unit corresponds to an increase by a factor of 10 in earthquake frequency.

Earthquakes cause destruction in several ways. Ground vibrations can shake structures and bring them to the point of failure and collapse. Certain kinds of soil lose their rigidity and "liquefy" when subjected to seismic ground motions. Avalanches, mudflows, fire and tsunamis may accompany earthquakes, and sometimes cause much greater damage than the shaking itself.

We conclude this chapter with a brief discussion on the problem of "maximum possible magnitude" in a given region, which is of considerable importance in the present study. That there must be an upper limit to seismic magnitudes is physically obvious, and it appears in fact that this limit is between 9 and 10 for interplate earthquakes. On the other hand, even the largest *intraplate* earthquakes are usually of much lower magnitudes; only in China have intraplate earthquakes of M = 8 and above been reported in this century.

Chinese earthquakes do appear to be anomalous in this respect, and it would probably be unduly conservative to assume that such large earthquakes can be expected in any intraplate area. With the limited data that are available for Norway and the Norwegian continental shelf, it is still necessary to consider other intraplate areas in order to get indications as to the maximum magnitude that might be expected. The region which points itself out in this respect is the eastern part of North America. Like Norway, this region is well removed from any plate boundary, and tectonically the Appalachian mountain chain, which is the dominant geomorphological lineament of the region was formed during the same orogeny as the Caledonides when America and Eurasia " collided". Post-glacial uplift is also a common feature to parts of eastern North America and Scandinavia.

Several large earthquakes of magnitudes 7-7.5 have struck eastern North America during the past few hundred years. They include the 1663 St. Lawrence Valley earthquake, and three major earthquakes of New Madrid, Missouri, during the winter 1811-1812, the 1886 Charleston, South Carolina, earthquake and the 1929 earthquake near the Grand Banks of Newfoundland. Even though such earthquakes are rare, it is nonetheless firmly established that earthquakes of magnitude 7 and slightly above are possible in widely distributed locations in eastern North America (Stein et al, 1979). Other intraplate areas from which we have reliable records of earthquakes of similar magnitudes include the USSR and Australia.

While numerous examples thus exist of a world-wide basis of large intraplate earthquakes of magnitude 7 to 7.5, we know of no example of any limited area being hit by such an earthquake more than once during historical times (we consider the three New Madrid earthquakes as a single instance of stress release). Phrased in another way, this would indicate that the next such earthquake would most likely occur in an area where no similar size event is previously known to have happened through historical times.

Characteristic effects of shallow shocks in populated areas	**Approximate magnitude**	**Number of earthquakes per year**
Damage nearly total	8.0	0.1-0.2
Great damage	7.4	4
Serious damage, rails bent	7.0-7.3	15
Considerable damage to buildings	6.2-6.9	100
Slight damage to buildings	5.5-6.1	500
Felt by all	4.9-5.4	1,400
Felt by many	4.3-4.8	4,800
Felt by some	3.5-4.2	30,000
Not felt but recorded	2.0-3.4	800,000

Table 4.1.
Earthquake magnitudes, effects and statistics (After Gutenberg & Richter, 1956)

5. Earthquake occurrence on the Norwegian Continental Shelf

In this chapter we survey past and present known earthquake activity offshore Norway. Furthermore, as the available seismicity information is fragmentary at best, we shall supplement these data with those of the earthquake activity of Scandinavia where the seismicity information is reasonably complete for historical times. In particular we shall concentrate on the known occurrence of large earthquakes in the region, and in addition present details on such earthquakes in separate appendices.

5.1 Data bearing on earthquake occurrence

Before going into detailed discussion on the earthquake occurrence, it is important to be aware of both the basic types and limitations of the observational data available. In general we differentiate between two types of seismicity data: i) macroseismic data which reflects how people actually felt an earthquake and ii) analysis of recordings of elastic waves generated by earthquakes using specifically designed instruments, i.e., seismometers and accelerometers. Both of these types of seismicity data are important, and their relative merits with reference to the present study will be discussed in the following.

5.1.1 Macroseismic data

Macroseismic data simply mean written descriptions on how people living in the area where the earthquake took place actually felt the earthquake and, equally important, observable damage to buildings, bridges, roads, etc. The systematic collection of macroseismic data on earthquake occurrence in Fennoscandia began in the 1880's when widespread use of questionnaires was initiated. Macroseismic data prior to that time had to be extracted from newspaper reports and other often very obscure sources and are therefore less reliable, although the large earthquakes are affected less in this respect. The oldest known report on seismic activity in *Denmark* dates bake to year 1073 (Lehman, 1956), in *Sweden* to year 1497 (Kjellén, 1903, 1909), in *Norway* to 1612 (Keilhau, 1836; Kolderup, 1905, 1913) and in *Finland* to 1610 (Renquist, 1930). Only after around 1650 does the written documentation appear sufficient to consider reported earthquakes as tectonic events from a scientific point of view. For example, the earliest reported earthquakes are often coincident with very stormy weather, which in turn appears to be the real cause of the reported damages. This tendency of coupling earthquake occurrence with other geophysical phenomena like storms, thunderstorms, auroras, particular celestial constellations, etc., is well exemplified in Horrebow's (1765) description of the large 1759 earthquake.

The available macroseismic information for an earthquake is primarily used for estimating maximum *intensity* and radius of perception. The intensity parameter is a measure of the size of the earthquake in question and in this respect the 12-graded modified Mercalli (MM) scale is commonly used (Wood and Neumann, 1931). Details on the MM-scale are given in Table 5.1 and demonstrate that the intensity parameter has no obvious physical meaning. Furthermore, several empirical relations have been proposed from which typical earthquake parameters like epicenter location, focal depth and magnitude are related to the basic macroseismic parameters intensity and radii of perception (Båth, 1972; Karnik, 1969). Despite some of

I.	Not felt
II	Felt by persons at rest or on upper floors.
III.	Hanging objects swing. Light vibration.
IV.	Vibrations like heavy truck passing nearby. Windows and dishes rattle. Standing cars rock.
V.	Felt outdoors. Sleepers wakened. Small objects fall. Pictures move.
VI.	Felt by everybody. Furniture displaced. *Damage*: broken glassware, merchandise falls off shelves. Cracks in plaster.
VII.	Felt in moving cars. Loss of balance while standing. Church bells ring. *Damage*: broken chimneys and architectural ornaments, fall of plaster, broken furniture, widespread cracks in plaster and masonry, some collapse in adobe.
VIII.	Steering trouble in moving cars. Tree branches broken off. Cracks in saturated soils. *Destruction*: elevated water tanks, monuments, adobe houses. *Severe to mild damage*: brick construction, frame houses (when unsecured to foundation), irrigation works, embankments.
IX.	Sand craters in saturated silty sands. Landslides. Cracking of ground. *Destruction*: unreinforced brick masonry. *Severe to mild damage*: inadequate reinforced concrete structures, underground pipes.
X.	Widespread landslides and soil damage. *Destruction*: bridges, tunnels, some reinforced concrete structures. *Severe to mild damage*: most buildings, dams, railway tracks.
XI.	Permanent ground distortion.
XII.	Nearly total destruction.

Table 5.1
Modified Mercalle Scale (Abridged) - after Wood and Neumann (1931).

the arbitrariness and subjectivity tied to the collection and analysis of the macroseismic data, this type of information is highly esteemed on two accounts, namely, in providing continuity of observational data over a time interval of several hundred years and in making possible a reasonable estimate of the location and magnitude of the earthquakes in question.

It is difficult to judge the information potential of the macroseismic material even after the collection of such observation was sysematized. We have reviewed available material, and found it to be of marginal use in determining intensity decay curves and attenuation parameters. The main reason for this shortcoming is the relatively scarce spatial sampling provided, as often only one questionnaire per postal district has been available. In the case of offshore earthquakes an additional problem is that seaward observations naturally are lacking. A likely consequence of this is a landward bias in epicenter locations, and this is in turn rather obvious when comparing seismicity maps based respectively on macroseismic and instrumental observations. (See Section 5.2.)

5.1.2 Instrumental data

Instrumental observations of Fennoscandian earthquakes date back to 1904 and 1905 when the first mechanical pendulum seismographs were installed in Uppsala and Bergen. Due to their low magnifications (around 400 and 200), these instruments did not contribute much new information about the seismic activity in the area under consideration. However, in the period 1955-1965 the Fennoscandian seismograph network was expanded and the instrumental quality vastly improved by installation of modern, high-gain electromagnetic seismographs with magnification ranging from 15,000 to 150,000. In 1971 another generation of instruments was introduced with the large aperture Norwegian Seismic Array (NORSAR) in southeastern Norway (Bungum et al, 1971; Bungum and Husebye, 1974). The present Fennoscandian network of stations (Fig. 5.1) represents a vast improvement in the capability of monitoring the seismic activity in the area, relative to what was available before 1970, although we will demonstrate that it is still not adequate for a complete seismo- tectonic study of local earthquakes - an illustrative example here is the initial confusion as concerns the Meløy earthquake sequence, which is described in detail in Chapter 6.

The shortcomings of the local seismograph network are the large station separations, the poor azimuthal coverage for earthquakes in the coastal areas of Norway, and the difficulties in obtaining large numbers of original seismograph records (which are stored in 4 different countries). With regard to the latter, it means that the crucial phase identification or interpretation of the seismic records is often based on second-hand information, i.e., as given in local seismic bulletins. The most serious problem, however, is that of discrimination between the relatively few (tectonic) earthquakes and the very many artificial events from quarry blasts, naval activities in the adjacent seas, etc. The above shortcomingts of the seismograph network are, however, not critical for earthquakes with magnitudes greater than 4.5-5.5, because these events are also recorded by stations outside Fennoscandia and usually may be reliably distinguished from man-made explosions. Actually such data were used by Husebye et al (1975) when discussing the seismicity of the Greenland and Norwegian Seas and adjacent coastal areas. Also Dahlman et al (1975) have published a seismicity map for Fennoscandia

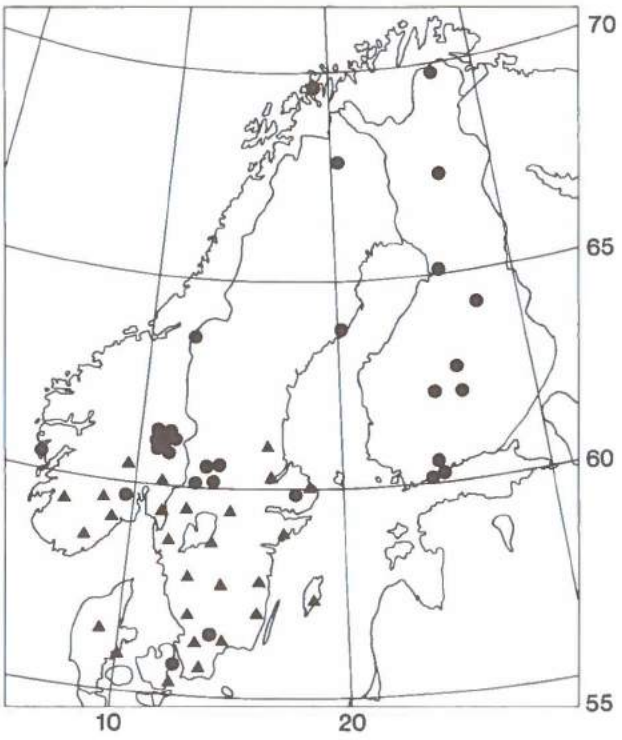

Fig. 5.1.
The Fennoscandian seismograph network. Circles indicate permanent seismic stations (or arrays if clustered), and triangles indicate temporary microearthquake stations (in operation since 1979/80).

which is based on a detailed study of instrumentally recorded earthquakes in the interval 1968-72. In addition, Noponen (1971-77) has reported on a routine basis both earthquakes and large chemical explosions occurring in Fennoscandia.

The seismograph stations which are located closest to the Norwegian coast are Bergen (BER) and Tromsø (TRO). However, the detectability of these stations is very poor, partly due to their coastal location, and the data have not proved very useful for the present study. Other seismograph stations in southern Norway are Kongsberg (KON) and the large aperture seismic array NORSAR, which became operative in 1963 and 1971, respectively. As mentioned above, seismograph stations located in coastal areas generally are significantly less sensitive than those far inland due to the surf-generated microseismic noise. This has clearly been demonstrated by Pirhonen et al (1976) for Fennoscandia and by Ringdal et al (1977) on a global scale. Although we have not directly computed the seismic event detectability offshore Norway as a function of time, our estimate is that prior to 1960 the event detectability in the general North Sea area was not significantly better than 5.0 magnitude units. Further north it was certainly not much better.

5.2 Seismicity maps for Fennoscandia

In the previous section we have described and commented upon types and amount of seismological data bearing on earthquake occurrence in Fennoscandia, and with regret noted that the quality of the data available at most stations is rather poor, even for the last decade.

In Figs. 5.2, 5.3 and 5.4 the seismicity of Fennoscandia from 1497 to 1980 is presented for different time intervals; 1497 to 1890, 1891 to 1950 and finally 1951 to 1980. In this respect we follow Husebye et al (1978) whose time differentiation was motivated by quality and

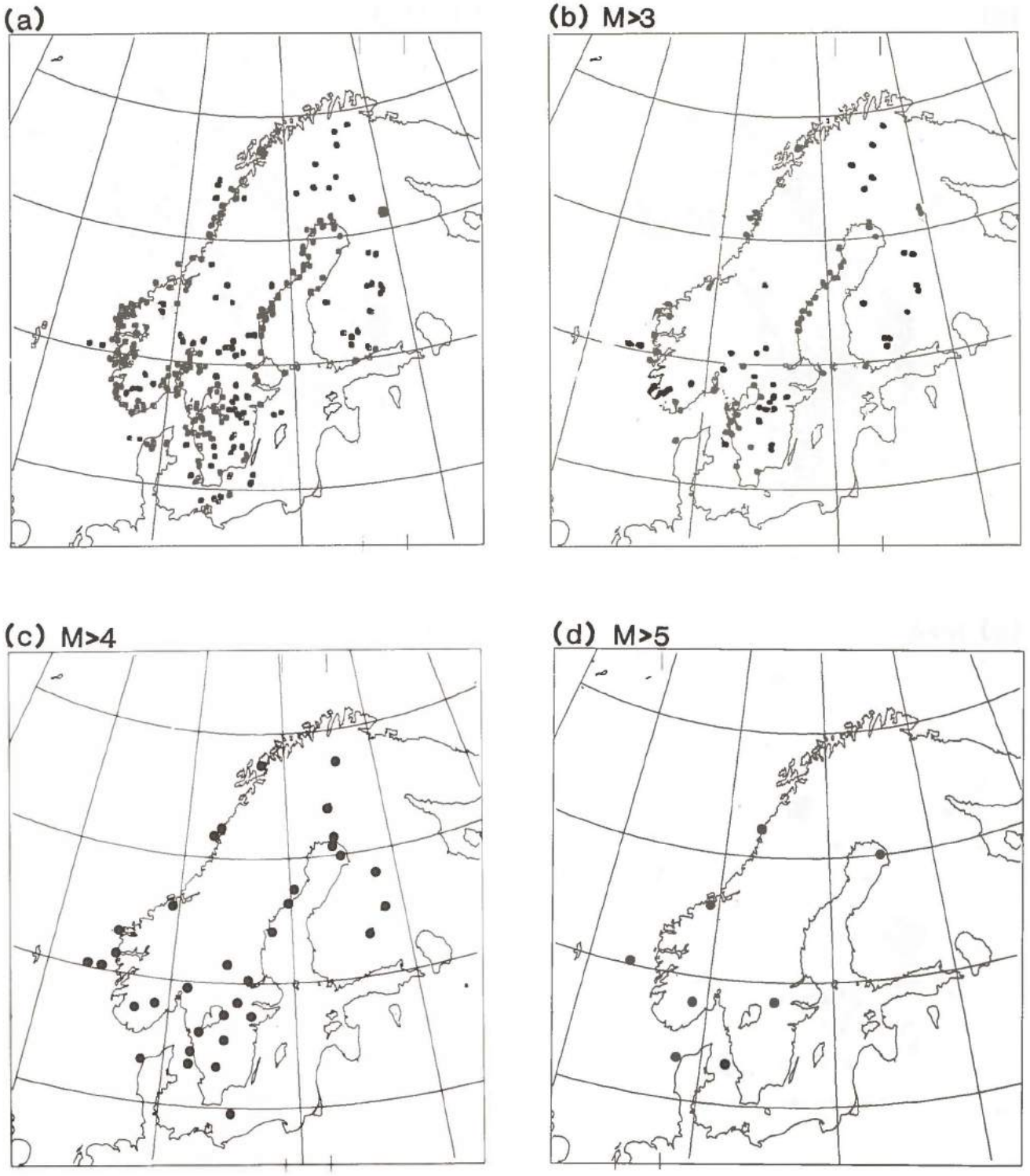

Fig. 5.2.

Seismicity map for Fennoscandia covering the interval 1497-1890 based on macroseismic data:

a) All earthquakes in the NTNF/NORSAR catalogue
b) Earthquakes of magnitude > 3
c) Earthquakes of magnitude > 4
d) Earthquakes of magnitude > 5

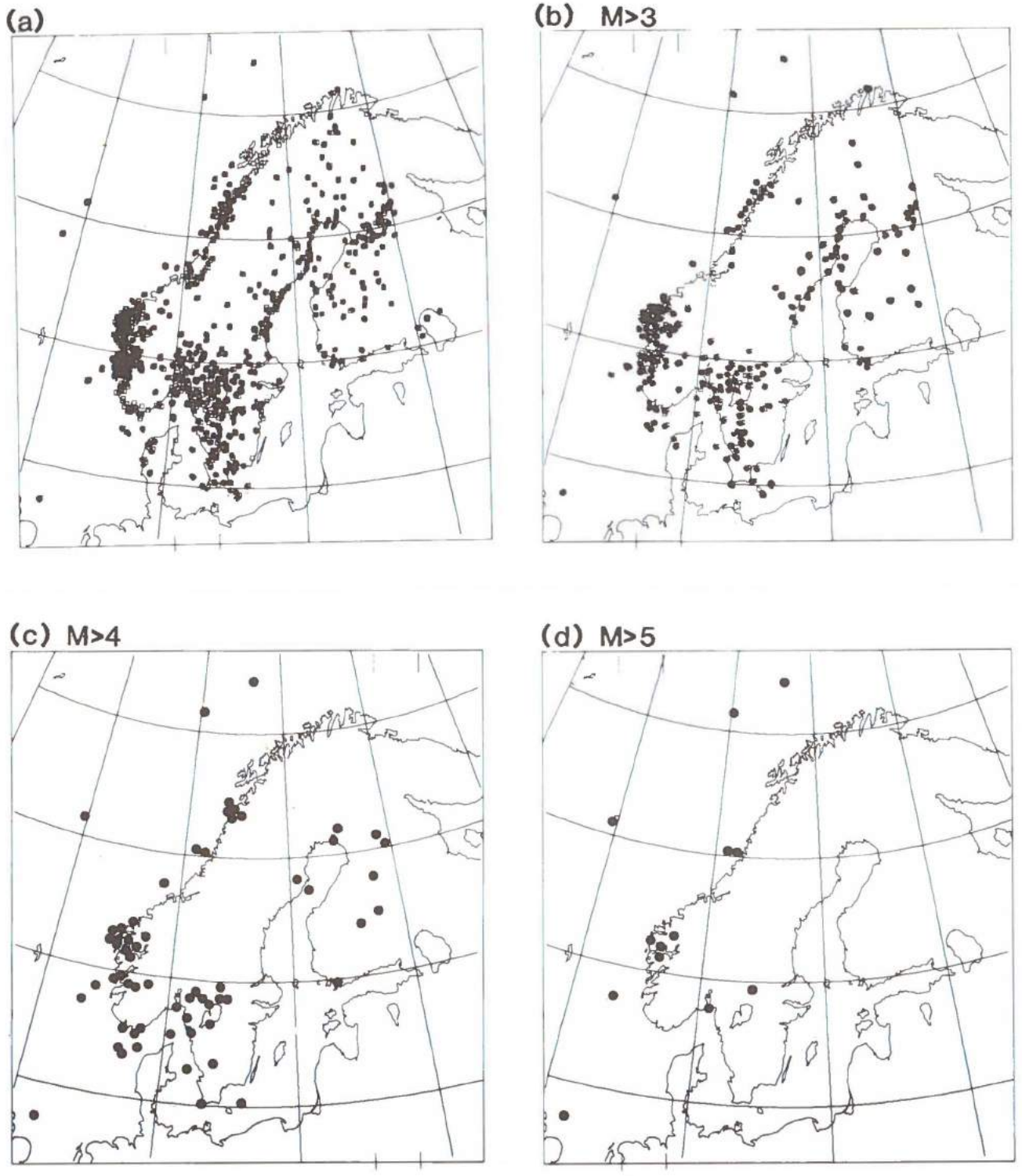

Fig. 5.3.

Seismicity map for Fennoscandia covering the interval 1891-1950 based on mostly marcroseismic data but also a few instrumental observations:

a) All earthquakes in the NTNF/NORSAR catalogue
b) Earthquakes of magnitude > 3
c) Earthquakes of magnitude > 4
d) Earthquakes of magnitude > 5

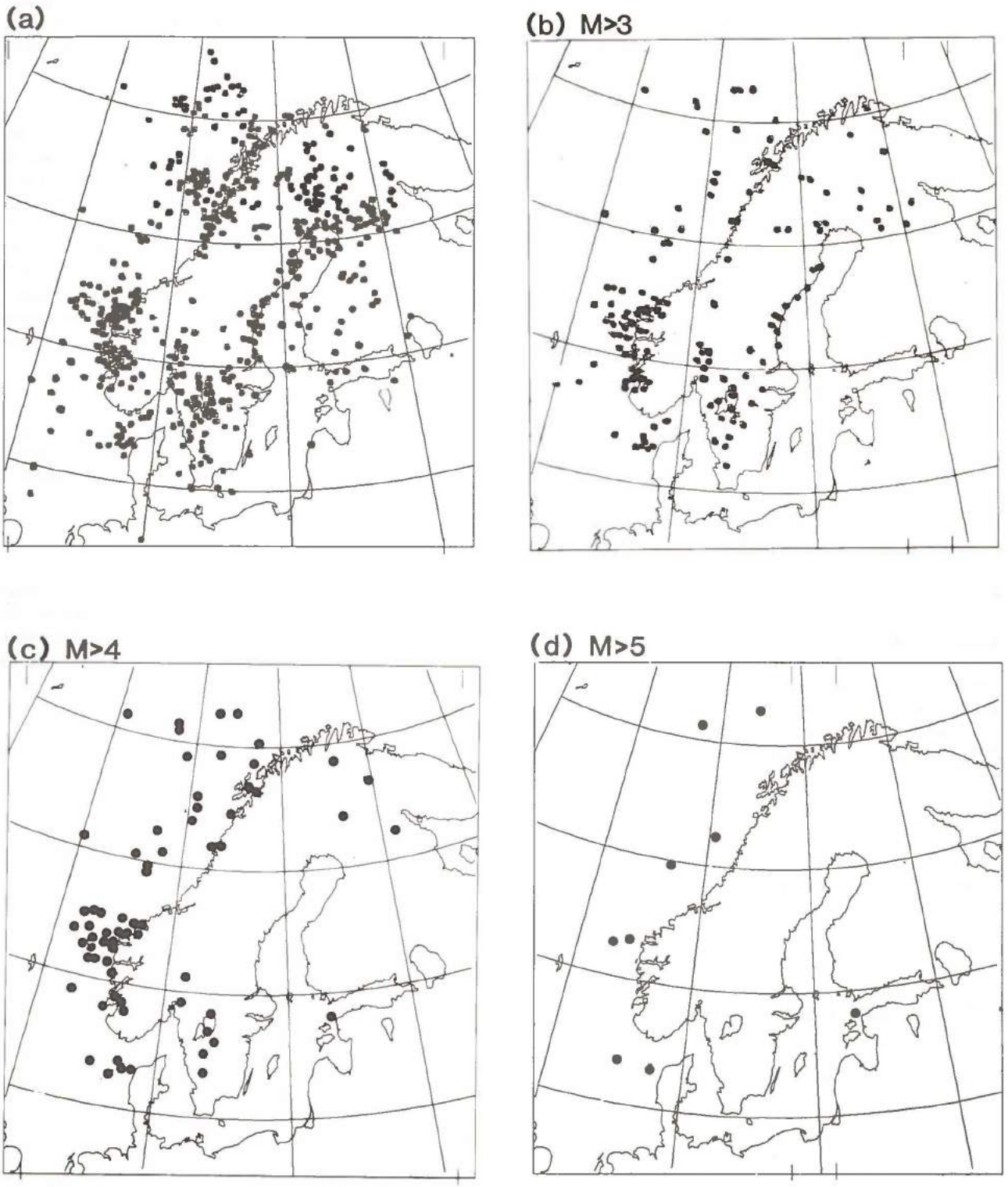

Fig. 5.4

Seismicity map for Fennoscandia covering the interval 1951-1980 mostly based on instrumentally detected earthquakes:

a) All earthquakes in the NTNF/NORSAR catalogue
b) Earthquakes of magnitude > 3
c) Earthquakes of magnitude > 4
d) Earthquakes of magnitude > 5

Note in particular that almost all of the larger earthquakes have occurred offshore Norway.

homogeneity constraints on the original macroseismic and instrumental data. In each figure, we present complete maps based upon the NTNF/NORSAR earthquake catalogue as well as maps showing earthquakes greater than magnitude 3, 4 and 5, respectively.

The first interval, 1497-1890, is based on what we may term historical data, that is, more or less arbitrary reports in different types of chronicles, newspapers, etc. The main sources here are the works of Keilhau (1836), Kolderup (1905, 1913), Kjellén (1903, 1909), Renquist (1930) and Lehmann (1956). The interval 1891-1950 is characterized by a systematic collection of macroseismic data, and in this respect we have relied on the excellent earthquake cataloque for this interval as published by Bâth (1956). Finally, the interval 1951-1980 is mainly based on instrumental data, and the data used here have been extracted from various seismograph station bulletins, catalogues from different international seismological centers and so on. For details we refer to Husebye et al (1978) and Bungum and Fyen (1979) who both have discussed extensively the tectonic aspects of the Fennoscandian seismicity.

Although the general patterns of the seismicity maps for the three periods are similar in some respects, there are some important differences. Most noteworthy, and very relevant to the present study, is the almost complete lack of earthquakes located offshore Norway before 1950. This is due to lack of adequate instrumental coverage as discussed earlier, and demonstrates that we have indeed a very limited time period of relevant coverage of earthquakes offshore Norway. Fig. 5.4, which covers the interval 1951-1980, is also noteworthy in another respect: whereas part a) of this figure might indicate that the seismic activity level offshore is similar to that onshore, this is indeed not so. Almost all of the larger earthquakes ($M > 4$) in this time interval have occurred offshore Norway, and we therefore may conclude that the earthquake hazard offshore Norway is significantly greater than for the remainder of Fennoscandia.

Thus, in order to obtain a reliable assessment of earthquake risk offshore Norway, it is necessary to take earthquake detectability for this region into account, for all the time periods considered. This will be further elaborated in Section 7 of this report.

5.3 The largest known earthquakes offshore Norway

Of special interest in any seismic risk study are the largest earthquakes known to have occurred in the region under consideration. Both instrumentally recorded events and earthquakes for which we have only historical records are of importance here. The "size" of the earthquakes must be determined on the basis of a number of observed characteristics, and the most prominent in use are:

(a) **Macroseismic intensity**

This quantity reflects how human beings have experienced an earthquake. For assigning a specific intensity to a given observation, the Modified Mercalli scale, which was already presented in Table 5.1, is most commonly used today. As noted earlier, intensity is a highly complex quantity reflecting mostly ground acceleration but also ground displacement and ground velocity during passage of earthquake-generated seismic waves. Besides, soil amplification effects must be considered carefully when assessing intensities. Despite its shortcomings, macroseismic intensity, and in particular the maximum intensity I_o of an earthquake is a very valuable parameter not only for historical earthquakes (where no instrumental observations exist), but also in supplementing instrumental observations of present-day earthquakes in Fennoscandia.

(b) **Area of perception**

The size of the area over which an earthquake has been felt is tied to the size of the earthquake, its depth of focus and the local wave attenuation characteristics. The area of perception is often indicated by using an equivalent radius R corresponding to the "average" distance from the epicenter to the furthest point (in any direction) where the earthquake was felt. This parameter is especially useful in the present study since maximum intensities cannot be properly assessed for earthquakes with offshore epicenters.

(c) **Earthquake magnitude**

This parameter is a measure of the size of an earthquake and its definition is physically tied to the kinetic energy of a wavetrain in a seismogram record. A general magnitude M definition is

$$M = \log A/T + f(\Delta, H) + C_{S,R}$$

where A = maximum signal amplitude, T = signal period, $f(\Delta, H)$ = correction term for epicentral distance and focal depth and $C_{S,R}$ = calibration term depending on seismograph location and earthquake source region.

(d) **Acceleration**

Instrumental measurements of ground motion in the vicinity of an earthquake source are best made by accelerometers or strong-motion instruments. Ground acceleration is in fact probably the most important single seismic parameter for risk analysis. Unfortunately, in Scandinavia no direct measurement of acceleration from a large or moderate size earthquake exists, and we therefore have to base risk assessment on a conversion from intensity or magnitude to acceleration. In this respect, we have to rely on data from either Europe, Japan and/or western United States. We remark in passing that accelerometer records of occurring earthquakes have a clear physical meaning, in contrast to what is the case for reported intensity.

(e) **Other parameters**

A number of additional parameters exist and are sometimes used in risk estimation. To complement the acceleration spectrum, spectra of ground displacement and velocities of strong-motion recordings are sometimes used. Complete time-histories of selected strong-motion records are very useful for engineering purposes. Apart from intensity and magnitude, the size of earthquakes is often measured using the *seismic moment*, which, as opposed to the other two parameters, is a measure with a clear physical significance at the source. Seismic moment is related to fundamental parameters of the faulting process (e.g., see Doornbos, 1982)

$$M_o = \mu S \langle d \rangle$$

Year	DATE Day	Hour	EPICENTER Lat	Long	DEPTH* (km)	MAGNITUDE	INTENSITY MM-Scale	FELT RADIUS (km)
1759	22/12	01.00	57.0N	11.5E	-	6	VII	500
1819	31/8	15.00	66.5N	13.0E	-	6	VII	500
1834	3/9	19.15	59.3N	8.5E	-	5½	VI	400
1841	3/4	02.16	57.0N	8.0E	-	5½	VII+	250
1865	7/5	13.21	60.5N	3.0E	-	5½	VI	400
1866	9/3	01.15	63.2N	9.0E	-	6	VII	400
1879	25/9	00.15	59.0N	7.0E	-	4½	IV	250
1884	22/4	09.15	51.9N	0.9E	-	5½	VIII	150
1886	24/10	23.30	60.5N	4.0E	-	4½	IV	300
1892	15/5	14.51	60.9N	6.0E	-	5½	VII+	240
1895	4/2	23.40	61.9N	7.0E	-	5	VI+	250
1901	18/9	01.24	57.4N	4.1W	30	5.8	VIII	240
1903	24/3	13.30	53.0N	1.7W	25	5.5	VII+	150
1904	3/7	15.21	53.0N	1.7W	20	5.2	VII	142
1904	23/10	10.26	59.2N	10.5E	55	6.4 (2)	VIII	560
1905	23/4	01.37	53.5N	0.9W	40	5.4	VII	119
1906	27/6	09.45	51.6N	4.0W	30	5.3 (3)	VIII	237
1907	14/1	13.03	65.5N	11.0E	-	5	V+	250
1907	27/1	04.58	65.5N	11.0E	-	5½	VI	315
1913	19/7	15.50	64.0N	8.0E	-	5.0 (1)		200
1913	4/8	07.38	61.4N	5.8E	-	4.9 (1)	V+	270
1924	25/7	19.36	72.5N	16.0E	-	5.6 (1)		
1927	24/1	05.18	59.0N	3.0E	-	5.1 (10)	VI	440
1929	10/6	23.03	71.0N	10.0E	-	6.0 (26)		600
1931	7/6	00.25	54.0N	1.4E	(70)	6.0 (27)	(VIII)	600
1934	20/5	19.04	64.5N	2.0W	-	5.6 (1)		
1935	17/7	00.04	65.5N	11.5E	-	5.6 (1)		
1938	11/3	16.08	61.9N	4.2E	-	4.8 (1)	V+	268
1946	11/5	16.25	66.0N	0.5W	-	5.0 (2)		
1946	11/5	18.39	66.0N	0.5W	-	5.1 (8)		
1954	7/7	00.48	59.8N	4.8E	-	4.9 (1)	VI+	350
1955	3/6	11.39	61.9N	4.0E	-	5.0 (2)		
1958	23/1	13.35	65.0N	6.5E	-	5.5 (1)		
1958	6/8	17.16	59.5N	6.0E	-	5.1	VI	300
1959	29/1	23.24	70.9N	7.3E	-	5.8		
1962	15/12	03.48	67.5N	14.2E	-	5	VI	235
1967	21/8	13.41	57.0N	4.9E	-	5.2 (9)		
1975	20/1	10.47	71.7N	14.2E	-	5.0		
1977	6/4	19.31	61.6N	2.5E	-	5.0		

* Depth estimates are those of Karnik (1969).

Table 5.2
Known, large earthquakes offshore Norway and in adjacent areas. The events listed have either a magnitude of at least 5.0 or a radius of perception of at least 250 km. Magnitudes are estimated from instrumental observations when possible (number of stations in parentheses), otherwise the magnitude values have been inferred from macroseismic data.

where S is the area of the fault, $\langle d \rangle$ is the average displacement on the fault, and μ is the shear strength of the faulted rock. Moment can be independently determined from spectral analysis of an earthquake. Because moment is corrected for radiation pattern as a function of fault geometry and observed azimuth, it is a more consistent measure of earthquake size than is magnitude and, most importantly, is not intrinsically upper bounded. However, in the present study, the available data have not allowed a measurement of seismic moment, and we have therefore at this stage limited the analysis to magnitudes and intensities.

The largest known earthquakes in Norway and adjacent seas are shown in Figs. 5.5 and 5.6. Fig 5.5 shows all known earthquakes within the indicated area which have either a magnitude of at least 6 or a radius of perception of at least 400 km. Fig. 5.6 covers the North Sea, and is an attempt to correlate earthquakes in the area with known tectonic features. The earthquakes of the two figures are listed in Table 5.2.

It is noteworthy from Fig. 5.5 that the major occurrence of large earthquakes takes place along the coast of Norway. From Fig. 5.6 there seems to be a slight correspondence between the earthquakes and the major faults of the map, but it is difficult to give definite conclusions because of the considerable location uncertainty of the earthquakes in question. This uncertainty is probably on the order of 25-300 km, highest for offshore and coastal epicenters and for earthquakes occurring before 1900.

Fig. 5.7 indicates the extent of the macroseismically felt area for six large earthquakes. In the following we give a brief description of each of the largest known events.

22 December 1759, 57°N, 11.5°E, M = 6, I_o = VII, R = 500

This earthquake is tentatively associated with movements along the Fennoscandian Border Zone (the Törnquist li-

ne). It was felt over southern Scandinavia and as far south as France.

31 August 1819, 66.5°N, 13°E, M = 6, I_0 = VII, R = 500

The earthquake was felt most strongly at Salten and Helgeland, with reports of muddy rivers, rocks rolling down from nearby hills and so on. A strong sea swell developed, and small-scale tsunami-like effects were reported. The felt area extended to the Kola peninsula in the east and to Stockholm in the south.

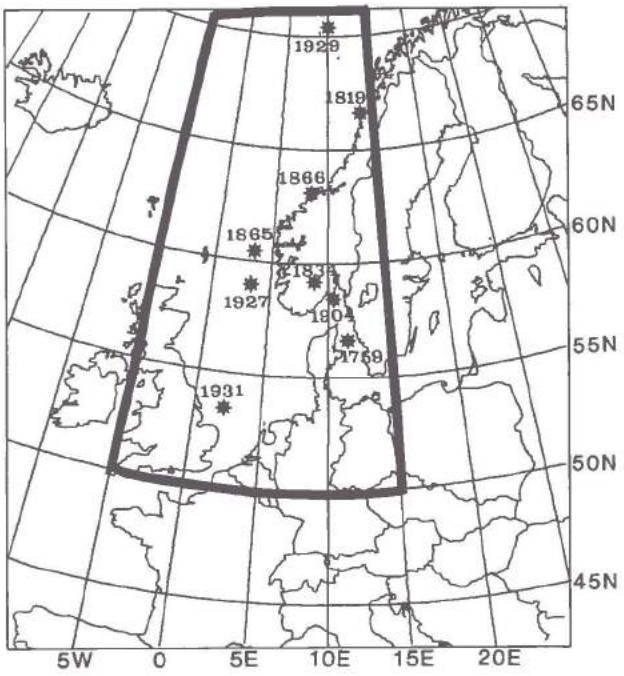

Fig. 5.5.
Map showing the estimated location of the largest known earthquakes in Norway and adjacent waters. All earthquakes shown have been felt over an area of radius at least 400 km.

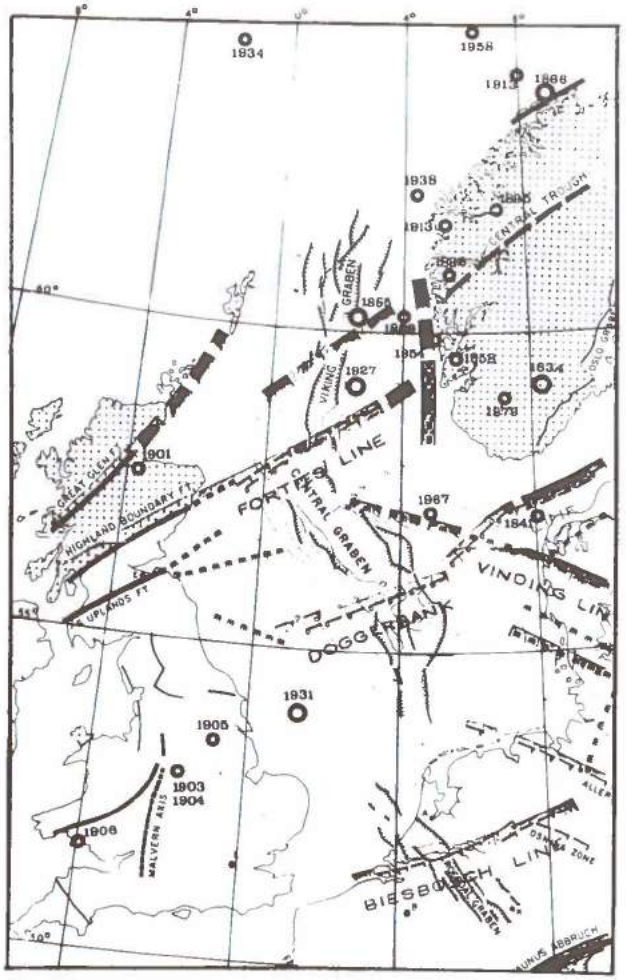

Fig. 5.6.
Map showing the estimated locations of known large earthquakes (magnitude M ≥ 5,0 or macroseismic radius R ≥ 250 km) in the North Sea and adjacent areas.

3 September 1834, 59.3°N, 8.5°E, M=5½, I_0 = VI, R = 400

This earthquake was felt over most of southern Norway, and also in Värmland (Kjellén, 1903). The maximum intensities were observed in inner Telemark.

7 May 1865, 60,5°N, 3°E, M=5½, I_0= VI, R= 400

The location of this earthquake is uncertain. It was felt from Kristiansund to Flekkefjord, but reports are available only from coastal sites. This indicates an offshore epicenter. We do not know whether this earthquake was felt at Shetland or in Scotland, and the proposed radius of perception is therefore also uncertain.

9 March1866,63.2°N, 9.0°E, M = 6.I_0 = VII, R = 400

This earthquake was felt from Bodø in the north to Langesund in the south; as far east as Søderhamn and as far west as the Shetland Islands, where the lighthouse is reported to have shaken violently. The strongest shaking is reported from Kristiansund and Trondheim, with some damage to chimneys and cracks in masonry. It is difficult to give a reliable epicenter for this earthquake; we have located it at the coastline near Kristiansund, but it is quite possible that the epicenter was in fact offshore, maybe as much as 50-100 km NW of Kristiansund. Apparent sea swells were reported near Molde, while ships anchored in Kristiansund and Trondheim were shaken as by a collision.

23 October 1904, 59.2°N, 10.5°E, M = 6.4(2), I_0 = VIII, R = 560

This earthquake, which had its epicenter in the outer Oslofjord (Fig. 5.8), is the largest one to have occurred in Fennoscandia in modern times, and consequently plays a major role in any seismic risk analysis for installations in southern Scandinavia. In the Oslofjord region, hundreds of chimneys collapsed, and tendencies to panic among the population were observed. The earthquake did not, however, result in casualties, and in only few instances were buildings severely damaged. The earthquake occurred along the Oslo Rift Zone, which is part of the fracture system in the North Sea.

The instrumental measurements are generally poor for this earthquake, and the magnitude value of M = 6.4 above is therefore uncertain. It appears that the true magnitude of this event should be somewhere in the range of 6.0- 6.5 and possibly slightly larger. The depth estimate of 55 km given by Karnik (1969) appears too high; a depth of 35 was estimated by Austegard (1975) based upon known macroseismic data.

24 January 1927, 59.0°N, 3.0°E, M = 5.1(10), I_0 = VI, R = 440

This is the best documented, large earthquake among those with an epicenter off the west coast of Norway. Nonetheless, its precise location is uncertain, as is of course the maximum intensity. The earthquake was felt with intensity V over most of the Norwegian west coast, and was given a magnitude M = 5.7 by Båth (1956) based upon macroseismic evidence. The instrumental magnitude of 5.1 appears too low in view of the great area over which the earthquake was felt, including most of Scotland, East England, the Shetland Islands and Norway

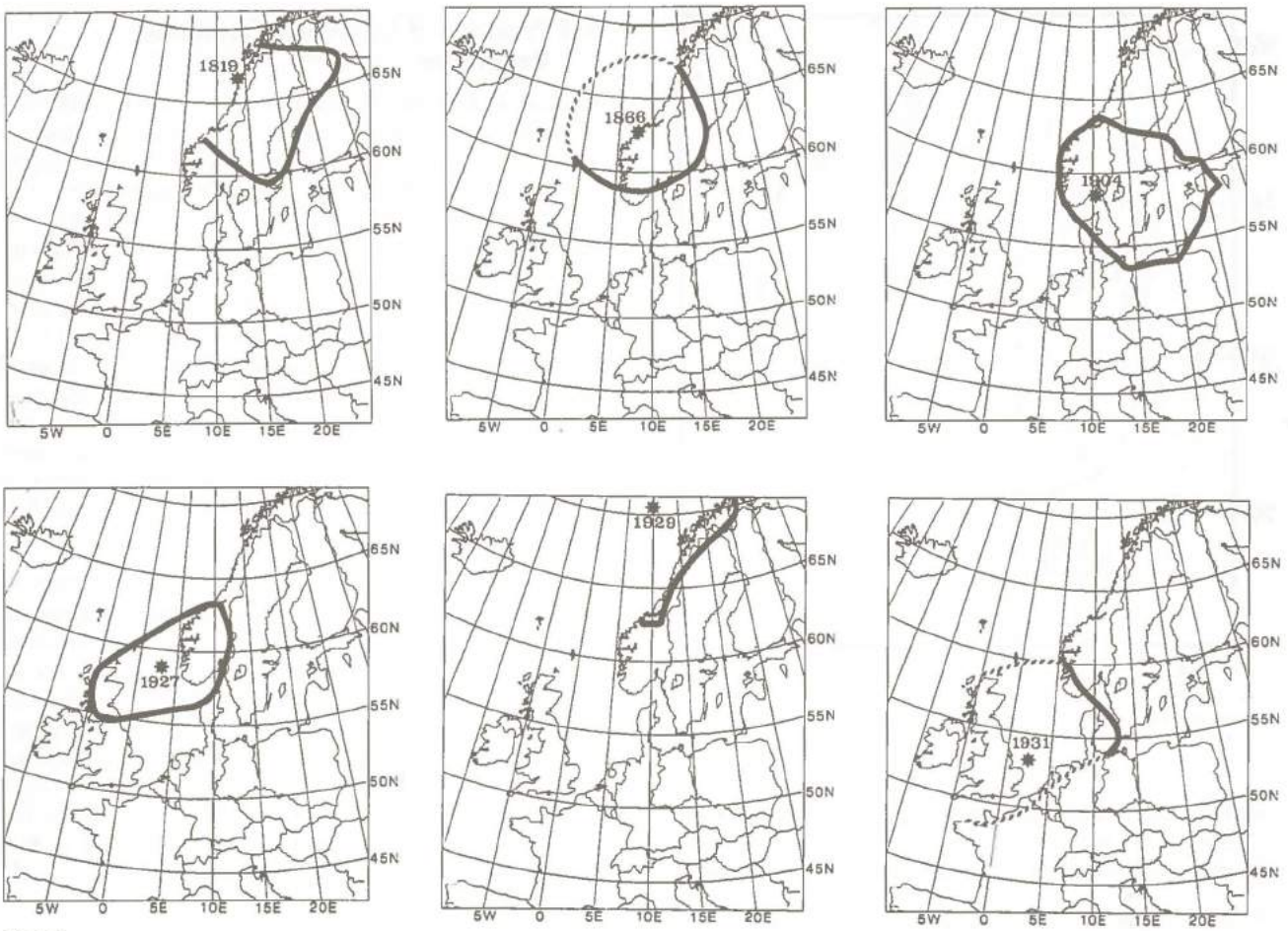

Fig. 5.7.
Estimated extent of the felt area for six large earthquakes.

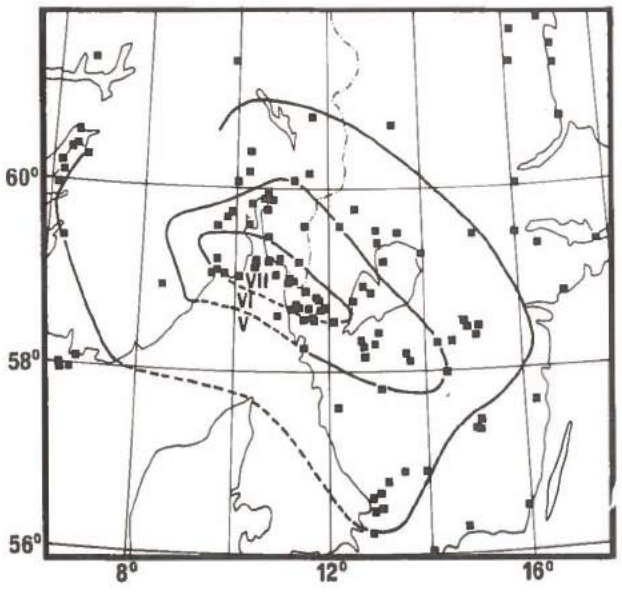

Fig. 5.8.
Isoseismals of the 1904 Oslofjord earthquake. "Aftershocks" of this event during the years 1904-1910 are also indicated. (After Austegard, 1975.)

south of Trondheim. It was also reported felt in the western part of Denmark, but not in Sweden. Associated with this earthquake were rumbling or roaring sounds of low pitch, and in some cases explosion-like bangs. The maximum intensity of 6 was reached in northeast Scotland, where ornaments and plaster were thrown down and cracks opened in conrete walls.

10 June 1929, 71.0°N, 10.0°E, M = 6.0(26), R = 600

This earthquake, with an epicenter in the Norwegian Sea, was felt over most of northern Norway. Unlike the other earthquakes discussed here, this event seems to have originated in a fairly active, concentrated seismic zone, from which a number of other earthquakes are also known.

7 June 1931, 54.0°N, 1.4°E, M = 6.0(27), (I_o = VIII), R = 600

This is the largest known earthquake in the North Sea, and had its epicenter in the Doggerbank area. From Fig. 5.6 it appears difficult to associate it to any particular surface fault structure; the uncertainty in the epicenter location should, however, be kept in mind. Karnik (1969) assigns a tentative depth of 70 km to this earthquake; this value must, however, also be considered highly uncertain and appears unreasonably deep. The Doggerbank earthquake was felt in Great Britain, Belgium, the Netherlands, northern France and Germany; in Norway its effects were mainly confined to the southwestern coast. The earthquake was in addition felt in Denmark, as far east as Copenhagen, according to Lehman (1956). (See Fig. 5.9.)

The earthquake damaged buildings in a coastal belt of Great Britain, some 30 km wide, extending between Scarborough and Grimsby; displaced boulders from Castle Hill, Scarborough; enlarged cracks in Lincoln Cathedral and changed the water levels of the four wells in the area, among many other effects. People in boats passing through the epicentral region at the time heard sounds of submarine origin which resembled muffled explosions

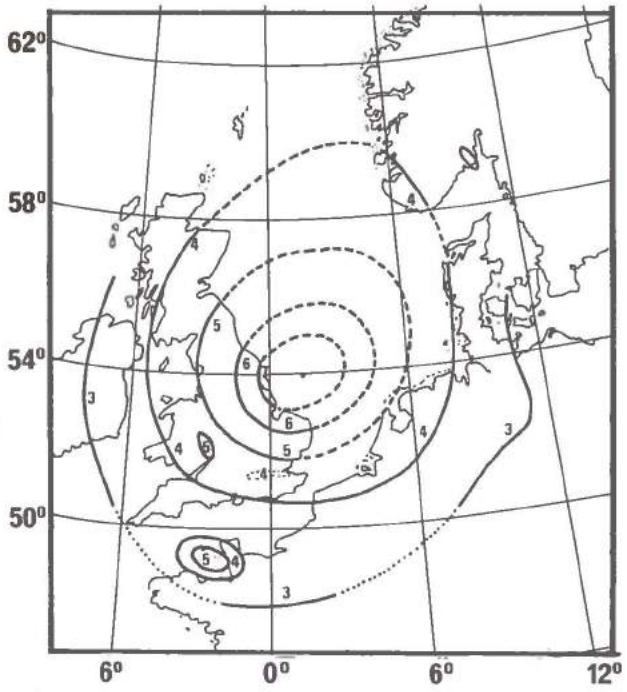

Fig. 5.9
Isoseismals of the North Sea earthquake of 7 June 1931. (After Versey, 1939)

and noticed a heavy, confused swell which developed in a calm sea but must have subsided relatively rapidly since no tsunamis were seen on the adjacent coasts of England.

In conclusion, the historical records of large earthquakes offshore indicate that such events have occurred over a wide geographical area. This is consistent with general intraplate tectonic considerations, and indicates that future, large earthquakes may occur even at locations where little indication of seismic activity presently exists. The largest of the earthquakes discussed here are of magnitude 6.0-6.5, but this does not imply that the maximum possible magnitude in the area in question would be so limited. In fact, historical records from comparable intraplate regions in other parts of the world show several examples of earthquakes which have exceeded M = 7.0 (northeast America (Stauder et al, 1976) and USSR (Prof. Keilis-Borok, Moscow, personal communication)). With the present knowledge, we therefore consider that seismic risk analysis for the Norwegian continental shelf must take into account the possibility of future occurrence of earthquakes in the magnitude range 7.0-7.5.

5.4 Precision of Estimated Earthquake Parameters

Obviously, macroseismic data are not suitable in the offshore-Norway area, as besides lack of seaward observations, there appears to be a distinct difference in macroseismic intensity decay rate, that is, attenuation in- creases significantly westward. This effect, which has not been studied in much detail in Fennoscandia, may also represent a source of bias in epicenter locations. Available instrumental data are neither well suited for precise locations due to relatively few station recordings and poor azimuthal coverage. For example, different seismological agencies have reported epicenter locations for the very same earthquake with separations exceeding 100 km! Instrumental data are significantly better than macroseismic for epicenter locations in coastal areas, which is clearly seen by a comparison between Fig. 5.3 and Fig. 5.4.

Problems involved in properly estimating earthquake intensity (macroseismic) or magnitude (instrumental) are similar to those involved for a proper epicenter location, i.e., a general lack of sufficient observational data. Furthermore, a useful, local magnitude scale has not been established for Fennoscandia. Precise focal depth estimates are difficult even where extensive observational data are available. All available evidence points towards foci locations within the crust and so-called normal faulting, but we again emphasize the need for more and better quality data in order to give reliable conclusions.

6. The Meløy, N. Norway, earthquake sequence 1978/79

6.1 The Earthquake Sequence

The Meløy earthquake sequence was a most remarkable seismological phenomenon which has given us a unique possibility for gaining insights into earthquake occurrence, mechanisms and source parameters for this area in particular, and for intraplate earthquake occurrence near passive continental margins in general. So far, the Meløy earthquakes have been discussed in five scientific papers (Bungum et al, 1979; Bungum and Husebye, 1979; Gabrielsen and Ramberg, 1979; Vaage, 1980; Bungum et al, 1982).

The first positively recorded earthquake out of what is now known as the Meløy sequence occurred on 3 November 1978 and was measured at ML (or local magnitude) = 2.4, using data from the NORSAR array which has an eipcentral distance of about 700 km. The first reports out of Meløy itself came a few days later, and during the week 12-19 November ground shakings were widely felt many times, particularly at night time. After 5 December, the activity decreased, having a minimum around 20 December, whereafter new outbursts of microtremors occurred on 27-28 December, 3-4, 8-10, and 18-20 January. A characteristic feature of the sequence is that the larger earthquakes (ML~3.0) are followed by microearthquake aftershocks lasting sometimes a few hours, sometimes a few days.

The authorities of the Meløy municipality asked NTNF/NORSAR on 16 November to monitor the area, and two days later the first seismographs were installed. Altogether 7 different sites were used (Fig. 6.1), and at any one time a maximum of 5 stations were in operation. During the first 10 weeks of instrumental coverage, more than 10,000 tremors were recorded, and the largest number of events recorded in one single day occurred on 2 December with 820 at Enga, 750 at Neverdal and 270 at Ørnes. Hypocenters were computed for 255 events evenly distributed in time throughout the recording period and on the basis of Pg-Sg time difference and also absolute Pg travel times when such were available. In Fig. 6.1, 66 events with at least 5 readings (phases), and RMS values less than 0.15 s are plotted. The epicenters are confined within an area of roughly 10 km N/S, 8 km E/W, with a concentration around 66.81°N, 13.63°E. The computed hypocenter depths for the 66 events in Fig. 6.1 are in the range 3-9 km, and the corresponding uncertainty is of the same order as for the epicentral coordinates, i.e., usually within ±1 km.

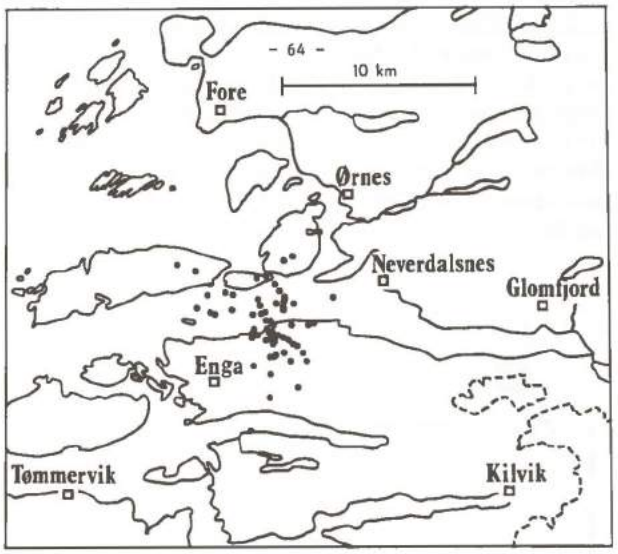

Fig. 6.1.
Map of the Meløy area with the seven locations used as sites for the three to five seismographs available. The three permanent sites are Ørnes, Neverdal and Enga. The black dots are computed epicenters for 66 earthquakes for which the depth range is 3-9 km. (From Bungum and Husebye, 1979)

Most of the events above ML = 2.0 were felt, and the maximum intensity on the Modified Mercalli scale was 6. Interestingly, very many earthquakes were heard and the reported sounds can be classified in three groups: (1) sounds without any felt tremor, (2) sounds associated with

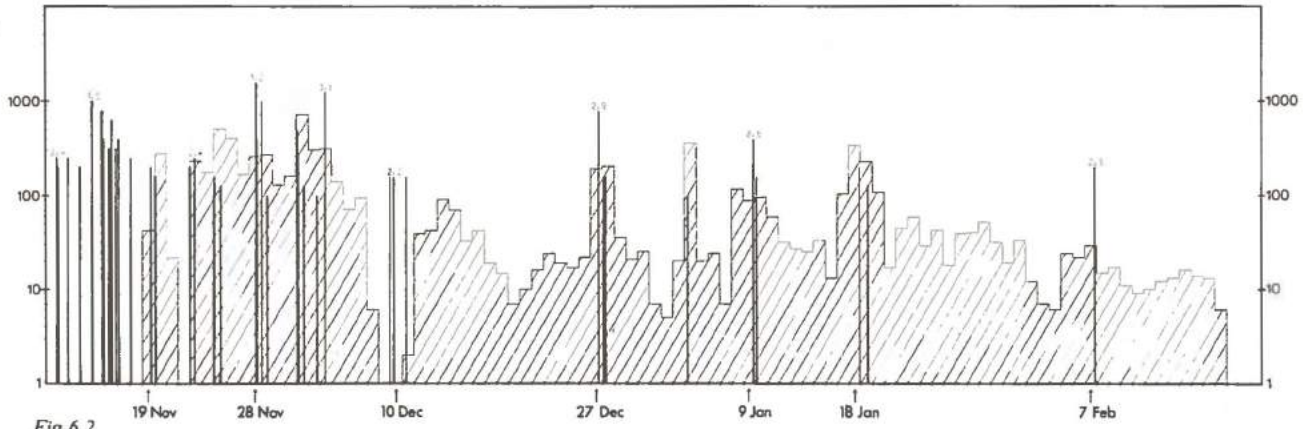

Fig 6.2
Time development of the Meløy earthquake sequence as recorded at the Neverdal station (see Fig. 6.1). The histogram shows number of events on a daily basis (non-operational gaps on 21-22 Nov, 8-11 Dec 78 and 2-3 Jan 1979). All events with an ML magnitude at 2.0 or above are plotted separately as vertical lines with height proportional to magnitude. For some of these larger earthquakes, magnitude is also given directly. (From Bungum and Husebye, 1979).

earthquakes felt, and (3) sounds generated in the epicentral area. The latter sounds (described as similar to when a load of snow slides off a roof) were quite different from group (2). The above information was partly derived from newspaper ads used as a substitute for conventional macroseismic questionnaires.

The time development of the sequence up to the middle of February 1979 is shown in Fig. 6.2, where we can see that the largest of the events had a magnitude (ML) of 3.2 and occurred more than two weeks after the onset of the sequence, while the frequency-magnitude distribution was quite normal (with b = 1.1). By the end of January 1979 the activity level had much decreased, and from March 1979 and throughout July 1980 (when the last seismograph was removed) only a few shocks were recorded, months apart. Even though the largest of these had a magnitude of more than 2.0, they appeared to be isolated events, in contrast to the typical shock clustering pattern when the activity was at its peak. Bungum et al (1982) have taken this as an indication of a development towards a more uniform and relaxed stress distribution in the Meløy area, which is part of a relatively active seismic zone after Fennoscandian standards (Husebye et al, 1978; Bungum and Fyen, 1979).

6.2 Focal mechanisms, tectonic implications

The seismic recordings at Meløy were obtained at hypocentral distances of only a few kilometers, resulting in some very good records even for low- magnitude events. Fig. 6.3 shows some examples here, obtained from three-component seismometers with analog tape recording and a flat velocity response in the 5-80 Hz frequency range (Vaage, 1980).

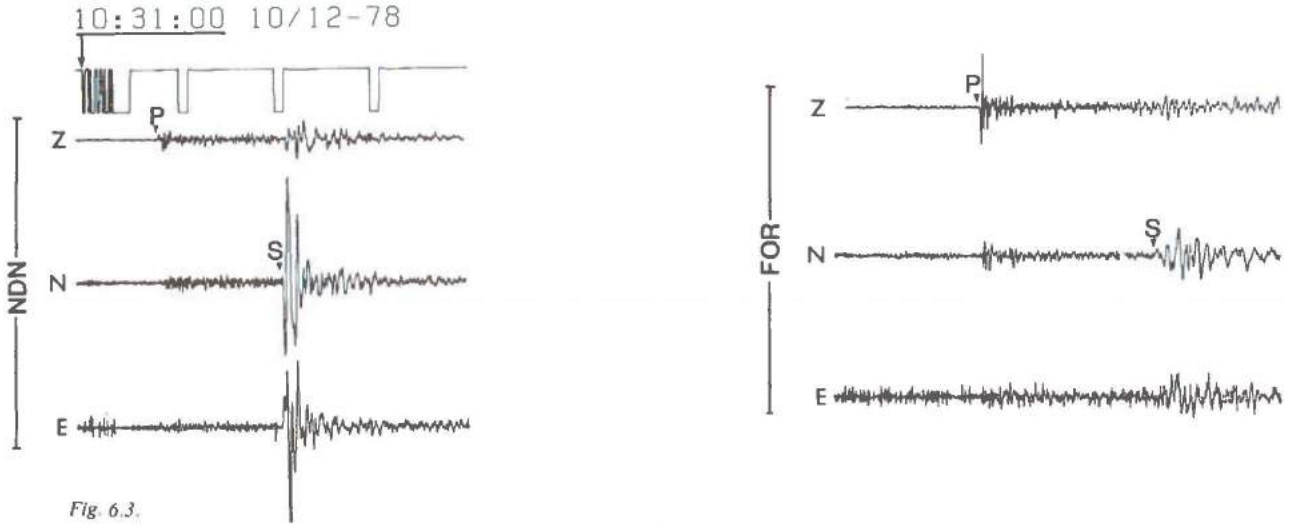

Fig. 6.3.

Examples of three-component recordings from NDN (Neverdal) and FOR (Fore) along with the timing signal as received from radio. Z = vertical component, N = north-south horizontal and E = east-west horizontal components. Time interval between each pulse is 1 sec. (From Vaage, 1980)

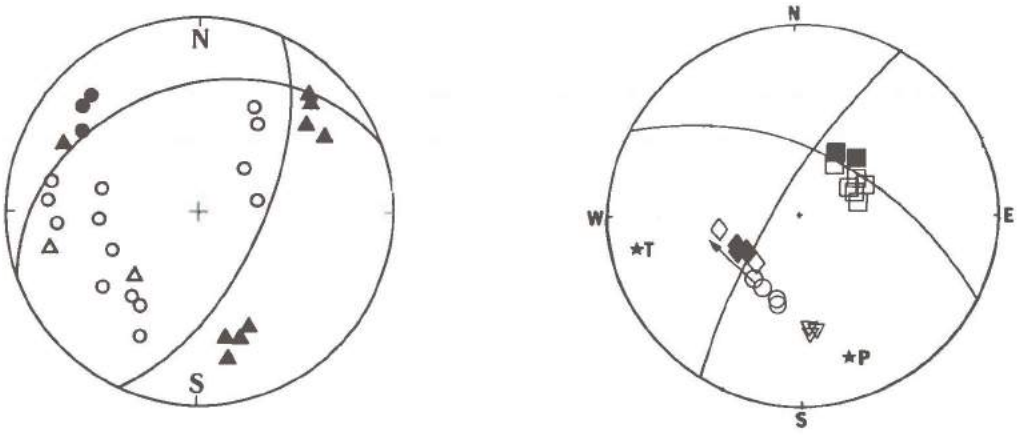

Fig 6.4

Composite focal mechanism solutions for the Meløy earthquakes as taken from Bungum et al (1979) (left) and Vaage (1980) (right). The data are plotted in a lower hemisphere stereographic projection, with open symbols indicating dilations and solid symbols compressions.

Based on first-motion directions from local recordings, two different composite focal mechanism solutions have been published for the Meløy earthquakes, as shown in Fig. 6.4. The first one is a near normal dip-slip solution, derived from analog paper recordings (Bungum et al, 1979), and the other is a strike- slip solution with a normal dip-slip component, derived from data as presented in Fig. 6.3 (Vaage, 1980). None of the solutions are well-constrained due to lack of station coverage and moreover, the two solutions are obtained from completely different data bases and can therefore reflect genuine differences both in time and space. Vaage (1980) has discussed the differences between the solutions in greater details, and he finds arguments in favor of both of them. We therefore have to accept that a single focal mechanism that satisfies all of the recorded data are not tenable, although it seems as if a normal dip-slip component is present for most of the events. In fact, a variation like the one observed is to be expected as an effect of variations in the local geological conditions (Bungum and Fyen, 1979), and especially since no earthquake larger than ML 2.5 was included in any of two published mechanisms.

An essential problem is how to fit the Meløy earthquakes into the tectonic framework of the area. A tectonic analysis based on Landsat lineament mapping has been done by Gabrielsen and Ramberg (1979), who found lineaments in two main directions, one parallel to the fjords (N80-85^{o}E) and another striking NNE (N20-35^{o}E). Both of the solutions presented in Fig. 6.4 have one plane striking in the latter of these directions, which moreover shows the best fit to the lineation of epicenters as found by Bungum et al (1979). This strike direction is coincident with the Caledonian folding axis, with the sedimentary basin axes, and also with the Pärve fault, which is a spectacular 200 km neotectonic feature in Swedish Lappland (Lundquist and Lagerbäck, 1976). From the seismicity maps for Fennoscandia presented in Section 5, it is seen that Meløy is located in the middle of a distinct seismicity zone along the coastal area between 65^{o}-70^{o}N. One of the largest known earthquakes in Fennoscandia occurred here in 1819, the so-called Lurøy earthquake, with a presumed location about 50 km SW of Meløy and an estimated magnitude of the order of 6.0-6.5 on the Richter scale. Further to the west of the Meløy area (and southwest of the Lofoten islands) there is another seismicity zone which coincides with the passive continental margin (Talwani and Eldholm, 1972, 1977). The seas between these two seismicity zones are part of an epicontinental basin with maximum sedimentary thicknesses of the order of 8-9 km, where profiling surveys have given clear evidence of block faulting (Rønnevik and Navrestad, 1977). The early Eocene uplift of western Fennoscandia, contemporaneous with the Norwegian Sea opening, amounted to a maximum of 2 km.

It is doubtful from the available evidence that any simple tectonic interpretation can be given for the Meløy earthquakes. With the scatter in focal mechanisms taken into consideration, one cannot rule out a causal connection to the on-going glacial rebound, even though other factors seem to indicate that this is at most a contributing factor (Husebye et al, 1978; Bungum and Fyen, 1979). Other events of possible significance are the Eocene uplift and the offcoast sedimentary block tectonics, and we do consider it likely that some connection exists between the Meløy seismicity and the off-coast sedimentary basins, where a more specific explanation has been offered by Bungum et al (1979). It should also be kept in mind that the regional stress field in the area necessairly must receive some contribution from the on-going tectonic movements connected to the spreading of the American and Eurasian plates.

Whatever the stress generating mechanisms might be, we conclude that the Meløy earthquake sequence is a realization of the interaction between a regional stress field and local zone(s) of weakness, both with several possibly contributing factors. The fact that the seismicity zone was so spatially concentrated indicates that the latter factor may have been decisive for where it occurred, while the former factor determines the level of energy release.

6.3 Frequency characteristics, source spectra

During the peak of the Meløy earthquake activity, tape recorded data such as those displayed in Fig. 6.3 were collected for two time intervals: 6-13 December 1978 and 22-25 January 1979. These data were subsequently digitized with a 500 Hz sampling rate, and a total of 40 events with magnitudes up to 2.2 were selected, providing us with a rare possibility for analysis of frequency characteristics and source parameters (Bungum et al, 1982).

The S wave amplitude spectrum for one of the larger events in the sequence is given in Fig. 6.5. The event is almost identical to the one displayed in Fig. 6.3, and the strong SH waves and the weak P waves are typical for all the events analyzed. There are also frequent changes in the P wave polarity, which is taken to indicate that the station (NEV) is located close to a nodal plane for these events, and consequently in an area of strong S-wave radiation. We see from Fig. 6.5 that the SH waves have an energy peak at frequencies around 20 Hz, with some difference between the horizontal components.

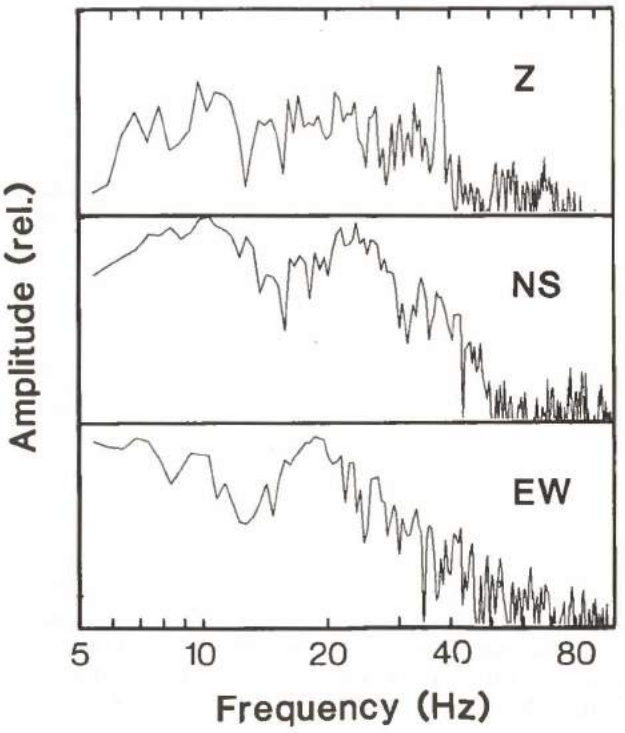

Fig. 6.5.
S wave displacement spectra for an event with ML = 1.4. The scaling is identical for the three traces, and logarithmic in amplitude. The hypocentral distance is about 10 km. (From Bungum et al, 1982)

The spectra displayed in Fig. 6.5 reflect only the frequency characteristics in the recorded data, which includes

the effect of the travel path, in particular the frequency-dependent attenuation. For the same event, such spectra will therefore be dependent on where the observation is made, and in particular on the hypocentral distance. These factors are removed in computing the source-displacement spectrum, which is displayed in Fig. 6.6 for a

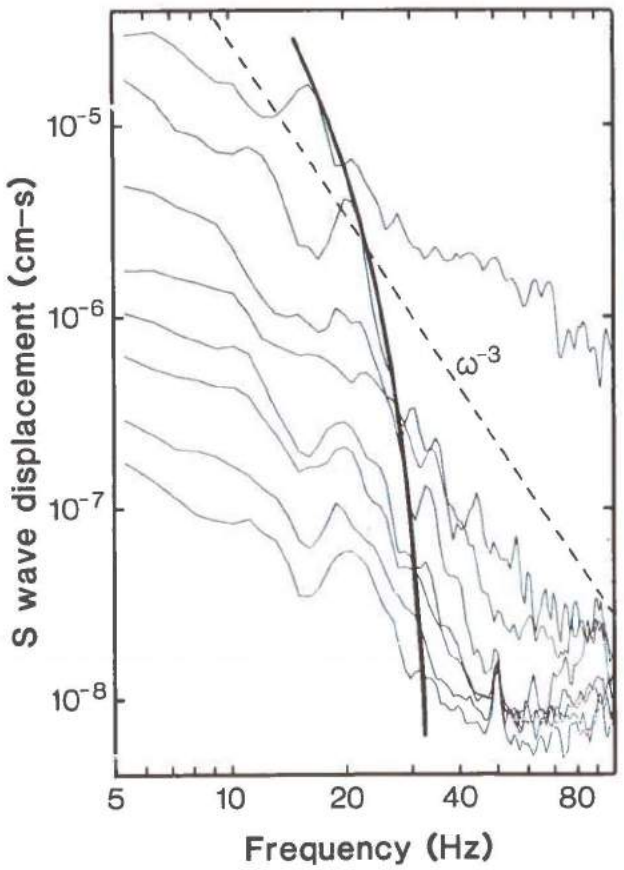

Fig. 6.6.
Path-corrected S wave displacement spectra for the 40 events, normalized to an observational distance of 10 km. Each curve, except for the uppermost one, represents the average of the spectra from several events (five in average), and the spectra were computed from data with a 500 Hz sampling rate. (From Bungum et al, 1982)

larger number of analyzed events (cf. Bungum et al, 1982). As for most source- displacement spectra, the curves are approximately flat up to the so-called corner frequency, above which they fall off at a certain rate, where a ω^{-3} curve is indicated in Fig. 6.6. It should be noted here that the large contributions for low frequencies are particular for the displacement curve, while in velocity and especially acceleration the curves will peak at higher frequencies.

6.4 Seismic Moments/Source Parameters

The seismic moment M_o is the low frequency value of the source-displacement spectrum, i.e.,

$$M_o = \text{limit}_{\omega \to o} M_\omega = 4\pi\rho R\beta^3 C R_s^{-1} \Omega_\omega(s)$$

where ρ = density, R = hypocentral distance, β = S wave velocity, C = free surface effect, R_s = radiation pattern coefficient and Ω_ω = S wave displacement spectrum. Using this formula, Bungum et al (1982) have computed seismic moments for some of the Meløy earthquakes, finding a relationship with magnitude as displayed in Fig. 6.7. Although the largest ML value in the sequence was 3.2, no earthquake above ML = 2.0 was recorded by the instruments used for the M_o computations.

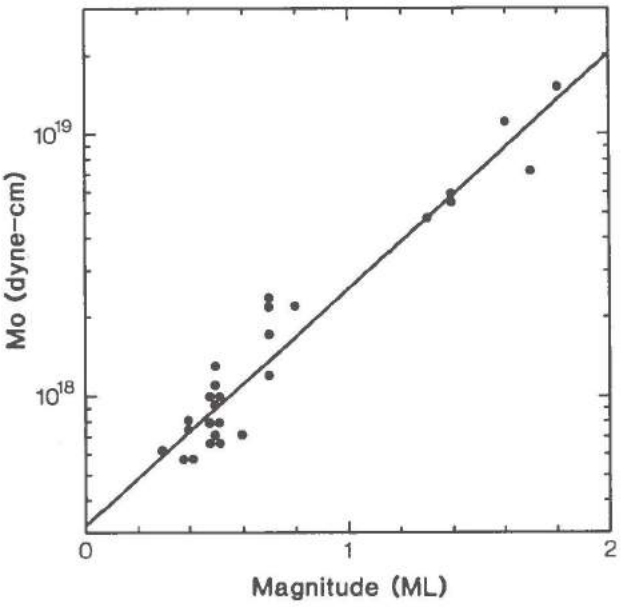

Fig. 6.7.
Seismic moment (M_o) versus local magnitude (M_L) for some of the Meløy earthquakes. (From Bungum et al, 1982)

Using the corner frequencies as obtained from Fig. 6.6, it is possible to compute various static source parameters and to look at their scaling with respect to seismic moment. Assuming a circular source model (Brune, 1970), the expressons for source radius (r), stress drop ($\Delta\sigma$)and average displacement across the fault will then be:

$$M = (7/16\pi)^{\frac{1}{2}} \beta f_o^{-1}$$

$$\Delta\sigma = (7/16) M_o \, r^{-3}$$

$$\bar{u} = (1/\pi\mu) M_o r \, -2$$

where f_o is corner frequency and μ is the shear modulus.

The results for the Meløy earthquakes are shown in Fig. 6.8, where also a rectangular model has been used for

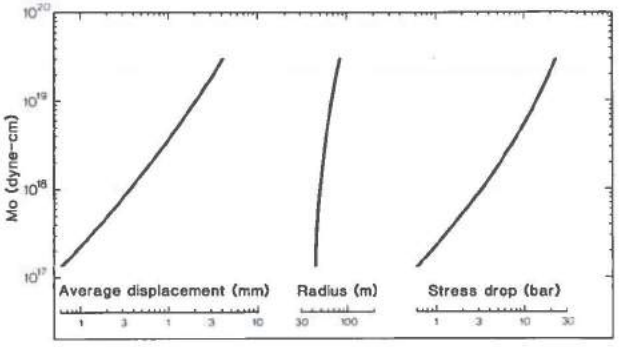

Fig. 6.8.
Relationship between seismic moment and average displacement, source size (radius and length) and stress drop, respectively, for a circular source model. The plot covers the moment range over which these parameters have been computed for the Meløy earthquakes. (From Bungum et al, 1982)

comparison. The differences are relatively small between the two models, the circular model giving displacements from 0.06 to 4.4 mm, source radii from 44 to 81 m, and stress drops from 0.6 to 25 bars. The most interesting feature is the strong dependency of stress drop with seismic moment, which is an effect of the slow increase of the corner frequencies with decreasing moment. It should be noted that our stress drop values of between 1 and 25 bars (41 for a rectangular model) cover much of the range over which stress drops normally are observed.

Outstanding features with the results presented in Figs. 6.7-6.8 are high signal and corner frequencies, small seismic moments and fault dimensions, and a rapid decrease in stress drop for moments below 10^{20} dyne-cm. This decrease in stress drop with decreasing seismic moment for small earthquakes, with a resulting approximate constancy of the source dimension, has been reported many times and from many areas. For larger earthquakes, on the other side, it is common to observe a falloff of the corner frequency curve proportional to ω^{-3} (cf. Fig. 6.6), resulting in a constant stress for all seismic moments.

The physical mechanism behind the decrease in stress drop with decreasing moment for small earthquakes remains unclear. Bungum et al (1982) discuss various explanations which have been suggested, and find that even though the Meløy data do not give particular clues as to the validity of these explanations, there is a point of possible significance in the nature of the earthquake sequence itself. This is tied to the fact that, as the main sequence developed and the average activity level decreased, the aftershock sequences following each of the larger events (up to ML = 3.2) decreased in size and finally disappeared altogether. This could be an indication that the source area originally did not contain a well-developed fault, but that a fault gradually came into being as the sequence progressed. This in turn could make it possible for single "large" earthquakes to occur at a later stage. If so, an explanation of the type forwarded by Johnson and McEvilly (1974), who suggested that corner frequencies for some reason do not reflect source dimensions as predicted by the theory, or alternatively that corner frequency is due to the rise time of the source function, would be more compatible with our data, since other explanations mostly involve preexisting faults. This possibility is moreover supported by ones intuitive problems in accepting that source dimension constancy can prevail over a moment range as large as our results seem to indicate.

7. Detectability of seismic events offshore Norway

7.1 Introductory remarks

The observed earthquake activity in the past forms the basis for any seismic risk study. A major problem in this regard is that adequate instrumental coverage only has been available for a very short time (in the case of Fennoscandia 20-30 years), while large earthquakes in intraplate regions generally have a return period that is much longer (often several hundred years or more). Furthermore, even for the time period with instrumental coverage, far from all significant seismic activity is actually detected, due to geographical factors. This problem is particularly severe for offshore areas, both because of the large distances to the nearest seismograph stations and since macroseismic evidence to complement instrumental observations is generally lacking. Offshore Norway, this implies that even recent seismicity maps such as that presented in Fig. 5.4 tend to give a biased picture of the relative seismic activity between areas close to shore and far offshore. As concluded in Section 5, there is reason to assume that the earthquake activity at some distance off the coast is larger than indicated in this and other available seismicity maps.

In order to assess quantitatively the effect of an inhomogeneous distribution of seismic stations, it is necessary to establish a model describing the detection capability of the station network for the area under consideration. NORSAR has therefore undertaken such a detection study for the area offshore Norway. The study is based on the station network shown in Fig. 7.1. This network is representative of those stations which have been available throughout the past 10-30 years, and in fact our seismicity maps for this period (Section 5) have mostly been based on information from this network.

After establishing a detectability map in this section, we will use the results later (in Section 10) to obtain estimates of the seismicity levels for various areas offshore Norway. These estimates will be determined from observed earthquake activity above a specified magnitude limit, where this limit is chosen in such a way that we can reasonably assume that the majority of earthquakes above the limit have been detected. In this way, we will obtain relative seismicity estimates that are not biased by detectability differences.

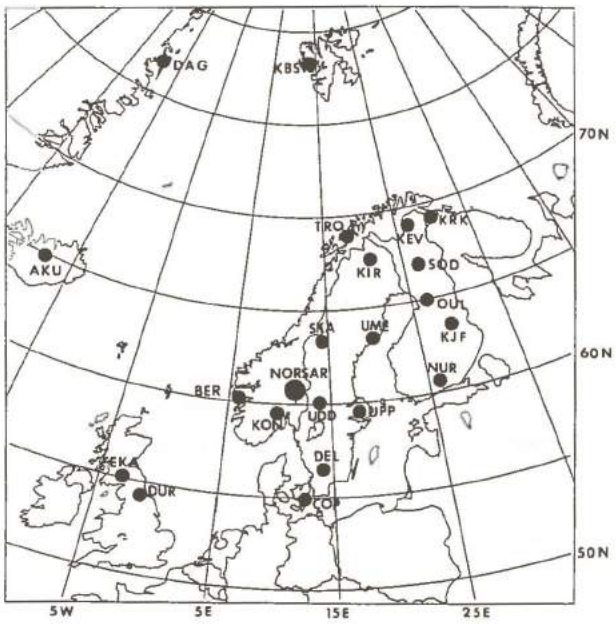

Fig 7.1
The seismograhp network used for estimating earthquake detectability offshore Norway. The full station names are: AKU - Akureyri, BER - Bergen, COP - Copenhagen, DAG - Danmarkshavn, DEL - Delary, DUR - Durham, EKA - Eskdalemuir array, KBS - Kings Bay, KEV - Kevo, KIR - Kiruna, KJF - Kajaani, KON - Kongsberg, KRK - Kirkenes, NORSAR - Norwegian Seismic Array, NUR - Jurmijärvi, OUL - Oulu, SKA - Skalstugan, SOD - Sodankyl, TRO - Tromsø, UDD - Uddeholm, UME - Umeå, UPP - Uppsala.

7.2 Development of a detectability map offshore Norway

The detectability of each individual station in a given network depends on the ambient noise level, local wave propagation effects and operational efficiency. To give an illustrative effect of the detection capability of four Fennoscandian stations we refer to Fig. 7.2, where the number of detected events out of a fixed data base is displayed together with the maximum likelihood detectability curve as described by Ringdal (1975). It should be noted that the figure refers to *teleseismic* detection capabilities in contrast to *regional* events which are the topic of our study. However, the principles are similar for detection of regional earthquakes, and the large variation in individual station detection capabilities shown in the figure would remain also for regional events.

The procedure is now to develop a model for the detection capability of a network of stations, given the capabilities of each individual station. Such a method was developed some years ago in connection with the problems of monitoring a nuclear test-ban treaty (Wirth, 1970), and we have adapted the associated computer program for the present purpose.

Data input to the program is the given station parameters and a set of epicenter locations. The computer output is the detection threshold as computed for the network. Optional output is also location confidence regions for all or certain subsets of stations.

Given a set of stations, assumed noise conditions and magnitude corrections, the program will determine "threshold magnitude" at which the probability of at least a specified number α of stations detecting is greater than a specified threshold for each of the specified sets of epicenters. In this case we have set $\alpha = 3$ since three stations is the minimum number of stations required to locate the epicenter of the event. The computer programs that evaluate the model are based on magnitude, in our case local magnitude. In Table 7.1 the most fundamental equations in the analysis with additional explanation of symbols is listed. Given an event j of magnitude m_j and

$$\log_{10} A_{ij} = m_j + b_\Delta + c_\Delta \log_{10} \Delta_{ij} + E_{ij} \qquad (1)$$

$$\hat{p}_{ij} = \phi \left[\frac{\log_{10} A_{ij} - (\mu_n + \log_{10} SDT)}{(\sigma_n^2 + \sigma_s^2)^{\frac{1}{2}}} \right] \qquad (2)$$

$$\phi(x) = \frac{1}{2\pi} \int_{-\infty}^{\infty} e^{-y\ 2/2}\, dy \qquad (3)$$

$$\hat{p}(\geq\alpha) = \sum_{k=\alpha}^{N} \hat{p}_j(k) \qquad (4)$$

Symbols above are defined as follows:

A_{ij}	-	signal amplitude at station i for event j
m_j	-	magnitude of event j
b_Δ, c_Δ	-	standard table entries
E_{ij}	-	station-epicenter bias corrections
μ_n	-	mean $\log_{10}$ noise amplitude
σ_n^2	-	variance of $\log_{10}$ noise
σ_s^2	-	variance of $\log_{10}$ signal
$\phi(x)$	-	normal cumulative probability function
N	-	number of stations in the network
$\hat{p}_j(k)$	-	probability that k stations will detect event j
$\hat{p}_j(\geq\alpha)$	-	probability that α or more station will detect event j
SDT	-	station detection threshold, i.e., signal-to-noise ratio required for detection at station
Δ_{ij}	-	epicentral distance from station i to event j
p_{ij}	-	probability that station i will detect event j

Table 7.1.
Basic equations and definitions used in the detection estimation.

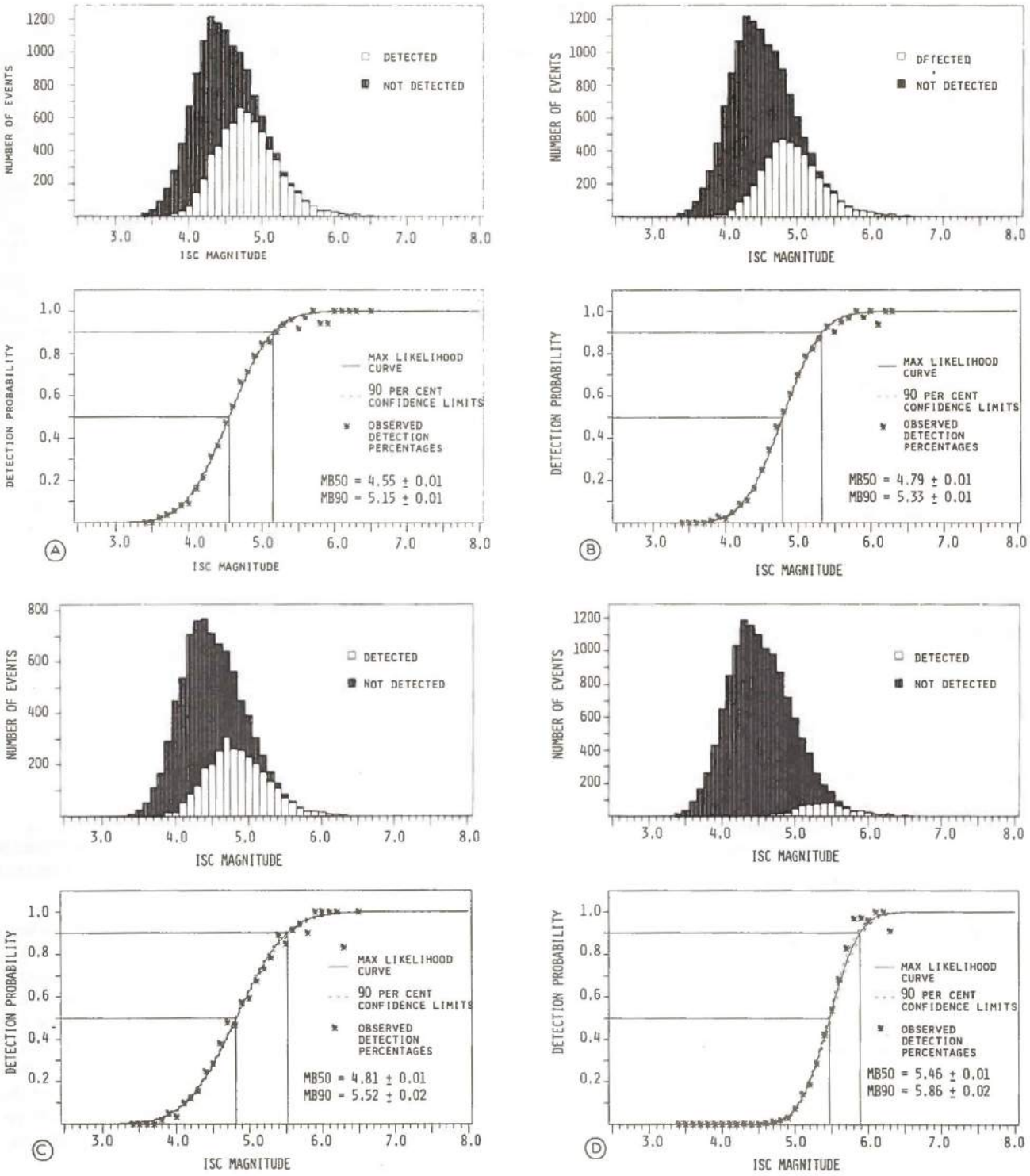

Fig. 7.2
Detection statistics for region 14 (30-90°). The upper half *is a histogram showing the reference event set and the number of events actually detected for each magnitude. The* lower half *shows the maximum likelihood detectability curve and its confidence limits. The actual percentage of detected events at each magnitude is also shown.*

A. For station NUR (Nurmijärvi, Finland)
B. For station UPP (Uppsala, Sweden)
C. For station xxx (Lillehammer, Norway)
D. For station COP (Copenhagen, Denmark)

STATION TABLE

I	IDENT	LAT.	LONG.	AMPL	NOISE SD	S/N RATIO	S-P MAG COR	SD TIME	RELIABILITY
1	NAO	60.80	10.80	2.00	0.20	2.00	0.0	2.83	0.90000
2	BER	60.40	5.30	30.00	0.20	2.00	0.0	2.83	0.90000
3	UPP	59.90	17.60	10.00	0.20	2.00	0.0	2.83	0.90000
4	KIR	67.80	20.40	8.00	0.20	2.00	0.0	2.83	0.90000
5	COP	55.70	12.40	30.00	0.20	2.00	0.0	2.83	0.90000
6	KON	59.60	9.60	25.00	0.20	2.00	0.0	2.83	0.90000
7	TRO	69.60	18.90	20.00	0.20	2.00	0.0	2.83	0.90000
8	UME	63.80	20.20	8.00	0.20	2.00	0.0	2.83	0.90000
9	KEV	69.70	27.00	8.00	0.20	2.00	0.0	2.83	0.90000
10	KBS	78.90	11.90	30.00	0.20	2.00	0.0	2.83	0.90000
11	NUR	60.50	24.60	6.00	0.20	2.00	0.0	2.83	0.90000
12	KJF	64.20	27.70	4.00	0.20	2.00	0.0	2.83	0.90000
13	KRK	69.50	30.00	30.00	0.20	2.00	0.0	2.83	0.90000
14	SKA	63.60	12.30	15.00	0.20	2.00	0.0	2.83	0.90000
15	DEL	56.50	13.90	15.00	0.20	2.00	0.0	2.83	0.90000
16	SOD	67.40	26.60	10.00	0.20	2.00	0.0	2.83	0.90000
17	OUL	65.10	25.90	10.00	0.20	2.00	0.0	2.83	0.90000
18	AKU	65.40	-18.60	50.00	0.20	2.00	0.0	2.83	0.90000
19	DAG	76.50	-18.50	12.00	0.20	2.00	0.0	2.83	0.90000
20	DUR	54.50	-1.40	50.00	0.20	2.00	0.0	2.83	0.90000
21	EKA	50.20	-3.90	12.00	0.20	2.00	0.0	2.83	0.90000
22	UDD	60.80	13.40	8.00	0.20	2.00	0.0	2.83	0.90000

Table 7.2
Station parameters for the detectability study offshore Norway. Station names, latitude and longitude are given together with assumed mean noise amplitude (0-peak amplitude in nm at 1 Hz), noise standard deviation, signal-to-noise ratios required for detection, magnitude correction factor, timing accuracy and assumed reliability (the value of 0.9 means 90 % uptime at the station).

distance Δ_{ij} from station i, the amplitude at that station is calculated as

$$\log_{10} A_{ij} = m_j + b_\Delta + c_\Delta \log_{10}(\Delta_{ij}) + E_{ij}$$

A_{ij} is the expected magnitude at station i for an event j at a given distance Δ_{ij} and magnitude m_j. Freedman (1967) showed that the amplitude distribution of body wave recordings closely approximated a log-normal distribution.

The amplitude-distance relationships used in this study are taken from Ringdal and Fyen (1979), and are specified below:

Deg	b_Δ	c_Δ
1.0	-1.4	0.0
2.0	-1.7	0.0
3.0	-2.0	0.0
4.0	-2.3	0.0
5.0	-2.6	0.0
10.0	-3.1	0.0
15.0	-3.3	0.0
25.0	-3.3	0.0
30.0	-3.5	0.0
85.0	-3.8	0.0
100.0	-4.5	0.0

E_{ij} allows for the inclusion of station-epicenter bias corrections; however, in the present study this correction was set to zero in all cases.

A station is assumed to detect provided that the ratio of signal-to-noise amplitude is greater than SDT (Station Detection Threshold). Signal and noise are assumed log-normally distributed. If the log of the noise amplitude has expectation μ_n and variance σ^2_n, and the log of the signal amplitude has expectation log A_{ij} and variance σ^2_s, then the probability that station i will detect event j is given

$$P_{ij} = \phi\left[\frac{\log A_{ij} - (\mu_n + \log_{10} SDT)}{(\sigma^2_n + \sigma^2_s)^{\frac{1}{2}}}\right]$$

where ϕ is the cumulative normal distribution, μ_n is the mean of the $\log_{10}$ zero-to-peak noise measurements at a given station in the frequency band of the expected signal.

The noise values are in fact the most important parameters bearing on the results of any network capability study. σ^2_s is the variance of the $\log_{10}$ signal amplitude. A signal standard deviation of 0.2 magnitude units was used in all the following analyses. The number of stations, N, was set to 22 in this study. SDT is the estimate of the signal-to-noise ratio required at a station the network to declare or recognize a detection. Given that the input parameters to the network estimation procedure remain the same, the change in the network threshold magnitude (δm_b) from SDT_1 to SDT_2 is $\delta m_b = \log_{10}(SDT_2/SDT_1)$.

Given N independent events with probability p_i, the probability of at least α of the events is

$$P(>\alpha) = \sum_{k=\alpha}^{N} p(k)$$

where

$$p(k) = E_k(p) - \binom{k+1}{k} E_{k+1}(p) + \ldots + \binom{N}{k} E_N(p)$$

is the probability of exactly k events, and

$$E_1(p) = \sum_{i=1}^{N} p_i;\quad E_2(p) = \sum_{i>j}^{N} p_i p_j;\quad E_3(p) = \sum_{i>j>k}^{N} p_i p_j p_k; \text{etc.}$$

A desired network detection probability based on detections at α stations is specified and $\hat{P}_j \geq \alpha$ is computed at each geographic node (j) for a low starting m_b which is incremented to higher values until the network threshold is met or exceeded.

Whenever, at a given node and a given m_b, $\hat{P}_j \geq \alpha$ is equal to or greater than the desired network detection probability, that m_b is assigned to that geographic node as the lower network detection capabilities.

The results of this method are contoured maps of m_b which give the network threshold magnitude for the specified probability, $P_j(\geq \alpha)$ based on detections at α or more stations (in our case α was set to 3).

The model described above has been applied to the network shown in Fig. 7.1. Parameter values used are listed in Table 7.2. The results have been used to develop a contour map of 50% detection thresholds offshore Norway as shown in Fig. 7.3. We see that the threshold varies from magnitude 3.0 in central Sweden to 4.0 on the outer Norwegian continental shelf. This is in good agreement with our observations from Section 5 (Fig. 5.4) regarding the observed seismicity in Fennoscandia.

It is clear that Fig. 7.1 would refer to detection capabilities only for the most recent time period (the past 10-30 years). Even so, the available stations have not been the same throughout this period, and we must therefore be somewhat cautious in our use of the results. In the risk studies in Section 10 we shall assume, based on our results here, that earthquakes above magnitude 4 on the Norwegian continental shelf have generally been detected in the period since 1950. We note here that other phases than P, in particular the Lg phase, often aid in detecting local and regional earthquakes, even though we have not incorporated these other phases in the present detectability study.

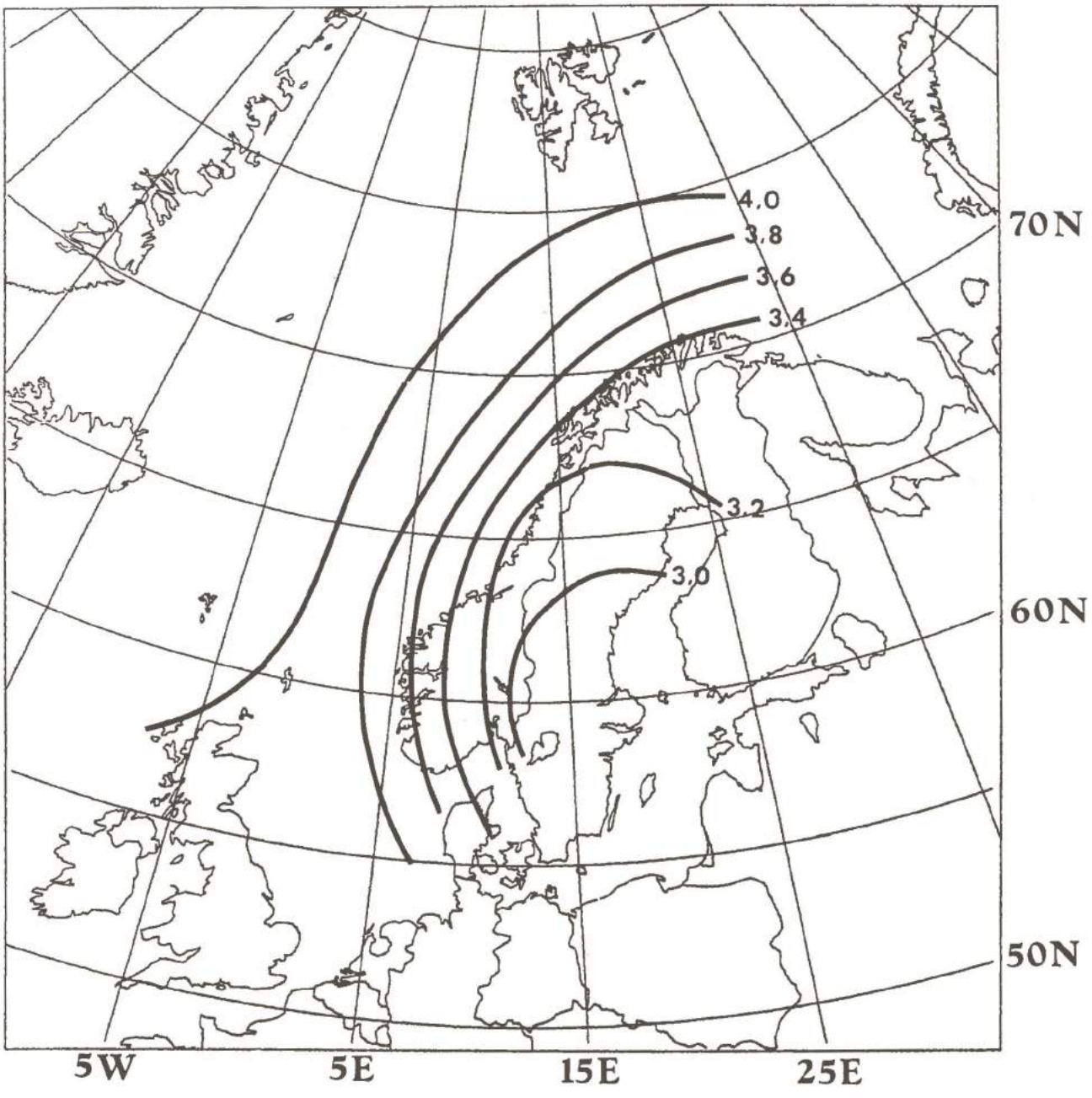

Fig. 7.3.
Estimated earthquake detectability offshore Norway based on the station network of Fig. 7.1. The contours correspond to a 50 per cent probability for P wave detection at at least 3 stations, using the attenuation relationship of Ringdal and Fyen (1979). The numbers on the contours are in terms of "local magnitude" (M_L).

8. Strong-motion attenuation

Proper knowledge and understanding of seismic wave attenuation is very important for a reliable assessment of seismic risk. The attenuation is governed by numerous factors as geometrical spreading, anelasticity, dispersion, interference (both constructive and destructive) of reflected and refracted waves, scattering, soil amplification and source radiation. The available amplitude data normally exhibit a large scatter and do not easily lend themselves to excessive statistical analysis of the relative importance of these factors. Hence, the attenuation model adopted should be of a simple kind. Indeed, it is customary to fit close-in amplitude data A by the empirical relation

$$A = A_0 R^{-N} \qquad (8.1)$$

where R is hypocentral distance and A_0 is a constant. Obviously, this relation does not incorporate specific attenuation mechanisms.

A similar approach commonly used in seismology is the derivation of a local magnitude relation m_b:

$$m_b = a + \log (A/T) + b \log \Delta \qquad (8.2)$$

where A is amplitude, T period and Δ epicentral distance in degrees. The derivation of a relation like (8.2) involves scaling among different events. But for a given period T, b in (8.2) corresponds exactly to - N in (8.1)

8.1 World-wide attenuation relationships

For a world-wide acceleration decay a value of 2.0 for-N in (8.1) has been considered appropriate (Trifunac and Brady, 1976). More recent investigations in stable shield areas tend to yield lower values for N, indicating that N = 2.0 might be typical only for tectonically active regions like California, Japan and Southern Europe.

Hasegawa et al (1981) have derived attenuation relations for Canada. For use in western Canada they propose N = 1.5 and N = 1.3 for acceleration and velocity, respectively. For eastern Canada, they find even smaller values for N, namely, 1.1 and 1.0, respectively.

Nuttli (1973) has derived a magnitude relation for earthquakes in the central United States and with propagation paths essentially in the whole area of North American east of the Rocky Mountains. His study is based on observations of the 1 sec period Lg waves. In the distance range 55-440 km he derives values 3.75 and 0.90 for the a and b parameters in (8.2). Street (1976) obtained similar results in a study of northeastern United States/southeastern Canadian earthquakes as well and established a basis for a unified magnitude scale between central and northeastern North America.

Nuttli (1978) has also investigated the attenuation of 10 Hz waves in the New Madrid seismic zone in southeastern Missouri, United States, and finds N = 1.4, for the

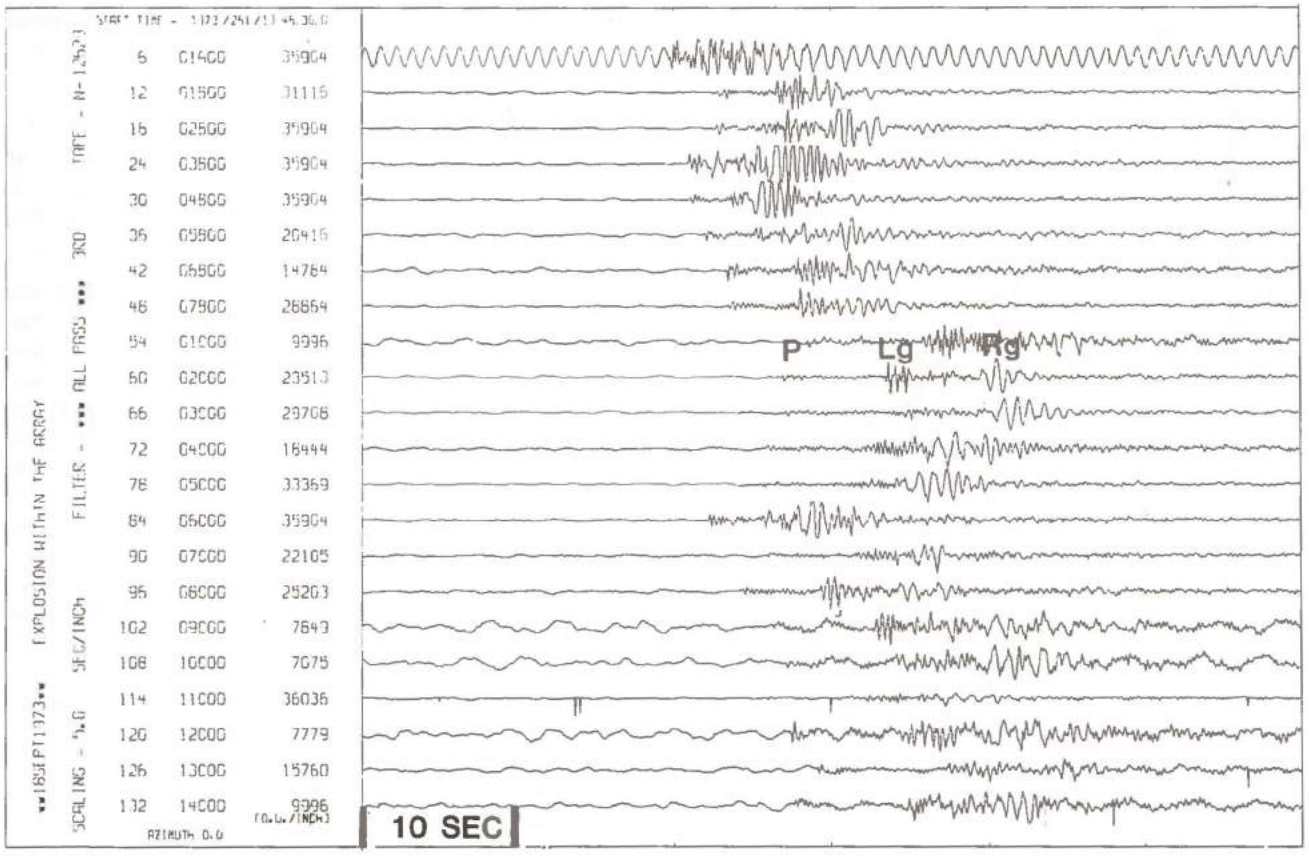

Fig. 8.1
Example of NORSAR recordings containing all phases P, Lg and Rg. The event is an explosion (event 4 in Table 8.2).

Event No.	Date	Time of Day (GMT)	M_L	Latitude	Longitude	Depth (km)
1	1 Oct 1973	16.44.14.3	2.3	59°55.1'	11°25.4'	7,3
2	23 Nov 1973	06.49.36.9	1.7	60°33.2'	11°28.2'	22,6
3	6 Dec 1975	14.15.58.3		59°39.6'	11°12.6'	0,0
4	18 Sep 1975	13.46.48.2		60°48.9'	11°00.9'	0,0

Table 8.1
Estimates of hypocentral coordinates for two earthquakes (nos. 1 and 2) and two explosions (nos. 3 and 4) which have occurred within or very near the NORSAR array (see Bungum and Fyen, 1979). M_L is local magnitude.

distance range 3 to 250 km, which is considered a modest fall-off of amplitude at such a high frequency.

8.2 Attenuation relationships relevant to the Norwegian continental shelf

From our general experience with data from NORSAR and other Fennoscandian seismic stations, the three phases P, Lg and Rg must be considered in the assessment of seismic risk offshore Norway. An example of a NORSAR record with these three phases is given in Fig. 8.1, showing one seismogram from each of the 22 subarrays of NORSAR. This event is number 4 in the event listing in Table 8.1.

The seismic phase Rg is a short period surface wave of Rayleigh type. The presence of this phase is an indicator of a shallow source. The hypocentral depth will normally be 0-1 km and according to Båth (1975) never exceeds 2-3 km whenever this phase is present in the records. The Rg phase also exhibits a limited range of propagation. Båth (1975) gives a limit of 300 km; in NORSAR records we have not observed this phase for ranges beyond 150 km. The distribution of earthquake focal depths for Fennoscandia is shown in Fig. 10.3, and clearly very few earthquakes are shallow enough for the Rg phase to be generated. Indeed, the presence of Rg is a reliable indicator for events having an artificial origin.

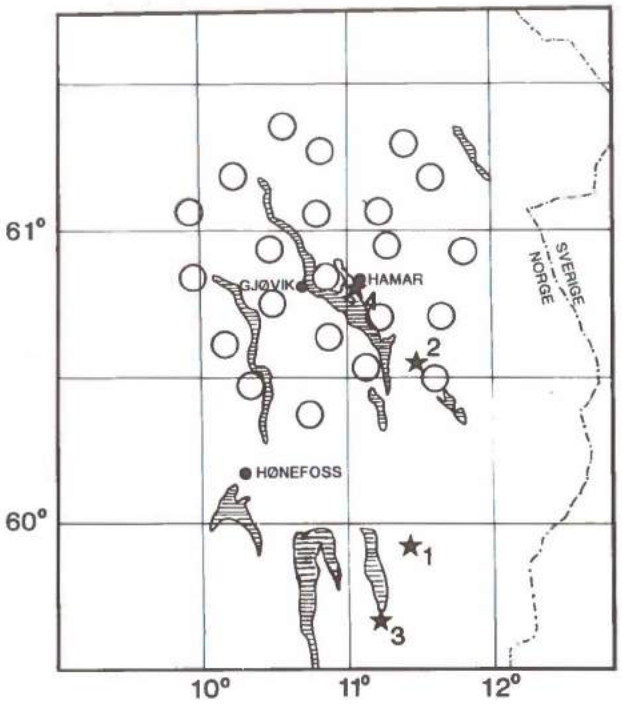

Fig. 8.2
The NORSAR array, consisting of 22 subarrays each with 6 seismometers. The four events studied are indicated by stars. Further information on the events is given in Table 8.1 and by Bungum and Fyen (1979).

Mykkeltveit and Ringdal (1979) have examined the relative attenuation characteristics of P and Lg records at NORSAR from 15 selected earthquakes and explosions, many of which have propagation paths containing parts of the Norwegian Continental Shelf. One of the conclusions from that study is that the Lg amplitude is larger than that of P by a factor of typically 3 or more in the distance range 100-500 km. Thus design earthquake motions in Norway and also the Norwegian Continental Shelf must primarily be concerned with Lg waves.

Now, the problem is how to obtain attenuation relations for Norway and the adjacent shelf areas. Some seismic refraction profile investigations have been undertaken in this region, but in neither of them has the station coverage been sufficient for reliable derivation of attenuation relations. Quite recently, however, two profiles have been shot with appreciably denser station coverage (in the order of 4 km between consecutive recording stations), but data from these experiments have not yet become available. So, for our analysis we have chosen NORSAR data from four events, two explosions and two earthquakes, all located within or near the NORSAR array. The configuration of NORSAR and the location of the four events are shown in Fig. 8.2. Each of the 22 subarrays (denoted by rings) has 6 seismometers within it, evenly distributed over an area of 8-9 km in diameter. For each event listed in Table 8.1 this gives us a total of 132 recordings.

In Fig. 8.3 all 132 records for event no. 2 in Table 8.1 have been arranged according to epicentral distance. All single seismograms have been normalized relative to its maximum amplitude and also subjected to 3rd order Butterworth bandpass filtering for the passband 0.5-1.5 Hz.

This gives a section of seismograms where two major phases, P and Lg, are seen propagating across the array. The Lg phase is seen to provide the largest amplitudes, except for very short distances. The maximum amplitude for each seismogram is plotted versus hypocentral distance in a log-log scale in Fig. 8.4 (event 2). The same procedure has been applied to the other events and results are presented in Fig. 8.4 for the frequency range 0.5- 1.5 Hz. The NORSAR instruments are velocity seismometers, so our results reflect decay rates for maximum ground velocity. In the lower left corner of each frame we have indicated various decay rates, i.e., various values of -N in (8.1).

The same four events were also analyzed in the frequency bands 1.5-3.0 Hz and 3.0-5.0 Hz and results are given in Figs. 8.5 and 8.6. For the two earthquakes (events nos. 1 and 2) we see no decay at all for these filters. This is due to strong high-frequency signals (main energy around 3 Hz) which are clipped on many seismometers. For all events and all three filters, the maximum amplitudes cor-

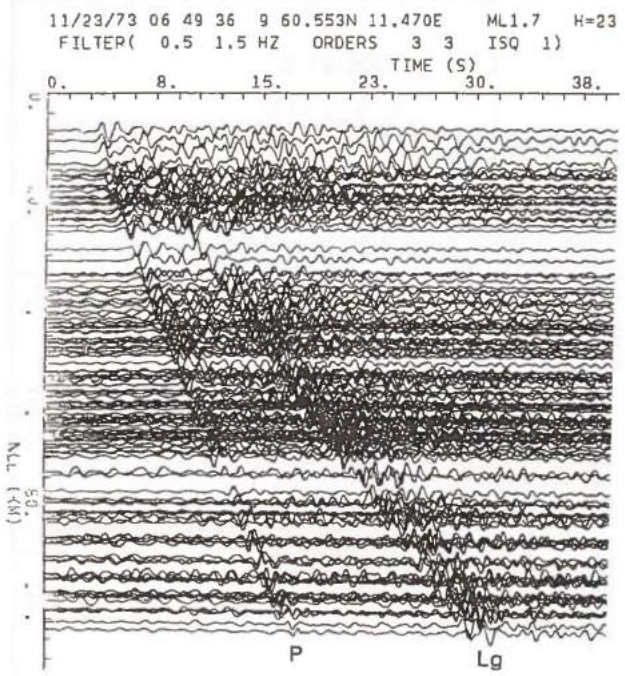

Fig. 8.3
Seismograms from event 2 arranged according to epicentral distance and normalized relative to the maximum amplitude in each trace.

respond to the Lg phase and hence our decay rates are those of Lg waves.

The results from our attenuation study are summarized in Table 8 2. The decay rates given represent rough fits of the data in Figs. 8.4, 8.5 and 8.6 to a straight line. Not surprisingly, scattering effects and henceforth the attenuation itself is strongest for relatively high signal frequencies. Decay rates for signals of frequencies of 1.5 Hz and above are seen to be in the order of -1.70. For frequencies in the range 0.5-1.5 Hz, however, it seems reasonable to adopt approximately -1.0 for this decay rate. This is the frequency range of major interest to offshore installations.

Accepting the above attenuation results to be valid also for the Norwegian Continental Shelf, our conclusion is that Lg waves that fall off as the inverse 1.0 power of the hypocentral distance is the phase of major importance and concern in the assessment of seismic risk offshore Norway.

Event No.	Distance Range Covered (km)	Decay Rates (N in (8.1)) 0.5-1.5 Hz	1.5-3.0 Hz	3.0-5.0 Hz
1	56-167	1.05	-	-
2	24-108	1.00	-	-
3	86-193	1.35	1.80	1.90
4	6-68	1.10	1.60	1.40
Average		1.12	1.70	1.65

Table 8.2.
Summary of maximum ground velocity decay values for the four events analyzed.

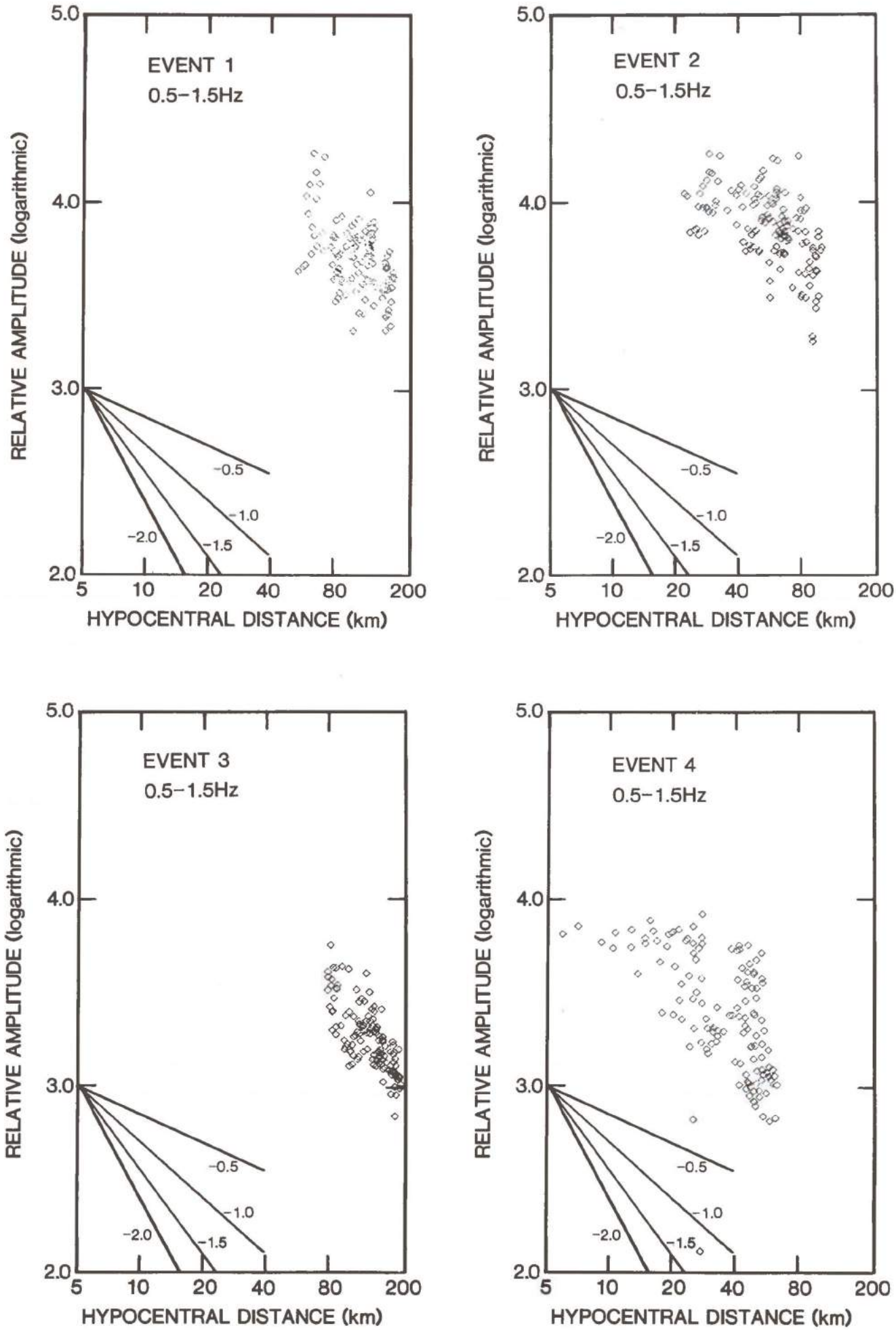

Fig. 8.4
Decay rates of maximum ground velocity for the frequency band 0.5-1.5 Hz for the four events in Table 8.1. Four different decay rates are indicated in the lower left corner.

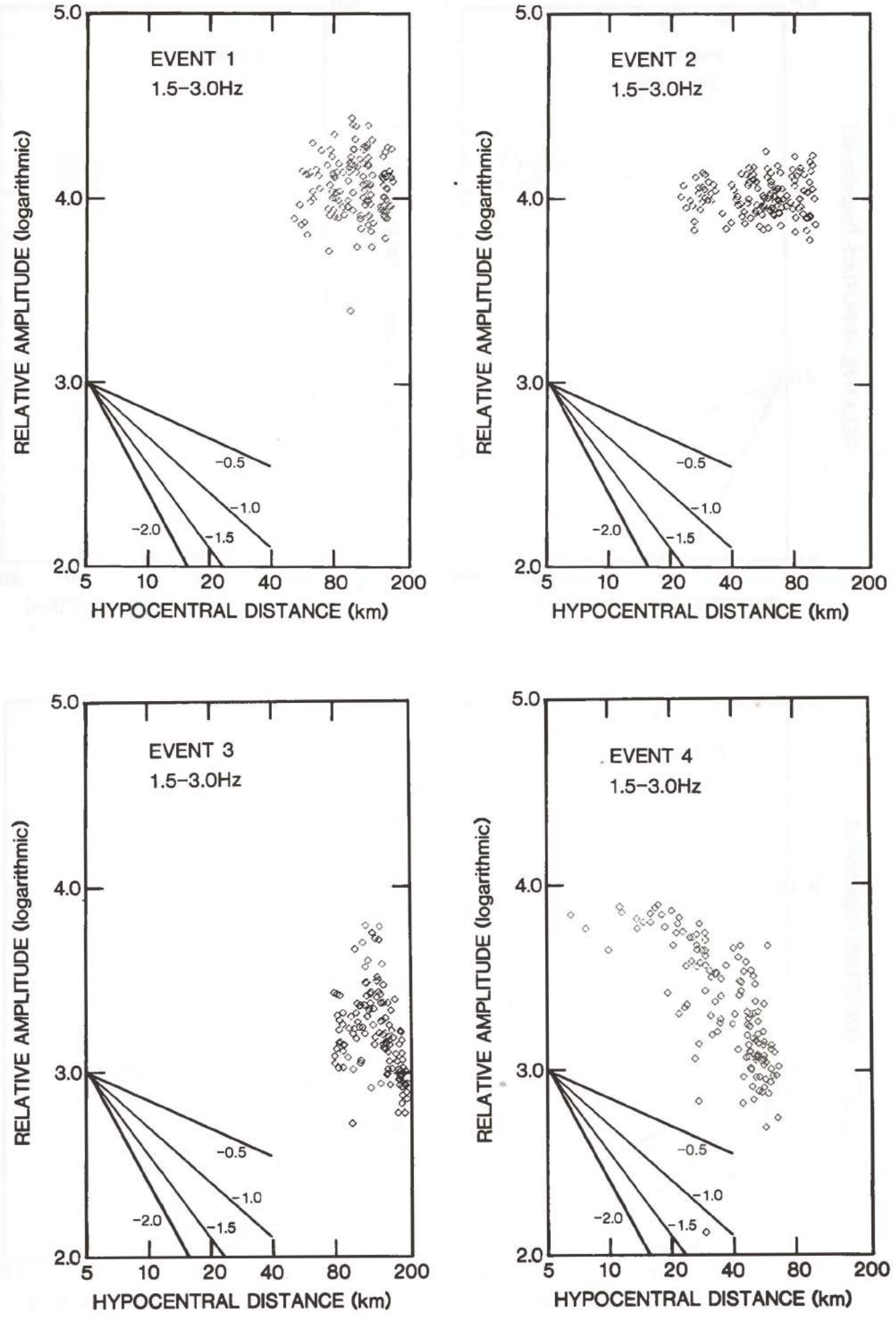

Fig. 8.5
Same as Fig. 8.4 for the frequency band 1.5-3.0 Hz.

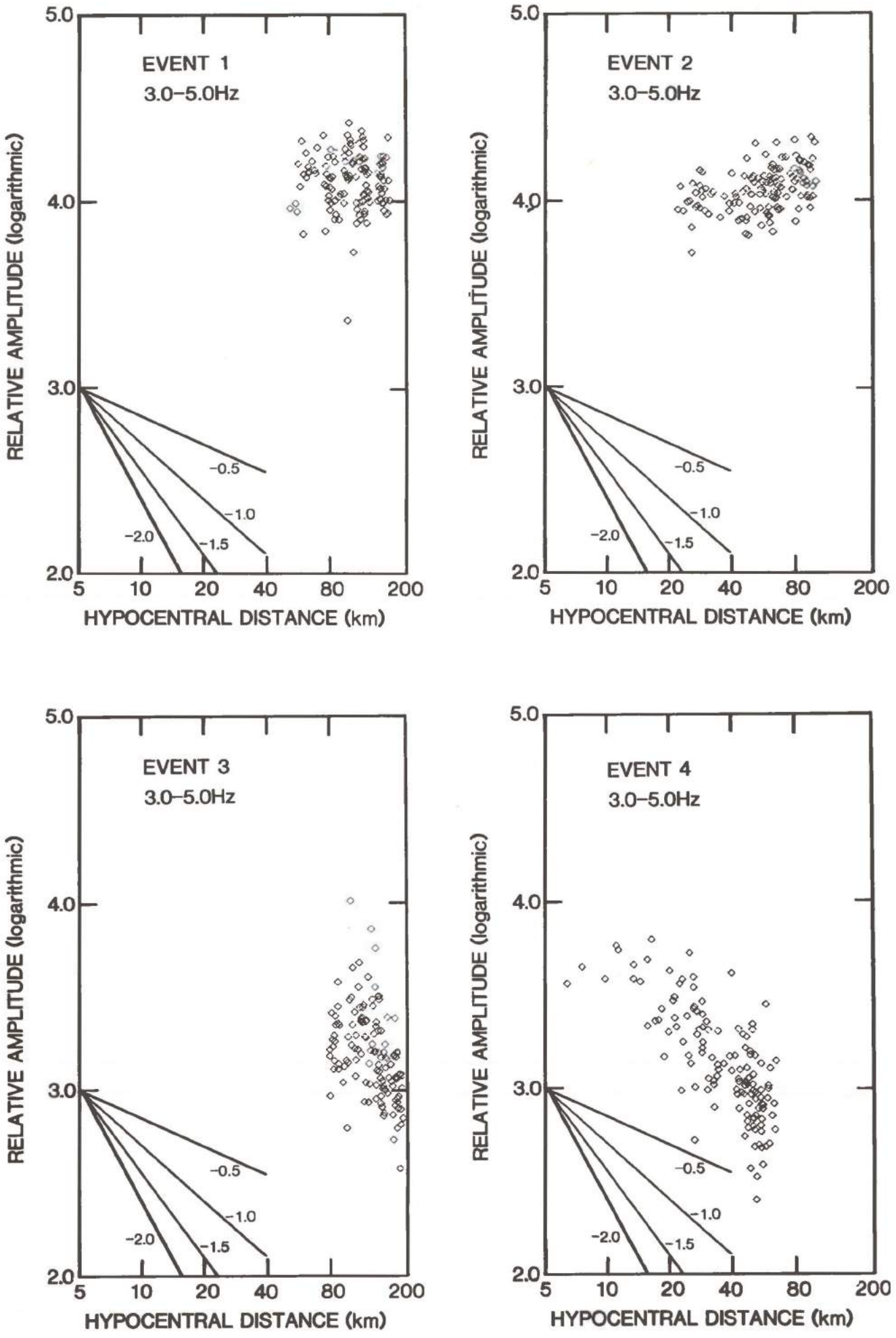

Fig. 8.6

Same as Fig. 8.4 for the frequency band 3.0-5.0 Hz.

9. Development of seismic risk maps - general considerations

9.1 Introduction

The general objective of seismic risk analysis is a quantitative assessment of the earthquake hazard to important constructions, such as nuclear power plants, large dams, offshore oil platforms and facilities for storage of nuclear wastes. The "risk" involved is by no means a simple concept; a number of geological, seismological, structural and economic parameters have to be considered before a rational earthquake resistant facility can be planned. The concept of *acceptable risk* is central throughout; in general the level of acceptable risk is lower the more disastrous the consequences of a structural failure will be (economic, environmental, loss of life, etc.).

Implicit in the expected seismic risk is a considerable element of future uncertainty. Therefore, it is not surprising that the principles of statistical forecasting and decision making are essential tools in the seismic risk analysis.

The basis seismological data for evaluating seismic risk comprise:

1. Current seismic activity.
2. Historical records of earthquakes
3. Tectonics and geological indicators
4. Observed seismological-tectonic patterns.

Point 4 above deserves special mentioning as it has formed the basis for recent studies applying advanced pattern-recognition techniques to the prediction of future earthquakes (Gelfand et al, 1974). Up to now, this method has shown promising results in areas of high seismic activity, but their application in intraplate situations is not yet proven.

9.2 Statistical prediction

The topic of assessing earthquake hazard for engineering purposes consists of predicting whether a certain engineering parameter (e.g., maximum ground acceleration) will exceed a critical value within a given time frame at a specific site. Thus "prediction" means here *not* the specification of actual time and place of occurrence of large earthquakes, but rather a statistical expectation based upon cumulative earthquake catalogues and tectonic/geologic information.

Although the concept of plate tectonics has provided a unified theory for the large-scale correlation between geology, tectonics and seismicity along plate boundaries, there is still a lack of understanding of how to associate intraplate seismicity (i.e., earthquakes within tectonic plates) to known geotectonic features. This means that the only acceptable way of assessing earthquake hazards in such areas is through observation of actual earthquake activity. Existing earthquake catalogues are often incomplete; only for the past 10-30 years have reliable instrumental observations been available on a global basis. For Scandinavia, historical records give evidence of earthquake activity from several hundred years back (Section 5) and, although incomplete, these data provide a valuable supplement to the more recent instrumental records.

The value of historical earthquake records becomes particularly pronounced in the "low risk" case. The expected life span of important industrial facilities may conveniently be classed into:

a) Short life span (less than 100 years)
   - Nuclear power plant
   - Offshore oil platforms
   - Facilities for short-term storage of nuclear wastes
b) Intermediate life span (a few hundred years)
   - Large dam constructions
c) Long life span (thousands of years)
   - Facilities for long-term storage of nuclear wastes.

It is important to note that

- Risk analysis under a) and b) can build upon the tectonic and seismological environment of the past few hundred years.
- Risk analysis under c) (long life span) must take into account likely changes in the tectonic environment.

Even for structures of short life span, the design ground motion values are sometimes to be specified corresponding to a probability of being exceeded as low as 10^{-4} or 10^{-5} per year. This requires, of course, a considerable extrapolation of the observed data, even when the longest available time history of known earthquakes is used.

approaches:

- *Time averaging:* use longest available time span, especially to identify recurrence times of large earthquakes.
- *Space averaging*: consider a large tectonic province of similar characteristics to where the site is located.

It is, however, necessary to take special precautions in those cases where major faults or tectonic boundaries are situated near the site. Such structures should be considered separately in the risk analysis.

The topic of this report concerns structures of *short* life span. We will assume that the known seismic history can be used as a guideline to predict future trends. Nonetheless, it is recognized that fluctuations in seismic activity levels over longer terms exist, as have been documented for the Mediterranean countries and China over the past several thousand years. This implies a statistical uncertainty in the end results that must not be forgotten.

9.3 Seismic risk versus other environmental risks

There are some similarities, but also important differences, in the assessment of the hazard to offshore constructions caused by earthquakes and other environmental factors, such as sea waves. Whereas a major storm will cause large (and similar) wave loads over a wide area, an earthquake will have its greatest effects in a very limited area near the source, with a rapid decay of ground motion at distances greater than a few tens of kilometers. In both of these cases there are obvious physical limitations involved, with respect to the largest wave height and the largest earthquake magnitude, respectively although the

exact specification of these limits is subject to some statistical estimation.

In an assessment of earthquake hazard, one must take into account both the probability that an earthquake of a given magnitude may occur and the probability that the focus will be within a given distance of the site of the construction. For example, within a 100-year period, it is very likely (in fact almost certain) that a large earthquake (magnitude 6 or above) will occur somewhere on the Norwegian continental shelf. However, the probability that such an earthquake will occur in the immediate vicinity of any given site within 100 years is very low. Nonetheless, if one considers the risk at a sufficiently low probability level, one will eventually arrive at a situation where the design parameters must be set to accommodate a major earthquake occurring very near the site.

By actually carrying out the probabilistic calculations, it can be seen that the expected ground motion at a given site due to earthquakes increases significantly with a lowering of the probability level. As found in Section 10, the expected ground acceleration due to earthquakes at a 10^{-4} per year probability of exceedance is larger by about a factor of 4 compared to that at a 10^{-2} per year level. This large increase is precisely due to the distance factor; given a lower probability level, one must expect large earthquakes to occur nearer to the site. In contrast, the expected load due to sea waves shows a much slower increase as the probability level is lowered, since the distance factor does not have the same importance here.

In practice, the calculation of loads due to earthquakes is of course much more complex than indicated by the qualitative comments given above, since one must take into account a statistical distribution of earthquake magnitudes, relative seismicity levels for different areas and detailed strong-motion attenuation relationships. However, the main conclusion remains: earthquake loads become an increasingly significant factor relative to other environmental loads when low risk levels are considered.

10. Development of seismic zoning maps

For engineering purposes, "seismic hazard" is most often expressed in terms of the expected maximum peak acceleration for a specified return period at a given site. This acceleration value is then used to scale a known strong-motion seismogram record or possibly a synthetic design spectrum in the subsequent response analysis of the structure.

10.1 Introduction

For offshore platforms, the most critical aspect of earthquake loads concerns the expected level of shaking at signal periods of approximately 2-4 seconds. It is noteworthy that the dominant period of known near- field accelerograms from earthquakes are much lower, typically 0.2-0.5 seconds. On the other hand, the *velocity* of ground motion usually has a dominant period at or above 1 second. It is therefore apparent that the actual level of velocity is more important to the risk of offshore installations than the acceleration level. While it would thus be desirable to develop zoning maps in terms of expected ground velocity at certain return levels, the available data on attenuation does not allow us to achieve this at the present time. Instead, we recommend that design spectra be based upon maximum acceleration, with the velocity level adjusted according to selected spectra from available strong-motion records. This will be further discussed in Section 11.

To estimate the acceleration in bedrock due to earthquakes at a given return period is in principle simple, but becomes difficult in cases where little is known about basic parameters. In order to conduct an adequate analysis, it is necessary to know or estimate the following:

i) **The complete seismic field surrounding the site**
This includes
- Extent and position of active faults
- Rate of seismic activity of each fault
- Statistical distribution of expected earthquake focal depths
- Frequency-magnitude relations of the earthquakes, including and estimate of the upper magnitude limit.

ii) **The relation between mangitude and accelrartion** (the "average" relationship as well as its statistical standard deviation)

iii) **Attenuation of accelration as a function of distance,**
including:
- The possible frequency dependence of this relationship
- Assessment of the effect of source dimension in the case of large earthquakes.

iv) **Amplification effects due to local soil conditions at the site**
(These are also frequency dependent.)

Needless to say, these factors can never be completely determined, and it is therefore necessary to apply average relationships that are considered adequate in the judgement of the expert. Especially for an area of relatively low seismicity like Scandinavia, the available data base of actual measurements is scarce, and one has to rely upon data from seismically more active regions such as California, Japan and Southern Europe. A considerable amount of judgement has to be applied in this respect, as it is clearly not appropriate to apply very sophisticated models in the calculations when our initial knowledge of basic parameters is as limited as is the case here. The aim of this study is to obtain an *initial assessment* of expected ground accelerations in bedrock due to earthquakes offshore Norway. We shall therefore in the following apply a simplified model and at the same time discuss the dependence of the results on the choice of model parameters.

Our main simplifications at this stage will be the following:
- We shall assume that the seismic field can be considered *homogeneous* over relatively large subregions offshore Norway. Thus we will not attempt to take specific faults into consideration.
- We shall assume that earthquakes occur as point sources in the statistical treatment.
- We shall assume that acceleration decay is independent of frequency.

In the following, we will develop zoning maps to provide an estimate of earthquake-induced ground accelerations in bedrock for the various regions within the Norwegian continental shelf area. Estimates will be given at two probability levels, corresponding to return periods of 100 resp. 10,000 years. While such estimates can be given with a reasonable reliability for return periods of 100 years, the values for 10,000 years are only tentative, and are based on an extrapolation procedure which must by necessity produce somewhat uncertain estimates.

10.2 Method and parameters

The basic method applied in this study is briefly described in the following. The method has been developed with the special area offshore Norway in mind, but would be applicable to other intraplate areas as well:

A. **Subdivision of area**
To compute the risk at any given site, we subdivide the surrounding area in blocks (typical size 100 km x 100 km or 200 km x 200 km) so that the site is the midpoint of the center block. We assume that the seismicity is evenly distributed within each block.

B. **Estimate of seismicity level**
Within each block, we estimate a seismicity recurrence relationship of the standard form:

$$\log N = a - b \cdot M$$

where N is the annual number of earthquakes exceeding magnitude M. The parameter **b** is kept fixed (see comments below) while the parameter **a** is obtained by *averaging the* **a** values obtained for three time periods, respectively:

i) 1950-1980 Threshold magnitude M_T = 4.0

ii) 1890-1980 Threshold magnitude M_T = 5.0

iii) 1780-1980 Threshold magnitude M_T = 5.5

Within each such time period, a is estimated by counting the observed number of earthquake N_0 exceeding the threshold magnitude M_T listed above. Thus, for each time period we obtain:

$$a = \log(N_0/NYEARS) + b \cdot M_T$$

where NYEARS is the length (in years) of the time period.

C. Strong motion attenuation

We assume a fixed strong motion attenuation relationship and relate acceleration to estimated earthquake magnitudes as desctibed in the comments below. To eliminate the need for several curves based on different attenuation characteristics, we have used a mean attenuation curve and an estimated standard deviation in the statistical model.

D. Calculation of acceleration

Using a Cornell technique, estimate the acceleration at a given location at the specified probability level by summing the contribution from seismicity within each block. A fixed source depth is assumed in these calculations (see discussion below).

Comments to A

The subdivision of the area in fairly large blocks is justified by the diffuse seismicity patterns observed offshore Norway, and the lack of any obvious correlation between earthquakes and known faults in this region. We have chosen a block size of 100 km x 100 km for our estimates at the 10^{-2} per year probability level, and 200 km x 200 km at the 10^{-4} per year level. At this latter, very low probability level, we consider that averaging over a large area as chosen is most correct, since the large earthquakes become the dominant factor at this level of risk estimation, and since we have little knowledge as to where future, large earthquakes may occur.

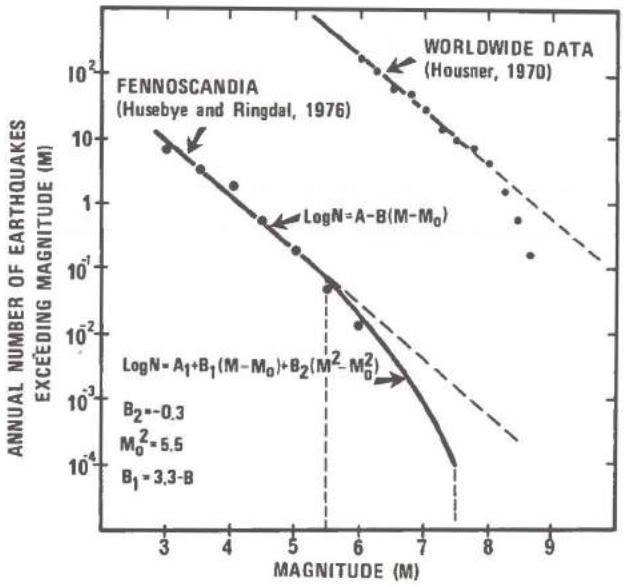

Fig. 10.1
Magnitude-frequency relationship used for this study. World- wide data (Housner, 1970b) are shown for comparison.

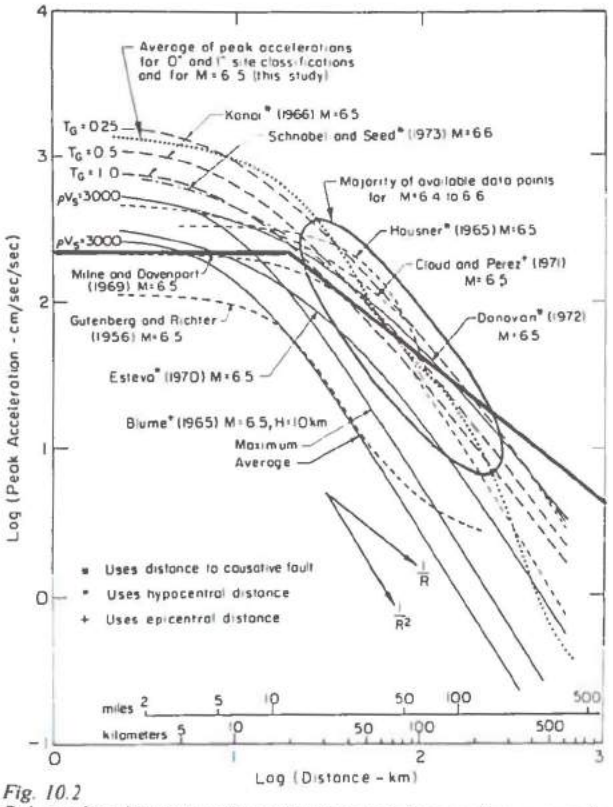

Fig. 10.2
Relationships between peak acceleration and distance from source for magnitude 6.5 earthquakes. (After Trifunac and Brady, 1976). The relationship chosen for this study, shown as a heavy line, is:

Comments to B

The seismicity coefficient **b** is usually relatively stable over wide areas, and this is the justification for keeping this parameter constant. We have chosen b = 0.8 in our calculations, which is consistent with general studies of earthquakes in Fennoscandia (Husebye and Ringdal, 1976, see Fig. 10.1). We have also assumed an upper magnitude limit of M = 7.0 in applying the seismicity formula for the Norwegian continental shelf.

Our consideration of three different time periods in estimating the parameter **a** is based upon the general quality of earthquake reporting in historic time in Fennoscandia (see Section 5). Our selection of thresholds is based on judgement, and is consistent with our observations on detectability in Section 7. Note that the averaging over the three periods has the combined effect of i) using the recent data base which is relatively good for offshore epicenters and ii) taking into account the occurrence of historic, large earthquakes offshore Norway.

For those blocks where little or no earthquake activityhas been observed, we have adopted a "background seismicity" level which is scaled to a level corresponding to one M = 4.0 or greater earthquake per 100 years per 10^4 sq. km. Thus, we obtain a non-zero probability of significant earthquakes occurring on the entire continental shelf.

Comments to C

The discussion in Section 8 shows that the near-field attenuation with distance of seismic waves in Scandinavia is relatively low compared to several seismically highly active regions. Similar results have been obtained for other intraplate regions (e.g., Hasegawa et al, 1981). Therefore, we must be careful when considering attenuation functions based on strong-motion recordings in interplate regions. Nonetheless, we have to resort to such relations

due to the lack of adequate observational data for intraplate areas. Fig. 10.2 shows a summary of a number of proposed relations for acceleration decay as a function of distance. The relation adopted for this study is also plotted on the figure. We have used the formula

$$acc = \theta \cdot b_1 \cdot e^{b_2 M} \cdot R^{-b_3} \cdot \varepsilon, \quad R > 20 \text{ km}$$

where acc is acceleration in fractions of g and the parameter values are $b_1 = 0.025, b_2 = 0.08, b_3 = 1.0$. Furthermore, ε is a lognormally distributed error term, i.e., ln ε is normally distributed with expectation 0 and standard deviation $\sigma = 0.3$.

We note from the figure that the slope of the adopted relation ($b_3 = 1.0$) is less steep than world-wide data indicate. On the other hand, in the distance interval of most significance to the risk calculations (20-200 km), our relation lies well within the ellipse comprising the majority of data points.

Whereas our choice of attenuation function is based on considerble judgement, we consider that it provides a reasonable " average" curve, and with the assumed standard deviation we consider that the inherent uncertainties in this relationship have been addressed adequately.

Comments to D

We have used the widely applied method of Cornell (1968) in computing the acceleration estimates. The assumption of a fixed depth of earthquake sources offshore Norway (selected as 20 km) is based upon statistics compiled by Husebye et al (1978), whose main results are shown in Fig. 10.3. An average depth of 20 km is representative of known earthquakes in this area. It is quite possible to assume a non-constant distribution of focal depths in the calculation; however, we consider that the quality of available data does not justify introducing this added flexibility. In this regard, we note that source depth is not necessarily magnitude independent; in fact the larger earthquakes (Section 5) appear to have greater focal depths than the smaller ones. Also, simulation experiments indicate that the risk levels are not greatly affected by assuming an average depth as opposed to a reasonable distribution around this value.

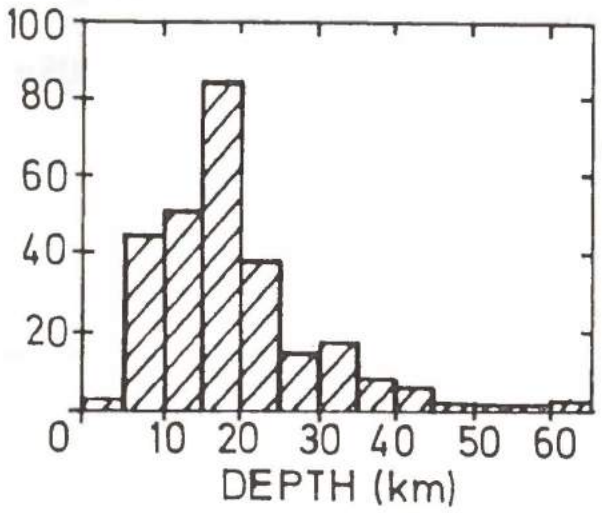

Fig. 10.3
Focal depth distribution for a group of Fennoscandian earthquakes (southern Sweden) as inferred from macroseismic data.

10.3 Seismic zoning maps offshore Norway

Peak acceleration maps at the two specified probability levels are shown in Figs. 10.4 and 10.5. At the 10^{-2} per year level (Fig. 10.4), the contours of this map delineate the zones of the acceleration 0.025 g and 0.050 g. The largest estimates within the most active seismic zones are found to be close to 0.06 g. At 10^{-4} per year probability level (Fig. 10.5), the contours are similar, but estimated accelerations are higher by a factor of typically 4. We emphasize, however, the degree of uncertainty in this second case, and consequently this map should be interpreted with caution. At the 10^{-4} per year level, the highest values offshore Norway are close to 0.20 g, corresponding to the seismically most active parts of the Norwegian offshore areas, i.e., the Møre coastline, offshore Nordland and in an area near 70°N, 10°E.

When considering a seismic zoning map of the above type, one should always bear in mind the limitations inherent in the statistical model. Basically these limitations are caused by the short time of observation combined with the low probability levels at which the risk is desired. A factor futher aggravating the situation is that seismic activity is by no means stationary in time and space, when considered as a random process. Historical records from earthquake-prone countries such as China and in the Middle East show in many cases that periods of relative quiet seismicity, lasting several hundred years, may be followed by a series of severe earthquakes over a relatively concentrated time period. Such factors are difficult to incorporate in a statistical model, but certainly justify a considerable degree of caution in interpreting the results.

We finally note that we have not taken any direct tectonic evidence into consideration in the present study. The main reason is that at present we do not have accurate enough estimates of earthquake location and depths offshore to perform any meaningful correlation between earthquake activity and known fault lines. Thus we have no means to determine whether a given fault can be considered seismically active, nor can we at present use information on fault dimensions to estimate the largest size earthquake that a given fault is capable of generating.

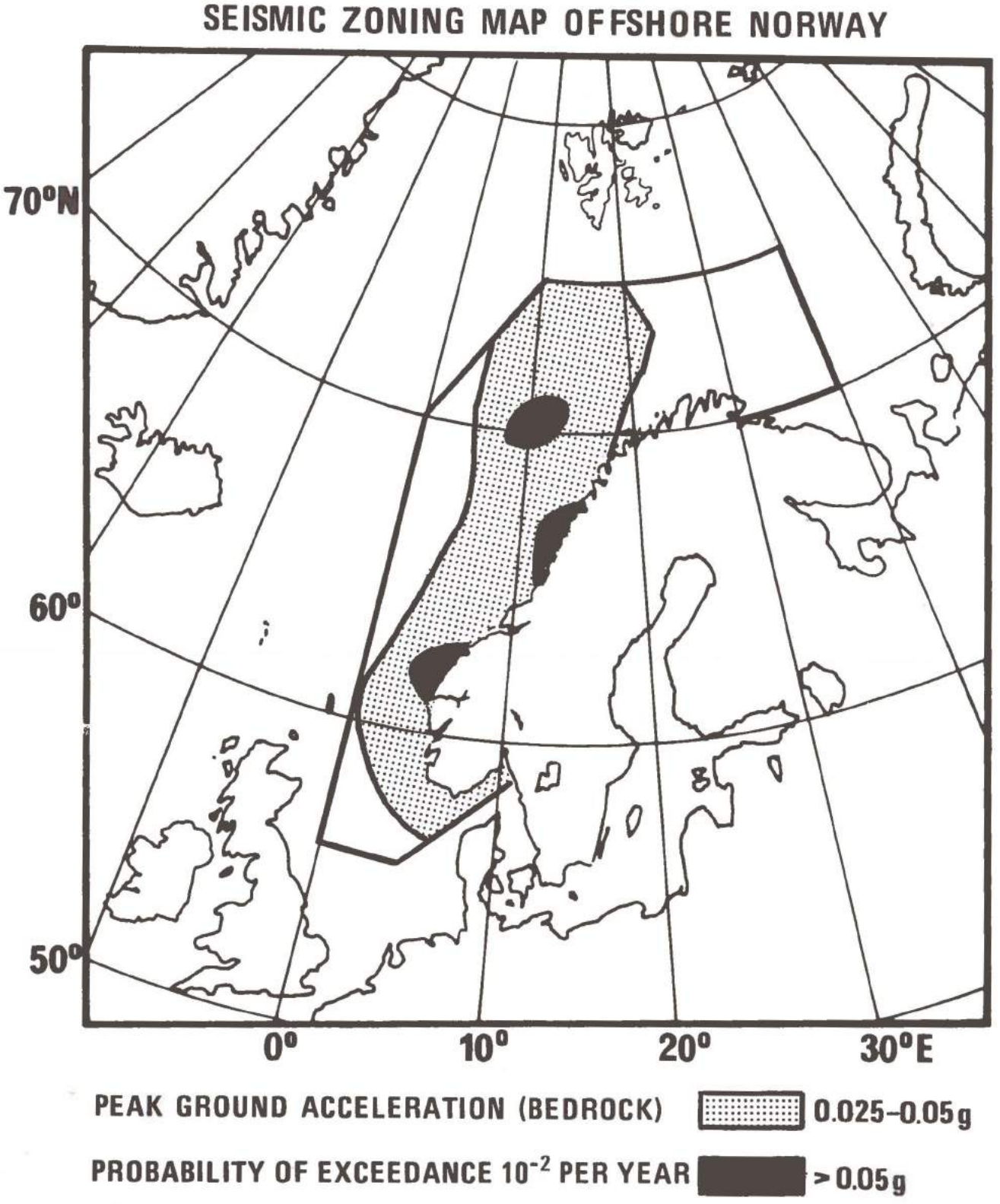

Fig. 10.4
Preliminary seismic zoning map offshore Norway showing expected peak ground accelerations in bedrock at a probability of occurrence of 0.01 per annum.

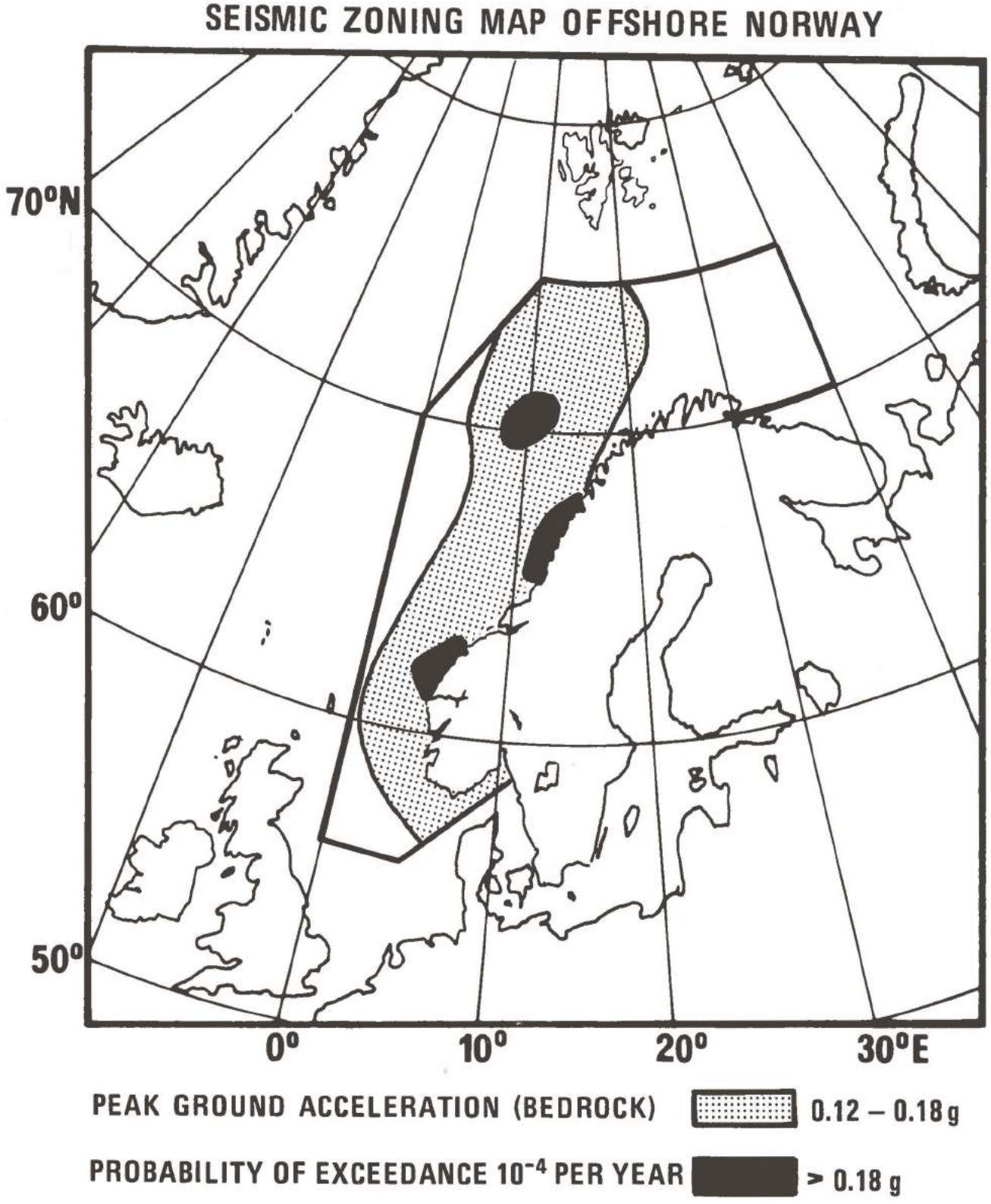

Fig. 10.5
Preliminary seismic zoning map offshore Norway showing expected peak ground accelerations in bedrock at a probability of occurrence of 0.0001 per annum. Note the reservations in the text regarding the uncertainty of these estimates.

11. Design spectra for the Norwegian continental shelf

The design spectrum is a response spectrum used for the seismic-resistant design of a structure. As such, it incorporates an estimate of what kind of strong-motion signature one should expect from a future earthquake with a magnitude at or close to the maximum possible in the area. It follows from this that the basis for constructing design spectra must be strong- motion recordings of past earthquakes. When no such recording is available from a particular area (such as Fennoscandia), one has to use strong-motion recordings from areas where such are available. This can be done either simply by adopting design spectra, such as those from the United States Nuclear Regulatory Commission (USNRC) or by developing "local" spectra, where differences in geologic and seismotectonic conditions have been taken into account.

It is the latter approach which has been adopted in this report, but before addressing the requirements for a "Fennoscandian" response spectrum we will discuss in more detail some general characteristics of and problems with design spectra.

11.1 Design spectra - General considerations

Although the concept of design spectra was introduced already in the 1930's (Biot, 1934), more systematic work in this area had to await the beginning of nuclear power plant construction at the end of the 1950's (Housner, 1959), with the first general design criteria being published a few years later (Lockheed et al, 1963).

Several different design spectra were then developed during the following years, based on statistical analysis of an increasing number of strong- motion records. The "classical" one was then published in 1973 by USNRC, based on the work of Newmark et al (1973), and 5 years after that came another update and refinement commissioned by USNRC (Newmark and Hall, 1978). With the exception of the latter one, each of these design spectra have been a bit more conservative than the previous one, with a difference of about a factor of two between Housner (1959) and USNRC (1973).

The seismic design spectrum is a specification of the requirements to relative strengths of a structure at different frequencies, and it is usually specified in terms of amplification factors for acceleration, velocity and displacement. The acceleration amplification factor, for example, is defined as the factor by which the peak ground acceleration is multiplied to obtain the absolute acceleration at a given frequency, and similarly for velocity and displacement. It is common now to display the amplification factors on tripartite plots where acceleration, velocity and displacement can be read from the same graph (see Fig. 11.1). The peak ground acceleration is now practically always standardized to 1.0 g, and if the velocity and displacement values are given in terms of amplification factors, we also need to know the peak ground velocity and displacement that correspond to the standard peak acceleration value. It is then common practice to plot the product of the amplification factors and the standardized peak values within

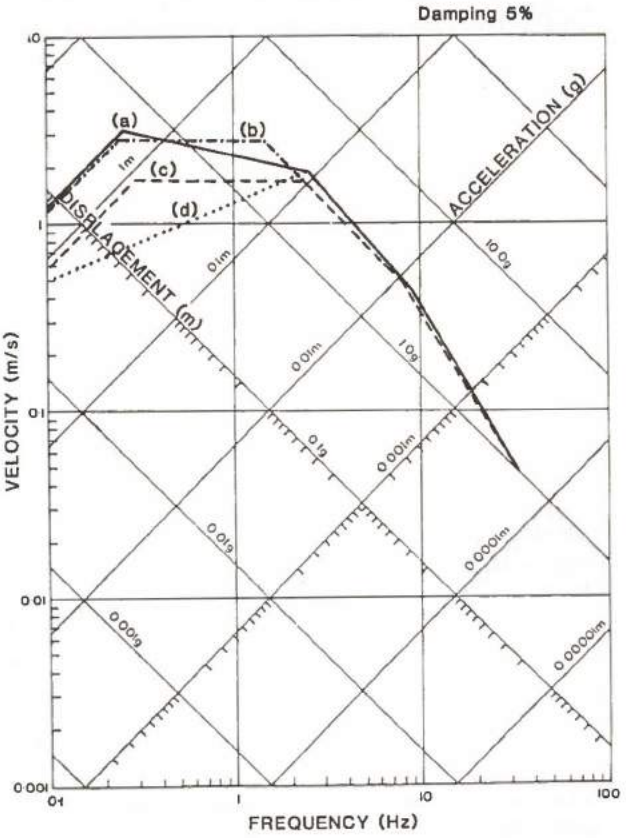

Fig. 11.1
Horizontal design spectra with 5% damping. The curves represent (a) USNRC RG No. 160 (USNRC, 1973); (b) NUREG/CR-0098 (Newmark and Hall, 1978); (c) Forsmark area, Sweden (Dames & Moore, 1976); and (d) Germany (also taken from Dames & Moore, 1976).

each of the three frequency bands, resulting in a spectrum which also so far as velocity and displacement are concerned is scaled relative to a peak acceleration value of 1.0 g.

It was found by Newmark et al (1973) that within the high, intermediate and low frequency bands the acceleration, velocity and displacement amplification factors (respectively) were nearly constants. It follows from that that the design spectrum can be plotted piecewise linearly within each of the three spectral bands, with values parallel to one of the tripartite axes. In addition to the three linear sections, a tapering of the acceleration values towards the peak ground acceleration is needed at higher frequencies, which implies the specification of two frequencies.

The presently used methodology for calculating design spectra was devised by Housner (1959), who realized that one could not with sufficient predictive accuracy specify or select an accelerogram that could be used as input for a dynamic analysis. The answer was to use statistical averaging over a number of earthquake records, and in the frequency domain. The idea here is that a good estimate of the effect or damage potential of an earthquake can be obtained by calculating the vibratory response (relative displacement) in a simple oscillator, with or without damping (Housner, 1970a). The displacement $y(t, \omega, \beta)$ of the mass relative to the base can then be given in terms of

time t, natural period of vibration $T = 2, \pi / \omega$ and damping β (expressed in fraction of critical damping). It can be shown that the total energy of this oscillator can be evaluated in terms of the Fourier amplitude spectrum of the recorded accelerogram, integrated over the duration of the shaking. The energy density values thus obtained are generally below those for the maximum energy, as the latter is tied to instantaneous values which may not be reached again during the earthquake (Housner, 1970b). If the maximum spectral displacement is S_d (defined as $y(t, \omega, \beta), \max)$, a pseudo-velocity S_{pv} and a pseudo-acceleration S_{pa} are defined as

$$S_{pa} = \omega S_{pv} = \omega^2 S_d$$

Even though S_{pa} and S_{pv} may differ somewhat from the maximum acceleration and the maximum velocity, the definitions are very useful because they make it possible to display all three quantities on the same tripartite logarithmic plot.

It is important to keep in mind now that the spectral values of maximum acceleration, velocity and displacement as computed for a particular earthquake (which is what Housner (1970b) calls a response spectrum) is not the same as a design spectrum. In fact, the maximum acceleration may sometimes have very little to do with the damage potential of an earthquake, and this happens when the level is reached only by a single, narrow pulse. This generally happens when the recording is made close to the hypocenter, very high accelerations can then be reached even for low magnitude earthquakes. Since these accelerations are associated with waves of very high frequencies, they contribute little to the velocity content of the record, and it is often the velocity response spectrum which is most important with respect to the effect of an earthquake (severity of the vibrations) on elastic structures (Housner, 1970a). The design spectrum is not a specification of a particular earthquake ground motion. It is obtained by averaging the spectral analysis results from many earthquake recordings, and then computing spectral bounds often defined as the average or the median with one standard deviation added. The curves are usually computed for a number of damping values, where a small value naturally leads to a more conservative design spectrum, or to larger amplification factors. The relationship between amplification and damping is usually now assumed to be logarithmic, expressed in terms of a regression equation (Newmark et al, 1973; API, 1981).

A final point about design spectra concerns the relationship between horizontal and vertical amplification factors. The vertical values are generally smaller, and usually found to be in the range between 1/3 and 2/3 of the horizontal ones (Housner, 1970a; Principia, 1981). In USNRC RG 1.60 (Newmark et al, 1973) a frequency dependent scaling was introduced (with values between 2/3 and 1), while a constant value of 2/3 was introduced in NUREG/CR-0098 (Newmark and Hall, 1978). The same relationship is also recommended by Principia (1981), who found that the value (of 2/3) for most frequencies was on the conservative side.

11.2 Design spectra for Norwegian continental shelf areas

Before addressing the question of the characteristics of design spectra appropriate for Norwegian off-shore areas, it is necessary first to look at some spectra for other areas.

In Fig. 11.1 is shown (a) the standard USNRC 1973 spectrum, (b) the USNRC 1978 spectrum, (c) the Forsmark spectrum, and (d) a German spectrum. These spectra are all quite similar for frequencies above about 2.5 Hz, while the U.S. (in fact Californian) spectra are far more conservative at lower frequencies than the European spectra. This is reasonable taking into consideration that (1) the U.S. spectra are based on larger earthquakes which generally have a more dominant low frequency source spectrum, and that (2) an interplate area like California has a relatively stronger high frequency attenuation than most intraplate areas.

For the United Kingdom, Principia (1981) has addressed the problem of developing design spectra by selecting a number of accelerograms from areas that should be reasonably comparable geologically, and with reasonably comparable source parameters. Their results are shown in Fig. 11.2, for three different soil categories (curves a-c). The USNRC 1973 spectrum is plotted also here, for comparison (curve d). It is seen that the U.K. curves are more conservative for high frequencies, but far less conservative for low frequencies, for all three soil categories. It should be noted here that curve (d) in Fig. 11.2 is a firm ground spectrum, where actually quite a range of soil conditions are included (Newmark et al, 1973).

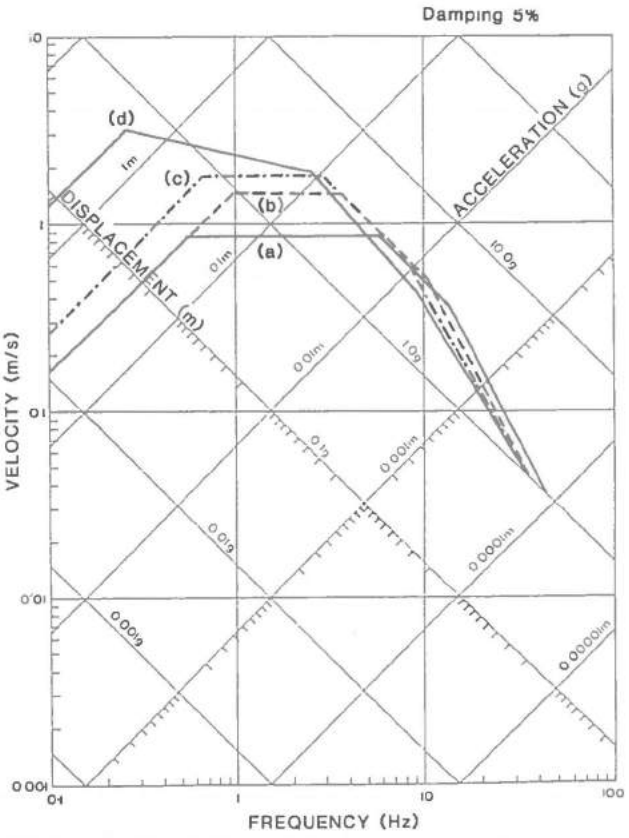

Fig. 11.2
Horizontal design spectra with 5% damping. Curves (a) - (c) represent Principia (1981) values developed for United Kingdom and covering (a) hard, (b) medium, and (c) soft ground. Curve (d) is from USNRC RG No. 1.60, for comparison.

In comparing the Californian spectra with Scandinavian ones, there are a few basic differences that should be kept in mind (see also Selnes, 1979):

- Californian earthquakes are larger, with lower corner frequencies and consequently relatively stronger low frequency radiation. In fact, the Meløy source spectra presented in Fig. 6.6 indicate higher frequencies than should be expected for similarly sized Californian earthquakes. An effect of this is that the peak ground

displacement and velocity values (scaled to an acceleration of 1.0 g) should be lower for Scandinavia.

- The focal depths in Fennoscandia are generally larger than in California, with most events in the range 10-30 km (Bungum and Fyen, 1979). In the NORSAR siting area, six precisely located earthquakes between 1971 and 1980 have depths of 7, 15, 22, 23, 30 and 30 km, respectively.
- The high-frequency attenuation in Fennoscandia is lower (see Chapter 8), with a Q-value probably in the range 500-1000 (see Chapter 6), and this has a similar influence on design spectra as the difference between source spectra.

These factors are similar to those used by Principia (1981) in their selection of earthquakes for U.K. design spectra. However, only earthquakes between 4.0 and 6.0 in magnitude have been used in their analysis, with an average of 5.2. This is about one magnitude unit below what would be reasonable estimate for an SSE earthquake (10^{-4} probability) in many areas of the North Sea. Mostly because of the way earthquake source spectra scale with magnitude (Bungum et al, 1982), an increse of one magnitude

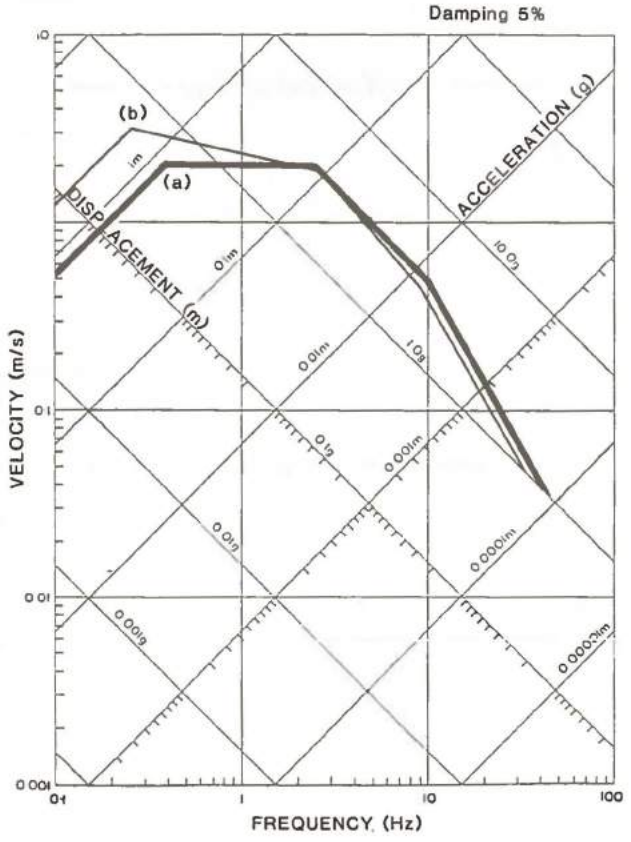

Fig. 11.3
Recommended horizontal design spectrum (5 % damping) for the Norwegian Continental Shelf (curve a). Peak acceleration, velocity and displacement is 3.2 g, 2.0 m/s, and 0.8 m respectively, and the high frequency tapering starts at 10 Hz and stops at 45 Hz. Curve (b) is from USNRC RG No. 1.60, for comparison.

(from 5.2 to 6.2) leads to a significant increase in the spectral amplification values for frequencies below 1 Hz, which is the frequency band of most importance for most offshore constructions. McGuire (1978) has found factors around 1.5-2.0 for the increase in velocity amplification around 1 Hz, and Iwasaki (1981) can refer to similar and higher values for the increase in accelera- tion in the 1-3 second period range.

Another factor which would support a North Sea design spectrum more conservative for lower frequencies than the Principia (1981) ones (which were developed for UK mainland), is the fact that longer period ground motion is often dominated by surface waves which may be strongly attenuated in the presence of thick sedimentary layers. Swanger and Boore (1978) have shown that for periods in the range 1.5-8.0 seconds amplification factors in the order of 3-4 may be introduced by typical offshore geology. Important here is not only the near-surface soil characteristics but also deeper structures, and especially important factors are seismic velocity gradients and possible sharp contrasts at depth.

We conclude therefore that while the USNRC spectra probably are too conservative at low frequencies (mainly because of the magnitude effect), the Principia spectra are probably not sufficiently conservative. For high frequencies, however, the Principia values seem to fit the North Sea requirements better. In consequence, we propose for the Norwegian offshore areas a design spectrum as shown by the heavy line (curve a) in Fig. 11.3. The spectral bounds for that curve are 0.8 m displacement, 2.0 m/s in velocity and 3.2 g in acceleration, with corner (tapering) frequencies at 10 and 45 Hz. Even though the proposed spectrum should be conservative enough to cover normal (North Sea) soft soil conditions, there might be cases where specific geological conditions may necessitate the introduction of an additional amplification factor at longer periods (above 1 second). We emphasize that this design spectrum is tied to a 10^{-4} probability level and to North Sea geologic conditions, for higher probabilities (lower magnitudes) or more typical Fennoscandian shield conditions a less conservative spectrum (at longer periods) could be chosen.

In comparing our recommendations with those of Dowrick (1981) for the UK offshore areas, we find that the *shape* of our design spectrum is fairly close to the one proposed by Dowrick for a 100 year return period. However, his absolute risk level (peak acceleration) seems unreasonably high in view of the results presented in this report.

The differences caused by variations in damping values must of course be allowed for. We recommend there to use a general logarithmic relationship of the type used by API (1981), where each of the spectral bounds in the proposed spectrum will be modified by a factor

$$D = \frac{\ln(100/\beta)}{\ln(20)}$$

for damping values β between 2 and 10.

With regard to the vertical design spectra, we recommend the standard solution here, namely, to use 2/3 of the horizontal values for the entire frequency band.

Since there is some tradition in plotting acceleration amplification values as a function of period, we have done that for the recommended spectrum in Fig. 11.4, together with a spectrum published by Selnes (1979) as a possible solution for Scandinavia. The values are about the same for periods around 1 second and above, while our curve is more conservative at shorter periods.

11.3 Time histories

Acceleration time histories are needed for dynamic analysis, and there are two basic ways of selecting such data,

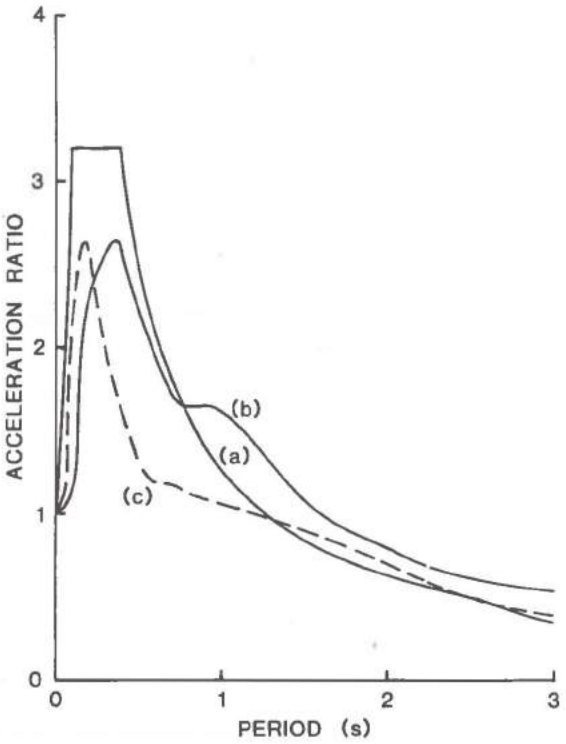

Fig. 11.4
Ratio between spectral acceleration and maximum acceleration as a function of period for (a) and the recommended design spectrum for the Norwegian Continental Shelf (Fig. 11.3); (b) a Californian spectrum for a deep soil deposit (Seed et al, 1974); and (c) a modification of (b) in accordance with specific Scandinavian conditions (Selnes, 1979).

either by generating artificial time histories or by selecting real accelerograms. There cannot be given any general recommendation on which solution to choose, as this will depend on the situation. Both solutions have their advantages and their disadvantages.

There are several methods in use for generating artificial time histories (Principia, 1981), and they all have the basic requirement to match a particular response or design spectrum. It is evident that this inversion is nonunique, as any number of different time histories can be generated for the same spectrum. Basic decisions here are tied to the length of the accelerogram, the envelope behavior, the phase angle distribution, and the relationship between the three components. Among these, the decision on the shape of the envelope is the most important one. With no previous accerelograms available from a particular area, it would not be much easier to select parameters for time history generation than it would be to select an accelerogram directly.

The latter procedure is still the most common one to use, and it is done by selecting strong-motion records (at distances typically 15-30 km from the zone of energy release) and scaling these to the appropriate acceleration value. Examples of earthquakes which might be appropriate to use here are the 1967 Koyna, India, earthquake ($M_S \sim 6.5$), and the 1976 Gazli, USSR, earthquake ($M = 7.0$). We consider both of these to be particularly relevant to the present case, as they are among the very few large intraplate earthquakes to have been recorded on nearby strong-motion instruments. They are both in a magnitude range close to the maximum possible (credible) for the North Sea areas, and they both show significantly higher predominant frequencies than typical interplate earthquakes. The Koyna earthquake is much disputed both with respect to cause (it is usually considered to be induced), to source parameters such as magnitude (where estimates range between 6.0 and 7.0) and faulting mechanisms (Langston, 1976), as well as to how to interpret the accelerogram (Guha et al, 1972). In comparison, it therefore seems to be more appropriate to recommend the Gazli earthquake, even though both of them from a geological point of view should be representative for shield areas like Fennoscandia.

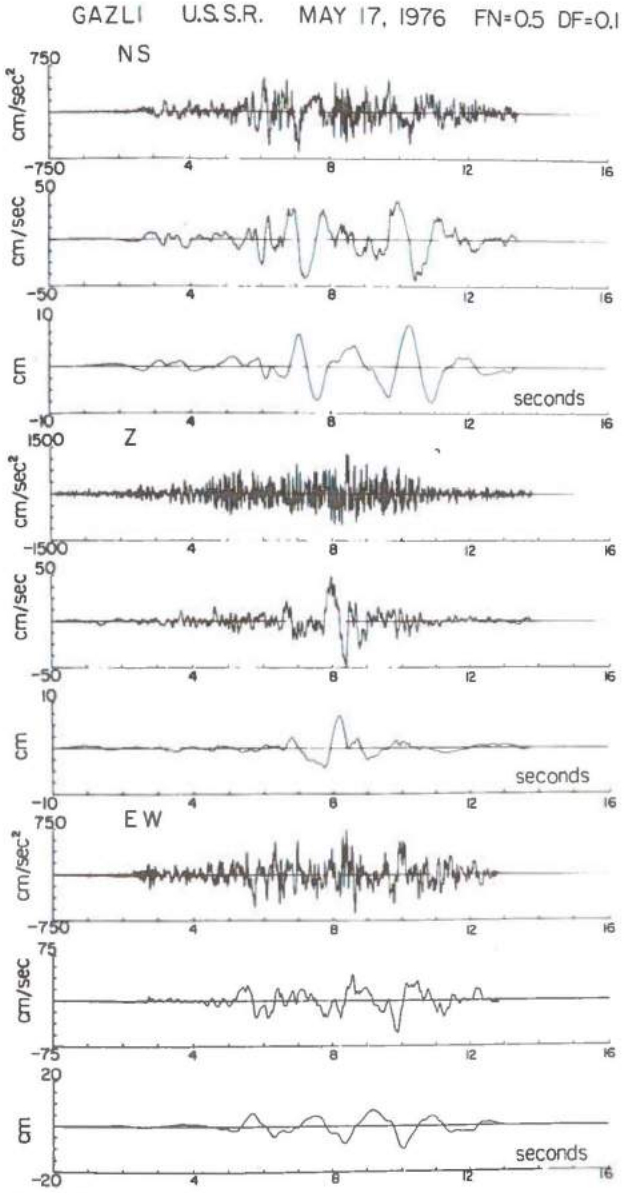

Fig. 11.5
Acceleration, velocity and displacement records for the Gazli earthquake (17 May 1976) from the Karakyr Point accelerograph about 10 km from the fault (from Harzell, 1980).

Three-component accelerograms of the Gazli earthquake of 17 May 1976 as recorded at Karakyr Point some 10 km away are shown in Fig. 11.5. We note that the durations of the strongest motion are relatively short, that is, about 8 sec on the vertical component. The corresponding amplitude spectra, shown in Fig. 11.6, give the vertical component spectra are reasonably flat out to 20 Hz while the horizontal spectra start falling off beyond 2 Hz. Tripartite spectra for the Gazli earthquake have not to our knowledge been published, but values on peak ground acceleration, velocity and displacement are available (Harzell, 1980). The strong-motion recordings are characterized by unusually high-amplitude (1.3 g), high-frequency (10 Hz)

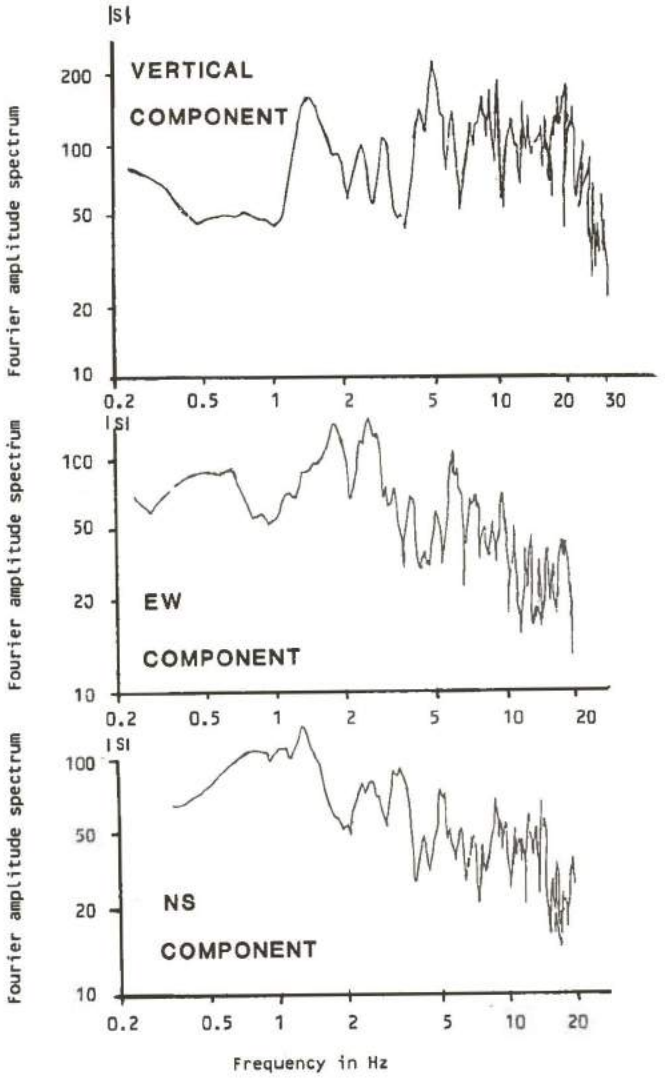

Fig. 11.6
Fourier amplitude spectra of Karakyr Point strong-motion recordings for the 17 May 1976 Gazli earthquake.

accelerations and low-amplitude (10 cm), low-frequency (0.8 Hz) displacements. In Table 11.1 the relative peak values are given together with similar values from U.S. (Newmark et al, 1973) and the Principia (1981) values developed for U.K., both for hard as well as soft ground conditions. For comparison, similar values are also given for the Koyna earthquake (Krishna et al, 1969). The recording site for the Gazli acclerograms is underlaid by 1 km thick sediments (Harzell, 1980), therefore probably qualifying for the "soft ground" category. In comparing with the other values in Table 11.1, we then find that the Gazli earthquake has peak velocity and displacement values very close to the U.K. soft ground values, except for vertical displacement. (The Gazli earthquake was not part of the Principia data base.) The peak values for Koyna, on the other side (Table 11.1), show anamously high displacement values as compared to acceleration. However, this most probably reflects quality problems with the accelerograms, and can thus be disregarded.

The results here therefore essentially confirm the usefulness of the Principia spectra with regard to more typical intraplate ("European") conditions, and the usefulness of the Gazli earthquake accelerograms (and possibly Koyna) for dynamic analyses. We maintain, however, for reasons given above, that somewhat more conservative spectral bounds (for longer periods) should be used for the North Sea areas. In order to accomodate for that in the selection of time histories, it may be appropriate also to consider using records such as those from the 1940 El Centro, the 1940 Helena, the 1971 San Fernando, or the 1977 Romanian earthquake.

	Velocity (cm/sec)		Displacement (cm)	
	H	V	H	V
U.S. - Hard Ground	71	43	30	28
- Soft Ground	122	74	91	84
U.K. - Hard Ground	37	21	9	6
- Soft Ground	66	35	15	13
Gazli, USSR (17 May 1976)	69	25	13	4
Koyna, India (10 Dec 1967)	39	50	(31)	(56)

Table 11.1

Values for peak ground velocity and peak ground displacement for horizontal (H) and vertical (V) components for U.S. (Newmark et al, 1973), U.K. (Principia, 1981), the Koyna earthquake (Kristy et al, 1980) and the Gazli earthquake (Harzell, 1980). The horizontal values are scaled to a standard peak acceleration of 1.0 g, and the vertical values are scaled to 2/3 g. The U.S. values are averages, the U.K. values are medians, and the Koyna and Gazli values are single measurements (horizontal components averaged).

References

Anonymous, 1978: *Norwegian Sea Symposium Proceedings*. Norw. Petroleum Society, Oslo, Norway.

API, 1981: *Recommended Practice for Planning, Designing and Constructing Fixed Offshore Platforms*. American Petroleum Institute, Washington, D.C.

Austegaard, A., 1975: The 1904-earthquake in the Oslofjord area, Appendix C of the Report: *Phase I studies - Preliminary seismic design criteria. Five alternative sites around the Oslofjord*. Report for NVE-statskraftverkene, Oslo, Norway. Prepared by Dames & Moore, New Jersey, 1975.

Båth, M., 1972: Zum studium der seismizität von Fennoskandia, *Ger-* 1981-1950. *Sveriges Geol. Unders. Årbok 50*, No. 1, 52 pp.

Båth, M., 1972: Zum studium der seismizit t von Fennoskandia, *Gerlands Beitr. Geophysik*, 81, 213-226.

Båth, M., 1975: Short period Rayleigh waves from near-surface events. *Phys. Earth Planet. Int.*, 10, 369-376.

Beaumont, C., 1978: The evolution of sedimentary basins on a viscoelastic lithosphere: theory and examples, *Geophys. J.R. astr. Soc.*, 55, 471-497.

Binns, R.E., 1978: Caledonian nappe correlation and orogenic history in Scandinavia north of latitude 67°N, *Geol. Soc. Am. Bull.*, 89, 1475-1490.

Biot, M.A., 1934: Theory of vibration of buildings during earthquakes *Zeitschr. für Angewandte mathematik und Mechanik*, Bd. 14, H4, 213-223.

Bjerhammar, A., 1982: Long wavelength heterogeneities in the upper mantle as seen by satellites. *Tectonophysics* (in press).

Blume, J.A., 1965: Earthquake ground motion and engineering procedures for important installations near active faults, *Third World Conference on Earthquake Engineering, New Zealand, Vol. IV*, 53-67.

Brune, J.N., 1970: Tectonic stress and the spectra of seismic shear waves from earthquakes. *J. Geophys. Res.*, 75, 5997-5009.

Bungum, H., and J. Fyen, 1979: Hypocentral distribution, focal mechanisms and tectonic implications of Fennoscandian earthquakes, 1954-1978. *Geol. För Stockh. Förh.*, 101, 261-271.

Bungum, H. and E.S. Husebye, 1974: Analysis of the operational capabilities for detection and location of seismic events at NORSAR. *Bull. Seism. Soc. Am.*, 64, 637-656.

Bungum, H. and E.S. Husebye, 1979: The Meløy, northern Norway, earthquake sequence - a unique intraplate phenomenon. *Nor. Geol. Tidsskr.*, 59, 189-193.

Bungum, H., E.S. Husebye and F. Ringdal, 1971: The NORSAR array and preliminary results of data analysis. *Geophys. J.R. astr. Soc.*, 25, 115-126.

Bungum, H., B.K. Hokland, E.S. Husebye and F. Ringdal, 1979: An exceptional intraplate earthquake sequence in Meløy, Northern Norway, *Nature*, 280, 32-35.

Bungum, H., B.J. Mitchell and Y. Kristoffersen, 1982: Concentrated earthquake zones in Svalbard, *Tectonoplysics*, 82, 175-188

Bungum, H., S. Vaage and E.S. Husebye, 1982: The Meløy earthquake sequence, Northern Norway; source parameters and their moment scaling relations, *Bull. Seism. Soc. Am.*, 72, 197-206.

Christie, P.A.F. and J.G. Sclater, 1980: An extensional origin for the Buchan and Witchground Graben in the North Sea. *Nature*, 283, 729-731.

Cloud, W.K., and V. Perez, 1971: Unusual accelerograms recorded at Lima, Peru, *Bull. Seism. Soc. Am.*, 61, 633-640.

Cornell, C.A., 1968: Engineering seismic risk analysis. Bull. Seism. Soc. Am., 58, 1583-1606.

Dahlman, O., Å. Ohlson and R. Slunga, 1975: Jordskalv och jordskalvrisker i Sverige, preliminär studie. The Swedish Defence Research Establishment, Hagfors Observatory, *Report 1975-08-15*, Stockholm, 18 pp.

Day, G.A., B.A. Cooper, C. Andersen, W.F.J. Burgers, H.C. Rønnevik and H. Schøneich, 1981: Regional seismic structure maps of the North Sea, in: L.V. Illing and G.D. Hobson (eds.): *Petroleum Geology of the Continental Shelf of North-West Europe*. Heyden & Son Ltd., London, pp. 76-84.

Dames & Moore, 1976: *Seismic risk analysis and design ground response spectra for the Forsmark area*. Report for the Swedish Power Board.

Dickinson, W.R., 1977: Tectono-stratigraphic evolution of subduction-controlled sedimentary assemblages, in: M. Talwani & W.C. Pitman III (eds.): *Island Arcs, Deep Sea Trenches and Back-Arc Basins*, Maurice Ewing Series 1, Am. Geophys. Union, 33-40.

Donato, J.A. and M.C. Tully, 1981: A regional interpretation of North Sea gravity data, in: L.V. Illing and G.D. Hobson (eds.): *Petroleum Geology of the Continental Shelf of North-West Europe*, Heyden & Son, Ltd. 65-75.

Doornbos, D.J., 1982: Seismic moment tensors and kinematic source parameters, *Geophys. J.R. astr. Soc.*, 69,235-251.

Dowrick, D.J., 1981: Earthquake risk and design ground motions in the UK offshore area. *Proc. Inst. Civ. Engrs.*, Part 2, 71, 305-321.

Eldholm, O. and M. Talwani, 1977: Sediment distribution and structural framework of the Barents Sea, *Geol. Soc. Am. Bull.*, 88, 1015-1029.

Esteva, L., 1970: Seismic risk and seismic design decisions, in: R.J. Hansen (ed.), *Seismic Design for Nuclear Power Plants*, M.I.T. Press, Cambridge, Mass., USA.

Freedman, H.W., 1967: Estimating earthquake magnitude. *Bull. Seism. Soc. Am.*, 57, 747-760.

Furnes, H., D. Roberts, B.A. Sturt, A. Thon and G.H. Gale, 1981: *Proc. int. Ophiolite Symp.*, Nicosia.

Gabrielsen, R.H. and I.B. Ramberg, 1979: Tectonic analysis of the Meløy earthquake area based on Landsat lineament mapping. *Nor. Geol. Tidsskr.*, 59, 183-187.

Gelfand, I.M., S.A. Guberman, V.I. Keilis-Borok, L. Knopoff, F. Press, E.Y. Ranzman, I.M. Rotwain and A.M. Sadovsky, 1975: Pattern recognition applied to earthquake epicenters in California, *Phys. Earth & Planet. Inter.*, 11, 227-284.

Guha, S.K., S.P. Aggarwal and P.D. Gosavi, 1972: Accelerogram of Koyna earthquake of December 11, 1967. *Bull. Seism. Soc. Am.*, 62, 413-414.

Gutenberg, B., and C.F. Richter, 1956: Magnitude and energy of earthquakes, *Ann. Geophis.*, 9, 1-15.

Harzell, S., 1980: Faulting process of the May 17, 1976 Gazli, USSR earthquake. *Bull. Seism. Soc. Am.*, 70, 1715-1736.

Hasegawa, H.S., P.W. Basham and M.J. Berry, 1981 : Attenuation relations for strong seismic ground motion in Canada, *Bull. Seism. Soc. Am.*, 71, 1943-1962.

Horrebow, C., 1765: Beretning om Jorskiaelvet, som skedde d. 22 dec. Ao. 1759, *Kongelig Dansk Videnskapselskab Skrifter*, Bd 9, 261-372, Copenhagen, Denmark.

Housner, G.W., 1959: Behavior of structures during earthquakes. *Proceedings of the American Society of Civil Engineers (ASCE)*, Vol 90, No. EM1, 113-150.

Housner, G.W., 1965: Intensity of earthquake ground shaking near the Causative Fault, *Third World Conference on Earthquake Engineering*, New Zealand, 94-111.

Housner, G.W., 1970a: Strong ground motion, in: R.L. Wiegel (ed.): *Earthquake Engineering*, Prentice-Hall Inc., Englewood Cliffs, N.J., 75-91.

Housner, G.W., 1970b: Design spectrum, in: R.L. Wiegel (ed.): *Earthquake Engineering*, Prentice-Hall, Englewood Cliffs, N.J., 93-106.

Husebye, E.S., H. Bungum, J. Fyen and H. Gjøystdal, 1978: Earthquake activity in Fennoscandia between 1497 and 1975 and intraplate tectonics, *Norsk Geol. Tidsskrift*, 58, 51-68.

Husebye, E.S., H. Gjøystdal, H. Bungum and O. Eldholm, 1975: The seismicity of the Norwegian and Greenland Seas and adjacent continental shelf areas, *Tectonophysics*, 25, 55-70.

Illing, L.V. and G.D. Hobson (eds.), 1981: *Petroleum Geology of the Continental Shelf of North-West Europe*. Heyden & Son, Ltd., London, 521 pp.

Iwasaki, T., 1981: Free field and design motions during earthquakes. *Proc. Int. Conf. on Recent Advances in Geotechnical Earthquake Engineering and Soil Dynamics*. Univ. of Missouri-Rolla, Rolla, MO, USA, 757-786.

Jarvis, G.T. and D.P. McKenzie, 1980: Sedimentary basin formation with finite extension rates. *Earth & Planet. Sci. Lett.*, 48, 42-52.

Johnson, L.R. and T.V. McEvilly, 1974: Near-field observations and source parameters of Central California earthquakes, *Bull. Seism. Soc. Am.*, 64, 1855-1886.

Jørgensen, F. and T. Navrestad, 1981: The geology of the Norwegian shelf between 62°N and the Lofoten Islands, in: L.V. Illing and G.D. Hobson (eds.) *Petroleum Geology of the Continental Shelf of North-West Europe*. Heyden & Son, Ltd., London.

Kanai, K., 1966: Improved empirical formulae for characteristics of strong motion earthquake motions, *Proceedings, Japan Earthquake Symposium, 1-4 (in Japanese)*.

Kanamori, H., 1977: The energy release in great earthquakes.

J.Geophys. Res., 82, 2981-2987.
Karnik, V., 1969: *Seismicity of the European Area, Vol. 1*, D. Reidel Publ. Co., Dordrecht, The Netherlands, 364 pp.
Keilhau, B.M., 1836: Efterretninger om Jordskjælv i Norge. *Mag. for Naturvidenskaperne*, 12, 83-165.
Kjellén, R., 1909: Sveriges jordskalv, forsök til en seismisk landsgeografi. *Göteborgs högskolans årsskrift*. Bd XV.
Kjøde, J., K.M. Storetvedt, D. Roberts and A. Gidskehaug, 1978: Paleomagnetic evidence for large-scale dextral movement along the Trollfjord-Kamagelv fault, Finnmark, North Norway, *Phys. Earth Planet. Int.*, 16, 132-144.
Knopoff, L., 1981: The nature of the earthquake source,in: E.S. Husebye and S. Mykkeltveit (eds.) *Identification of Seismic Sources, Earthquake or Underground Explosion, D. Reidel Publ. Co. Dordrecht, The Netherlands, 49-70.*
Kolderup, C.F., 1905: Jordskjelvet den 23. oktober 1904, *Bergens Museums Aarbok 1905*, 1, 172 pp.
Kolderup, C.F., 1913: Norges jordskjælv, *Bergens Museums Aarbok 1913*, 8, 152 pp.
Krishna, J., A.R. Chandrasekaran and S.S. Saini, 1969: Analysis of Koyna accelerogram of December 11, 1967. *Bull. Seism. Soc. Am.*, 59, 1719-1731.
Kristy, M.J., L.J. Burdick and D.W. Simpson, 1980: The focal mechanisms of the Gazli, USSR, earthquakes. *Bull. Seism. Soc. Am.*, 70, 1737-1750.
Langston, C.A., 1976: A body wave inversion of the Koyna, India, earthquake of December 10, 1967, and some implications for body wave focal mechanisms. *J. Geophys. Res.*, 81, 2517-2529.
Lehman, I., 1956: Danske jordskjælv, *Bull. Geol. Soc. Danmark*, 13, 88-103, Copenhagen.
Lockheed Aircraft Co. and Holmes & Narver, Inc., 1963: *Nuclear reactors and earthquakes*. Report for the United States Atomic Energy Commission TID 7024, 415 pp.
Løset, F., 1981: Neotectonic movements in Norway. *Internal Report 40009-7*, Norwegian Geotechnical Institute, Oslo, Norway.
Lundquist, I., and R. Lagerbäck, 1976: The Pärve fault: A late glacial fault in the Precambrian of Swedish Lappland, *Geol. Fören. Stockh. Förh., 98, 45-51*
Madariaga, R., 1981: Dynamics of seismic sources, in: E.S. Husebye Husebye and S. Mykkeltveit (eds.) *Identification of Seismic Sources, Earthquake or Underground Explosion, D. Reidel Publ. Co. Dordrecht, The Netherlands, 71-96.*
McGuire, R.K., 1978: Seismic ground motion parameter relations. *J. Geotech. Eng. Div.*, 104, 481-491.
McKenzie, D., 1978: Some remarks on the development of sedimentary basins. *Earth Planet. Sci. Lett.*, 40, 25-32.
Milne, W.G., and A.G. Davenport, 1969: Distribution of earthquake risk in Canada, *Bull. Seism. Soc. Am.*, 59, 729-754.
Morner, N.A. (ed.), 1980: *Earth Rheology, Isostasy and Eustacy*, J.F. Wiley & Sons, 589 pp.
Mykkeltveit, S. and F. Ringdal, 1979: P and Lg wave attenuation in selected frequency bands in the 1-5 Hz range using NORSAR short period records, in: *Sci. Rep. No. 1-79/80*, NTNF/NORSAR, Kjeller, Norway.
Mykkeltveit, S., E.S. Husebye and C. Oftedahl, 1980: Subduction of the Iapetus Ocean crust beneath the Møre Gneiss Region, southern Norway, *Nature*, 288, 473-475.
Newmark, N.M. and W.J. Hall, 1978: Development of criteria for seismic review of selected nuclear power plants. United States Nuclear Energy Regulartory Commission, *NUREG/CR-0098*.
Newmark, N.M., J.A. Blume and K.K. Kapur, 1973: *Seismic Design Spectra for Nuclear Power Plants*. American Society of Civil Engineers (ASCE) Power Div., November, 287-303.
Noponen, I., 1971-77: *Seismic events in northern Europe*, Monthly bulletins from March 1971 to December 1977, Institute of Seismology, Univ. of Helsinki, Finland.
Nuttli, O.W., 1973: Seismic wave attenuation and magnitude relations for eastern North America, *J. Geophys. Res.*, 78, 876-885.
Nuttli, O.W., 1978: A time-domain study of the attenuation of 10 Hz waves in the New Madrid seismic zone. *Bull. Seism. Soc. Am.*, 68, 343-355.
Oftedahl, C., 1980: *Norges Geol. Unders. 356*, 3-114.
Pirhonen, S.E., F. Ringdal and K.-A. Berteussen, 1976: Event detectability of seismograph stations in Fennoscandia, *Phys. Earth Planet. Inter.*, 12, 329-342.
Principia, 1981: *Seismic Ground Motions for UK Design*. Report for British Nuclear Fuels Ltd. and Central Electricity Generating Board, by Principia Mechanica Ltd.
Renquist, H., 1930: Finlands jordskalv. *Fennia*, 54, 113 pp.
Richardson, R.M. and S.C. Solomon, 1979: Tectonic stress in the plates. *Rev. of Geophys. and Space Phys.*, 17, 981-1019.
Richter, C.F., 1958: *Elementary Seismology*, W.H. Freeman & Co., San Francisco, Calif., USA, 768 pp.
Ringdal, F., 1975: On the estimation of seismic detection thresholds, *Bull. Seism. Soc. Am.*, 65, 1631-1642.
Ringdal, F. and J. Fyen, 1979: Analysis of global P-wave attenuation characteristics using ISC data files, in: *Sci. Report No. 1-79/80*, NTNF/NORSAR, Kjeller, Norway.
Ringdal, F., E.S. Husebye and J. Fyen, 1977: Earthquake detectability estimates for 478 globally distributed seismograph stations. *Phys. Earth Planet. Inter.*, 15, 24-32.
Rønnevik, H.C., 1981: Geology of the Barents Sea, in: L.V. Illing and G.D. Hobson (eds.): *Petroleum Geology of the Continental Shelf of North-West Europe*, Heyden & Son, Ltd. London, 395-406.
Rønnevik, H. and T. Navrestad, 1977: Geology of the Norwegian shelf between 62° N and 69° N. *Geojournal*, 1, 33-46.
Sacks, I., A. Snoke and E.S. Husebye, 1979: Lithospheric thickness beneath the Baltic Shield. *Tectonophysics*, 56, 101-110, 1979.
Schnabel, P.B., and H.B. Seed, 1973: Acceleration in rock for earthquakes in the Western United States. *Bull. Seism. Soc. Am.*, 63, 501-516.
Sclater, J.G., and P.A.F. Christie, 1980: Continental stretching: An explanation of the Post-Mid-Cretaceous subsidence of the central North Sea basin, *J. Geophys. Res.*, 85, 3711-3740.
Seed, H.B., G. Ugas and J. Lysner, 1974: Site-dependent spectra for earthquake- resistant design. Univ. of California, Berkeley, College of Engineering Earthquake Engineering Research Center, *Report 74-12*, 15 pp.
Selnes, P., 1979: Earthquake parameters for use in engineering design in Scandinavia. *Geol. Foren. Stockh. Förh.*, 100, 301-305.
Stein, S., N.H. Sleep, R.J. Geller, S.-C. Wang and G.C. Kroeger, 1979: Earthquakes along the passive margin of eastern Canada. *Geophys. Res. Lett.*, 6, 537-540.
Stephansson, O. and H. Carlsson, 1976: Seismotektonisk analys av Fennoscandias berggrund - en studie för seismisk riskanalys i Forsmark, *Tech. Rep. 1976: 20T*, Dept. of Rock Mechanisms, University of Luleå, Sweden.
Street, R.L., 1976: Scaling northeastern United States/southeastern Canadian earthquakes by their Lg waves. *Bull. Seism. Soc. Am.*, 66, 1525-1537.
Sturt, B.A., and D. Roberts, 1978: Caledonides of northernmost Norway (Finnmark), in: E.T. Tozer and P.E. Schenk (eds.): *Caledonian-Appalachian orogen of the North Atlantic Region*, Geol. Survey of Canada, Paper 78-13, 17-24.
Swanger, H.J. and D.M. Boore, 1978: Importance of surface waves in strong ground motion in the period range of 1 to 10 seconds, *Proc. 2nd Int. Conf. on Microzonation for Safer Construction - Research and Application*, San Francisco, CA, USA, 1447-1457.
Sykes, L., 1978: Intraplate seismicity, reactivation of preexisting zones of weakness, alkaline magmatism and other tectonism postdating continental fragmentation, *Rev. Geophys. & Space Physics*, 16, 621-688.
Talwani, M. and O. Eldholm, 1972: The continental margin off Norway: A geophysical study. *Geol. Soc. Am. Bull.*, 83, 3575-3608.
Talwani, M. and O. Eldholm, 1977: Evolution of the Norwegian-Greenland Sea, *Bull. Geol. Soc. Am.*, 88, 969-999.
Thomassen, T.C., 1888: Berichte über die, wesentlich seit 1834, in Norwegen eingetroffenen Erdbeben, *Bergens Museums Aarsberetning 1888*, 52 pp.
Tozer, E.T. and P.E. Schenk (eds.), 1978: Caledonian-Appalacian orogen of the North Atlantic Region, *Geol. Survey of Canada*, Paper 78-13.
Trifunac, M.D., and A.G. Brady, 1976: Correlation of peak acceleration, velocity and displacement with earthquake, magnitude, distance and site conditions. *Int. J. Earthquake Engin. Struct. Dynamics*, 4, 455-471.
USNRC, 1973: Design response spectra for seismic design of nuclear power plants. United States Nuclear Regulatory Commission, *Regulatory Guide No. 1.60*, Directorate of Regulatory Standards, Washington, D.C.
Vaage, S., 1980: Seismic evidence on complex tectonics in the Meløy earthquake area, *Nor. Geol. Tidsskr.*, 60, 213-217.
Versey, H.C., 1939: The North Sea earthquake of 1931 June 7, *M.N.R.A.S. Geophys. Suppl.*, 4, No. 6, Jan 1939.
Watson, J., 1977: Eo-Europa: the evolution of a craton, in: D.V. Ager and M. Brooks (eds.), *Europe from Crust to Core*, J. Wiley & Sons London, 59-78.
Wegener, A., 1929: *Die Entstehng der Kontinente und Ozeane*. English translation The origin of continents and oceans by J. Biram. Dover Ed. 1966, 246 pp.
Windley, B.F., 1979: Tectonic evolution of continents in the Precambrian. *Episodes*, 4, 12-16.
Wirth, 1970: Estimation of network detection and location capability. *Seismic Data Laboratory Research Memorandum*, Teledyne-Geotech, Alexandria, Virginia, USA.
Wood, H.O. and F. Neumann, 1931: Modified Mercalli scale of 1931, *Bull. Seism. Soc. Am.*, 21, 277.
Woodland, A.W. (ed.), 1975: *Petroleum and the Continental Shelf of Northwest Europe*, J. Wiley & Sons London, 499 pp.
Yanshin, A.L. (ed.), 1966: *Tectonic Maps of Eurasia, part 2*: Geological Institute, Academy of Science, Moscow (in Russian).
Ziegler, P.A., 1981: Evolution of sedimentary basins in North-West Europe, in: L.V. Illing and G.D. Hobson (eds.): *Petroleum Geology of the Continental Shelf of North-West Europe*, Heyden & Sons, Ltd., London, 3-40.